2015

Synthesis and characterisation of novel astaxanthin metal complexes

Submitted by:

Nasreen Shuaith

Being a thesis presented for the award of Master of Science (by research)

Supervisor:

Dr. Garrett Farrell

Science department, Letterkenny Institute of Technology, Letterkenny, Co. Donegal.

Submitted to Quality and Qualifications Ireland in fulfilment of the requirements for the award of Masters of Science (by Research) in October 2015

Declaration

I hereby certify that the material, which l now submit for assessment on the programmes of study leading to the award of a Master of Science (by research), is entirely my own work and has not been taken from the work of others except to the extent that such work has been cited and acknowledged within the text of my own work. No portion of the work contained in this thesis has been submitted in support of an application for another degree or qualification to this or any other institution.

Signature of Candidate _____Date _____

Thereby certify that all the unreferenced work described in this thesis and submitted for the award of a Master of Science (by research), is entirely the work of Nasreen Shuaith. No portion of the work contained in this thesis has been submitted in support of an application for another degree or qualification to this or any other institution.

Signature of Supervisor _____Date _____

Acknowledgments

Firstly I would like to express my sincere gratitude to my supervisor Dr. Garrett Farrell for providing me with valuable advice, guidance, knowledge and encouragement along the way.

I thank the Letterkenny institute of technology for providing me with the opportunity to carry out my research and use of their equipment. Also a special thanks to LYIT technicians for providing technical support and guidance.

My sincere thanks go to my labmates Dr. Denis Mccrudden and Carla Harkin for their insightful discussions, advice and assistance.

Finally I would like thank my parents, sisters and brother for their support and I especially thank my sister Dunya Shuaith for being there, encouraging me along the way and supporting me through the rough times.

Abstract

Astaxanthin is produced in a wide range of organisms, its extractability from the native Irish brown crab (*Cancer pagurus*) was carried out using glacial acetic acid. The extractable natural astaxanthin yield is quantified using High performance liquid chromatography. In this research the possibility of yielding extractable astaxanthin from crustacean waste was examined to provide a natural source of the xanthophyll. Astaxanthin is popular in demand by the nutraceutical market due to its high radical scavenging activity. The question stands does this ability withstand the biochemical reactions undergone following ingestion. In order to assimilate these reactions examination of complex formation with transition metal salt were carried out a three temperatures of 20°C, 37 °C and 78 °C. Complexation with copper chloride proved successful at a higher activation energy (78 °C) as significant changes were confirmed in electronic spectra and cyclic voltammograms. Cobalt chloride proved unsuccessful in the formation of complexes with astaxanthin as no changes were observed apart from a stabilisation effect in cyclic voltammograms providing a two electron oxidation transfer. Astaxanthin is a natural powerful antioxidant but the involvement of the radical scavenging sites in biochemical reactions can hinder or improve it effects as proven in this research the metal chlorides exhibit a stabilisation effect on the molecules antioxidant activity but also changed the aggregation of the molecule when complexed with copper chloride at a higher temperature causing a more tight H-type packing. These effects require further examination before marketing this molecule as a nutraceutical as these reactions may negate it intake.

List of Acronyms

Ag/ AgCl	Silver silver chloride
β	Beta
Ca	Calcium
$Ca(ClO_4)_2$	Calcium perchlorate
Cd	Cadmium
C=O	Carbonyl
Cu	Copper
DMBA	Dimethylnemz(a)antracene
DMSO	Dimethyl sulfoxide
E	Potential
Fe	Iron
$(FeClO_4)_2$	Iron perchlorate
Hg	Mercury
HOMO	Highest unoccupied molecular orbital
HPCD	Hydroxypropyl-β-cyclodextrin
HPLC	High performance liquid chromatography
IUPAC	International union of pure and applied chemistry
KCL	Potassium chloride
LUMO	Lowest unoccupied molecular orbital
NMR	Nuclear magnetic resonance
O	Oxygen
OH	Hydroxyl
Pb	Lead

TBA TFO	Tetrabutylammonium tetrafluoroborate
V_o	Incident beam
V_m	Vibrational frequency of molecules
Zn	Zinc
π^*	Antibonding orbital
π	Bonding orbital
δ	Sigma
ΔE	Delta energy

Units

%	Percentage
℃	Degrees Celsius
cm	Centimetres
Dq	Electron to electron repulsion
g	Grams
µs	Microseconds
mg	Milligram
mM	Millimolar
nm	Nanometres
r.m.s	Raman band of water
V	Volts
V/s	Volts per second7

List of tables

List of figures

Table of contents:

Chapter 1

Introduction

1.0 Introduction

Over the last quarter of a century the nutraceuticals market has expanded into a multi-billion euro industry with the forecast of continued growth within the emerging global markets (Frost and Sullivan 2011). Nutraceuticals is a term that combines "nutrition" and "pharmaceutical", and is used to describe a food that functions in maintaining the wellbeing and health enhancement of an individual thus preventing and treating specific disease (Ramaa et al. 2006). There are numerous reasons for the continued growth in this sector but in essence the industry is catering for the consumer concern regarding traditional synthetic additives and the trend has been towards incorporating more natural substitutes which are viewed as a healthier alternative to traditional additives into food products. One particular area which has gained considerable attention is the role played by antioxidants within food products (Shahidi 2000) and also the preventative role these additives may play as free radical scavengers within the human body post consumption

(Capelli and Cysewki 2007). While numerous synthetic compounds have been used to achieve these goals in the past, the white paper by Frost and Sullivan (2011) predicts a push towards the development of natural nutraceuticals for the consumer market. The logic behind this driving force is the somewhat perceived notion that there is a lower risk of side effects associated with natural products while at the same time being potentially more bioavailable. Within this group of naturally occurring antioxidants the carotenoids represent a commercially important class of molecules.

1.1 Antioxidant Activity

On a daily basis the human body is exposed to free radicals whether it is from the surrounding environment (sun rays and pollutants) or through food intake. Irrespective of the source these free radicals can cause damage and the envisaged role of any ingested antioxidant is to eliminate these radicals and restore the cell to a normal state. Indeed many consumer foods are now marketed based on a products inherent natural antioxidants and their potential for antioxidant activity within the body. However the relative effectiveness of these natural antioxidants can and does vary considerably (Capelli and Cysewki 2007). But in such a consumer driven market products containing additives with the highest anti-oxidant activity will inevitably perform better from a commerical point of view. Recent studies have shown that in terms of antioxidant capacity astaxanthin out performs commercially available naturally occurring antioxidants which are well known and a popular choice amongst consumers. A few of which include vitamin E, based on singlet oxygen quenching tests astaxanthin proved 550 times stronger (Shimidzu et al. 1996) and Vitamin C studies based on oxygen free radical scavenging astaxanthin proved to be 64.9 times stronger (Bagchi 2001).

While there does exist a popular movement towards incorporating greater amounts antioxidants into food products it would be prudent to recognise the fact there is still some uncertainty regarding the potential to which these antioxidant molecules are assimilated through the intestinal wall (Alexandropoulou et al. 2005, Hu et al. 2000). However given the structural similarity of astaxanthin to the β-carotene molecule, a molecule that is known to be bio-assimilated by the human body it is not unreasonable to assume that astaxanthin may be absorbed through a similar metabolic process.

Irrespective of this assumption it is recognised that free radicals produced within the body can cause damage and play a role in the development of chronic diseases which are life limiting such as cataracts, cancer and rheumatism through disruption of the cell's regular state (Pham-Huy et al. 2008). Thus it is this potential to prevent this type of free radical damage that has driven much of the research interest into these free radical terminators.

Mechanisms of scavenging free radicals involve electron transfer reactions, the transfer of a hydrogen atom and radical addition. Carotenoids possess the ability to either donate or accept electrons for free radical scavenging purposes. In combating oxygen (O_2) free radicals dioxi-carotenoids can take up electrons and these mechanisms suggest that there is direct reaction between the antiradical and the free radical. The chelating of metals by molecules can have an indirect effect and inhibit the formation of free radicals. Studies have shown the Cu^{2+} chelating capacity of carotene and astaxanthin's capability of forming metal ion complexes with metal cations (Hernández-Marin et al. 2012).

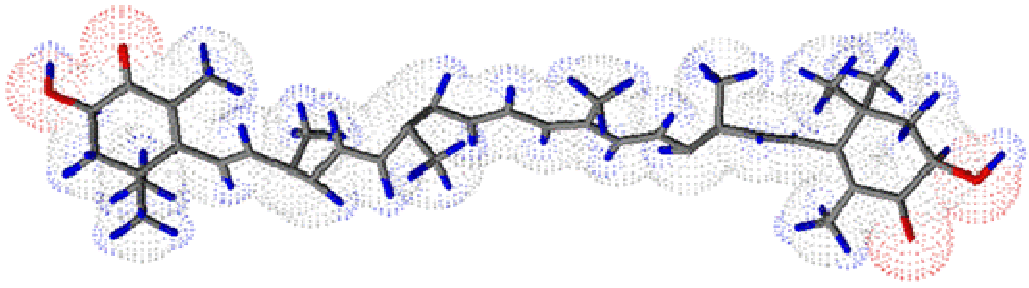

Figure 1.1: A stick model depicting the molecular structure of astaxanthin and the associated delocalised electron cloud.

These interactions can induce changes on the distinctive spectroscopic absorption characteristics of astaxanthin, i.e. there is a shift in the maximum absorption band of astaxanthin, usually a red shift (Hernández-Marin et al. 2012). These changes are of interest as they can induce changes on the efficiency of astaxanthin as a potential nutraceutical. Natural astaxanthin is of particular importance to the nutraceuticals sector but these benefits are intrinsically linked to the bioavailability of the unbound molecule. Any interactions between astaxanthin and metal ions inherently present within the digestive system has the potential to reduce this bioavailability and thus decrease its potential as a natural antioxidant, e.g. copper and cobalt. The metal cobalt

may be introduced into the digestive system as part of Vitamin B_{12} complex (Smith and Gropper 2012) and copper can be introduced through a large variety of different dietary intakes including meat, dried fruits, nuts and cocoa, mainly in the form of copper sulphate (Kamberg 2010, Smith and Gropper 2012). This metal binding capacity of astaxanthin may also represent an efficient way to preserve its antioxidant capabilities by providing a route for drug delivery.

1.2 Carotenoids

The carotenoids represent a large class of naturally occurring fat soluble molecules. These coloured pigments are found in both the plant and animal kingdoms and can vary from blue to red in colour. The carotenoid family includes over 800 individual molecules which is divided into two major groups: Carotenes and Xanthophylls. The essential difference between the carotenes and xanthophylls is the additional presence of oxygen atoms in the xanthophyll molecules. Both classes are structurally similar molecules based on a repeating isoprene subunit. This repeating isoprene subunit results in a conjugated sp^2 hybridised carbon backbone. This hybridised system results from unfilled p-orbitals which overlap with adjacent unfilled p-orbitals on neighbouring carbon atoms. These hybridised orbitals interact and allow for electron movement. In fact the carbon backbone can act as an electronic conductor and electrons are free to migrate along the molecules backbone (Palanna 2009). It is this hybridised orbital which is responsible for the interesting electronic properties of this molecule.

The colour of the of the particular carotenoid is due to the presence of the conjugated double bond system within the molecule and the greater the degree of conjugation the further red shifted the primary absorption band will be. A minimum of seven conjugated double bonds is required before a carotenoid molecule exhibits a visible yellow hue (DeMan 1999). In addition each double bond may exist in either the “cis” or “trans” form although the majority of the carotenoids found in food products are in the “trans” form. Irrespective of the stereo-isomeric configuration the inherent highly unsaturated nature of the carotenoids means that they are highly susceptible to oxidative damage and photodecomposition. While the bound molecules as they are found in natural systems are relatively stable, the purified molecules must be stored under controlled

conditions so as to minimise their exposure to oxygen and light. Failure to limit the exposure to these conditions normally results in the formation of breakdown products like monoesters of the parent carotenoids molecules (Siems et al 1999). The degree to which the formation of these breakdown products has occurred can be monitored using chromatographic techniques such as high performance liquid chromatography (HPLC).

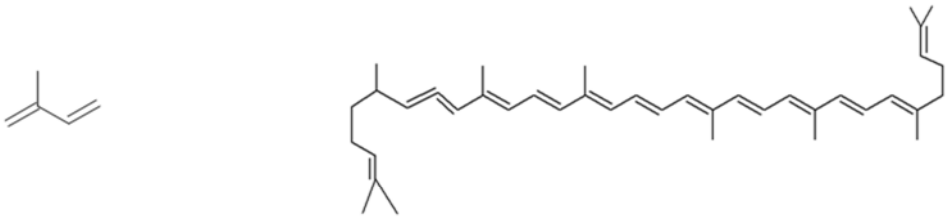

Figure 1.2 :(a) Basic Isoprene subunit with double bond conjugation, **(b)** Lycopene (generated using Chemsketch software)

Various different carotenoids have been shown to be extremely effective nutraceuticals in numerous studies, e.g. lycopene has been associated with the decreased risk of cardiovascular diseases and chronic cancer (Rao and Agarwal 2000) and lutein can reduce the risk of lung and breast cancer (Ribaya-Mercado and Blumberg 2004).

1.3 Astaxanthin potential as a nutraceutical

The most important and widely used xanthopyhlls is astaxanthin; it has many applications within the pharmaceutical, food and cosmetic industries. This pinkish-red pigment can be found in a variety of foods and some common examples of the natural occurrence of astaxanthin include salmon, seaweeds and crustaceans. The majority of these organisms with the notable exceptions of algae and bacteria cannot produce astaxanthin directly and it is thus introduced through their diet (Capelli and Cysewski 2007). Once it is absorbed it can have different effects on the organism's body, a few include: pigmentation, the ability to oxidise essential fatty acids and immunological reactions (Capelli and Cysewski 2007).

The consumer demand for commercial astaxanthin has resulted in a dramatic increase in the market in recent years. Natural astaxanthin is in great demand because of its

benefits including antioxidant activity, antimicrobial activity and anti-inflammatory activity (Capelli and Cysewski 2007). Until recently the main application for astaxanthin usage had been in fish farming where astaxanthin was added to the salmon's diet in order for the fish flesh to develop its popular pink/red pigmentation. It also had the additional benefit of conferring protection (cellular) from oxidation (Baker and Günther 2004).

The wide variety of benefits associated with astaxanthin gives it the potential to be a powerful nutraceutical. Studies have shown that ingestion of astaxanthin may confirm benefits such as antioxidant and anti-inflammatory activity (Bagchi et al. 2010). Further studies by Nagendraprabhu and Sudhandiran 2011 on rat colon carcinogenesis showed that astaxanthin exhibits anti-cancer and anti-inflammatory effects. In 7,12-Dimethylbenz(a)anthracene (DMBA)-induced hamster buccal pouch carcinogenesis astaxanthin has been found to have a chemo-preventative effect as it disrupts the NF-κ B and Wnt/ß-catenin signalling pathways through inhibiting phosphorylation of kinases and transcription factors (Kavitha et al. 2013). However these antioxidant and anti inflammatory functions can be disrupted through the formation of complexes with other atoms within the digestive system, e.g. transition metals (cobalt, copper, etc.). Recent research has shown the that the cyclohexane ring of a astaxanthin molecule can chelate metal to from complexes with Ca^{2+} and Zn^{2+} ions at low salt concentrations (Polyakov et al. 2010). The formation of similar complexes involving copper and chloride and their stability will be examined further during this research.

1.4 Sources of Astaxanthin

While astaxanthin can be obtained from numerous sources each with its own benefits the majority of commercially available astaxanthin is extracted from *Haematococcus pluvialis* flakes; an algae which is known to have the largest concentration of the pigment in nature. While a synthetic form of the molecule is available the natural form of the molecule has been found to have a greater bio-availability and thus more research has been placed into finding improved methods of its extraction from natural sources. Other sources of astaxanthin which have been exploited include red yeast

(*Xanthophyllomyces dendrorhous*), green algae (Haematococcus pluvialis) and oil extracted from krill (Dore and Cysewski 2003).

1.4.1 Algal sources

The algae are a primitive class of organism which inhabit both freshwater and saltwater aquatic ecosystems (Graham and Wilcox 2000). They are photosynthetic organisms which are less complex in structure when compared to land plants. Even so the algae represent the one of the largest marine sources for astaxanthin (Graham and Wilcox 2000). Within certain algae cells large accumulations of astaxanthin can occur after the cell has been subjected to high levels of sunlight. A similar effect can also be induced by varying the nutrient supply levels to the cell e.g. by altering the amount of available nitrogen. The accumulation of the astaxanthin occurs within the extra-chloroplastic lipid droplets where astaxanthin is considered to reduce cellular damage and photo-inhibition (Sigee 2005).

Figure 1.3: A 90 acre microalgae farm owned by Cyanotech on the coast of Hawaii (Capelli and Cysewski 2007).

An example of this protective effect in nature can be found in Snow algae (*Chlamydomonas Nivalis*), where in once the snow melts the algae cells are exposed to sunlight, which results in the algae producing astaxanthin as a protective agent. This is observed as a red coloured snow which can be found usually in open exposures on the

snow (Graham and Wilcox 2000). The commercial production of astaxanthin exploits this defensive mechanism for manufacturing purposes whereby cultures of algae are grown and then submitted to high levels of irradiation and once astaxanthin has been accumulated within the cell then the algae is harvested and the pigment is extracted from the cell and purified (Dore and Cysewski 2003).

1.4.1.1 Seaweed sources

The seaweeds are a group of algae but unlike simpler algae the seaweeds are autotrophic and multicellular in nature. They are similar in appearance to terrestrial plants and exhibit stems, roots and leaf analogues. Worldwide about 8 million tonnes of wet seaweed is harvested annually and recently its nutritional benefits have gained worldwide interest, due to the presence of proteins, vitamins, minerals and carbohydrates (Banerjee et al. 2009). Astaxanthin is also found in various red seaweeds (e.g. *Catenella repens*) and studies have demonstrated the effect of seasonal variations on the biomass of the seaweed along with ecological factors, population structure, water salinity and nutrient availability. Some of these seasonal variations can also effect the production of astaxanthin within the seaweed e.g. high temperature and lack of nutrients etc. (Banerjee et al. 2009). It was found that astaxanthin concentrations varied in India in pre-monsoon, monsoon and post-monsoon conditions with the highest concentration been found in pre-monsoon seaweed samples (which was probably attributed to the higher temperature) and the lowest in monsoon samples (Banerjee et al. 2009). This information can help in developing the conditions in which seaweed produces optimum levels of astaxanthin which can then be applied and used in astaxanthin manufacture.

1.4.1.2 Microalgae Haematococcus pluvialis

The microalgae *Haematococcus pluvialis* is a single celled chlorophyte which is found worldwide. It is noteworthy because it yields the highest concentration of astaxanthin from amongst all the algal sources. Under optimal growth conditions *Haematococcus pluvialis* normally exhibits a green coloration but when it is placed under an environmental stress the chlorophyte enters into a defensive mode hastily producing spores and accumulating astaxanthin. Environmental stresses like strong sunlight, lack of nutrients or dehydration can induce pigment production to form a barrier against the

harmful UV rays (Dore and Cysewski 2003). This stress induced pigment production is shown in figure 1.4 where the cell changes it structure into spore production. These spores can later hatch after dormancy, which can last for a number of years, back into free green swimming cells when reintroduced to an environment which exhibit suitable growth conditions.

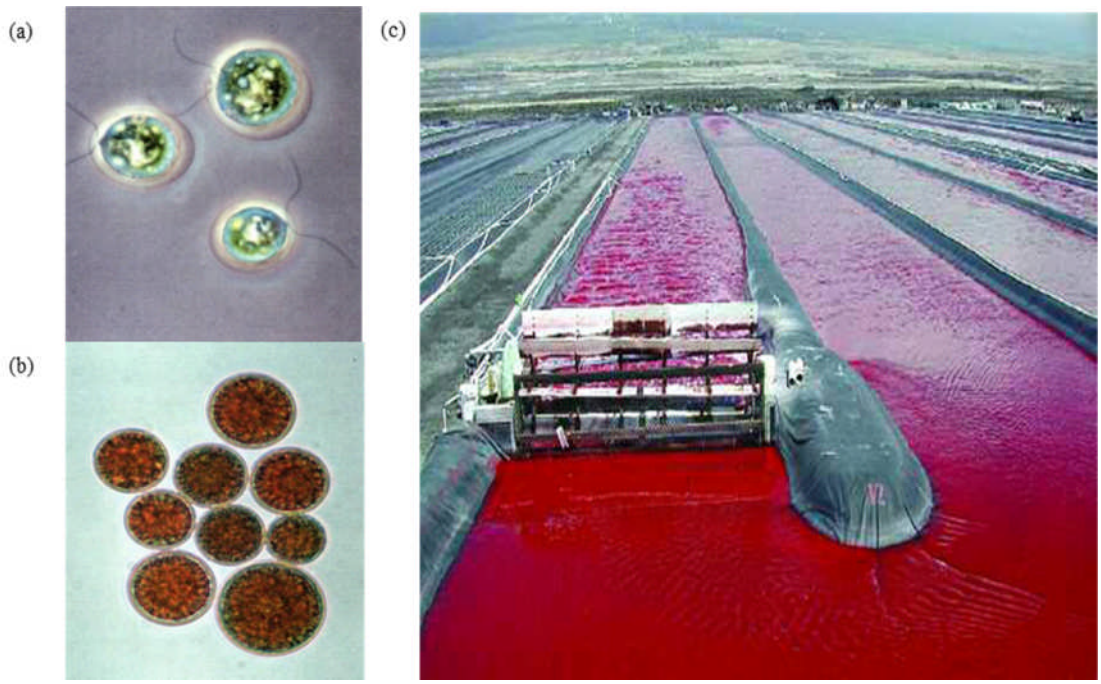

Figure 1.4: (a). *Haematococcus pluvialis* vegetative cell, **(b)**. Haematococcus pluvialis astaxanthin rich spores (Stressed) (**c)**. *Haematococcus pluvialis* algae pond ready for harvest (Capelli and Cysewski 2007).

The cultivation of these algae is a relatively straight forward process although care has to be taken to ensure the avoidance of contamination from wild algae and protozoa which can make their way into the culture medium. Although *Haematococcus pluvialis* algae is a potentially abundant source for natural astaxanthin and in the future it may replace the synthetic form especially in aquaculture feeds, it still suffers from disadvantages associated with its production. Some of these issues include the expensive extraction process, the slow algae growth rates, astaxanthin purity and low yields. Thus when compared to the production of the synthetic form its cost effectiveness suffers (Acton 2013, Dore and Cysewski 2003).

1.4.2 Echinoderms sources

Echinoderms intake various carotenoid precursors through their diet, they feed on the phytodetritus material deposited on the sea bed and play an important role in recycling the nutrients within this material (Gilpin 2006). The phytodetritus has been linked to reproduction and growth seasonal patterns in the benthic biomass. Several marine animals such as echinoderms accumulate the carotenoids within their integuments assisting in camouflage, protection and signalling (e.g. colour during breeding) (Maoka 2011). Research has shown that the carotenoid content of echinoids from different sampling sites is larger than that of holothurians (sea cucumbers), this can be due to the difference in diet intake as holothurians feed lower in the sediment rather than the phyto detrital layer (Wigham et al. 2008). Also numerous starfish species were also found to primarily contain the carotenoids astaxanthin, 7,8,7',8'-didehydroastaxanthin and 7,8-didehydroastaxanthin (Maoka 2011).

1.4.3 Crustacean sources

The crustaceans are part of the arthropods phylum and all the species of this phylum have an exoskeleton made up of protein, carotenoids and chitin. With over 40,000 individual species the malacostraca are the largest of the six crustacean classes (Bernie and Wislon 2001). Many species within the class are highly coloured due to the presence of various proteins bound to the carotenoid molecules within the exoskeleton. Indeed the actual amount of rare and unusual carotenoids within some of these species can result in them acting as a viable source of carotenoids for commercial usage once freed from the shell (Khanafari et al. 2007, Sachindra et al. 2005). Numerous astaxanthin extraction methods have been developed which can vary from a straight forward microbial digestion to numerous complex wet chemical extraction methods. Indeed both types of extraction procedure have been applied to the recovery of astaxanthin from Persian Gulf shrimp waste (*Penaeus Semisulcatus*) (Khanafari et al. 2007). Various studies have focused on optimising the extraction conditions by varying the choice of extraction solvents and extraction conditions (Khanafari et al. 2007, Sachindra et al. 2005, Vilasoa-Martínez et al. 2008). The major pigments found in this

species of shrimp were found to be dominantly astaxanthin and its esters. Astaxanthin recovery from waste shrimp shell has also been performed using microbial extraction methods with even greater effectiveness when compared to solvent extraction techniques (Khanafari et al. 2007). In a study on a marine crab (*Charybdis cruciata*) astaxanthin and its esters were also found to be predominant at concentrations of 65.5 g/100g of the total carotenoids extracted (Sachindra et al. 2005). The same results were found when testing the Snow Crab (*Chionoecetes Opilio*) shell from the North Atlantic as astaxanthin was the primary carotenoid along with smaller concentration of its esters (Vilasoa-Martínez et al. 2008).

1.4.4 Astaxanthin extraction techniques

Irrespective of the source material removing the astaxanthin from its bound matrix is intrinsically important commercially and the choice of purification strategy is an essential step in the recovery of a usable astaxanthin source. There are a number of astaxanthin extraction methods available, these include various acid treatments, organic solvent extraction and microbial extraction. Finding a suitable solvent system for an extraction is of key commercial importance. Like most carotenoids the backbone of astaxanthin is hydrophobic in nature but unlike most other carotenoids both of the cyclohexane ends (heaxatomic) of the molecule possess hydrophilic functional groups. This solubility character duality confers some unusual characteristics upon the molecule compared to other carotenoids and consequently astaxanthin exhibits an ability to solubilise in both aqueous (polar) and non-aqueous (non-polar) systems alike (Yuan et al. 2008).

One of the most popular solvents used in astaxanthin extraction is acetone primarily due to its higher solubility in the organic solvents (Yuan et al. 2008). Various extractions have been employed together for optimisation and production of the largest astaxanthin yield, e.g. Elumalai et al. (2014) employed a mixture of organic solvent extraction, acid treatments and dimethyl sulfoxide (DMSO) in the extraction of astaxanthin from *Haemotococcus pluvialis*. Khanafari et al. (2007) compared both chemical and microbial extraction of astaxanthin from shrimp (*Penaeus semisulcatus*) waste. In wet

chemical extractions both hexane and DMSO were used in combination whereas in the microbial extraction *Lactobacillus sp.* culture was used for fermentation and the collected culture was then subjected to chemical extraction using a 3:1 ratio of hexane to acetone. The results showed the microbial extraction proved to be more effective than the chemical extraction yielding 23 mg more astaxanthin per gram of starting material (Khanafari et al. 2007). Chunhua et al. (2013) employed an additional acid wash step in the organic solvent extraction from *Phaffia rhodozyma*. This step was employed to eliminate the cell wall and membrane to improve the efficiency of the solvent extraction increasing the astaxanthin yield by threefold. The use of different organic solvents has also been examined to determine the best ratio of polar and non-polar extracting solvent, which were found to be acetone and hexane respectively (Sachindra et al. 2006). A binary mixture of both a polar and non-polar solvent was found to be most effective as it resulted in a 60% increase in yield when compared to the use of a single solvent. Given the nature of the raw material to be utilised in the initial stages of this work the astaxanthin extraction from brown crab (*Cancer pagurus*) shell, starfish (*Asterias rubens*) and algae may prove difficult due to the presence of matrix effects and an acid washing step to free the astaxanthin may be added as an extra step to help improve the recoverable yields.

1.5 Astaxanthin chemical structure

The molecular formula for astaxanthin is $C_{40}H_{52}O_4$ and the molecule consists if two carbon hexagon cages connected by an alternating series of nine carbon- carbon single and double bonds. The IUPAC name for astaxanthin is (3S,3'S)-3,3'dihydroxy-β, β-carotene-4, 4'-dione) and it consists of a long hydrocarbon chain terminated in two cyclohexane rings, both of which contain hydroxyl (OH) and carbonyl functional groups (C=O). These presences of these two groups with their electronegative oxygen atoms give astaxanthin its unique functional abilities. A few of these abilities include bonding to muscle tissue, antioxidant activity and colouration (Naguib 2000). These functions have been the object of interest in an increasing number of studies as they have been found to help in the treatment and prevention of certain ailments such as cancer (Khanafari et al. 2007.

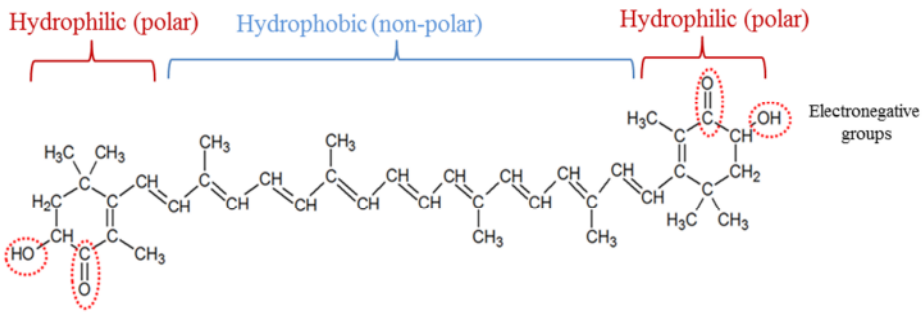

Figure 1.5: The Structure of Astaxanthin ($C_{40}H_{52}O_4$) showing the Hydroxyl "OH" ,Carbonyl group "O" groups and the non-polar / polar functionalities (molecular structure of astaxanthin generated using Chemsketch software.

The structure of astaxanthin is similar to lycopene except that it is cyclized at both ends. The alternating double bonds along the backbone of the molecule form a polyene chain which gives this and other similar like molecules their unique properties. The alternating sequence of single and double bonds allow for the possibility of a number of geometrical isomers to exist, with the number of possible steric forms exceeding over a thousand possible structures. However this number is greatly reduced when steric hindrance is taken into account (Britton et al 1996). In nature most carotenoids exist in the all trans configuration and in this regard astaxanthin is no exception. Exposure to light is known to isomerise parent carotenoid molecules, which can affect the shape of the molecule with the trans form being structurally more rigid. This change in confirmation can affect the solubility and absorbability of the molecule. The trans forms of the carotenoids also tend to crystalize or aggregate more easily and thus are less easily absorbed.

The end groups and the degree of oxygenation of these groups also effect the carotenoid properties. Most carotenoids are hydrophilic and are only soluble in organic non polar solvents (Yuan et al. 2008). Astaxanthin however is an exception and it possess the ability to solubilise itself in both polar and non-polar solvents. The presence of the conjugated double bond system with its associated delocalised π electrons provide carotenoid molecules like astaxanthin their unique electrochemical properties. These highly delocalised electrons only require a small amount of energy to promote them into an excited state. As a result visible light is sufficiently energetic enough to bring about an electronic transition with the molecule. Carotenoids like astaxanthin are susceptible

to oxidative dehydration during storage and processing and as such care has been taken when handling to prevent photobleaching and oxidative damage (Miao et al. 2013, Ahmed et al. 2015).

1.6. Transition metal complexes

Within the transition metals series, the d-block contains a number of elements which are of interest due to their presence in numerous biological systems. A prime example is the metal cobalt which is an essential constituent of the vitamin B_{12} which functions as a catalyst in numerous biochemical reactions (Mahaffy et al. 2014). The inherent properties of these metals which make them uniquely suitable for these types of biochemical applications are governed by their loosely bound d-electrons. Depending on the electron configuration of the *3d* and *4s* sub-shells these transition metals are able to exhibit various oxidation states and this affords them the opportunity to form many ionic or partially ionic compounds. Chromium and copper differ from the other transition metals by possessing only one electron in their respective *4s* orbitals. Various coordination complexes can be formed in solution between metal salts and halides with neutral molecules.

The type of complexes formed and their stability to spontaneous decomposition is dependant not only on the metal ion but also on the type and number of ligands attached to it. Ligands are molecules or ions possessing at least one electron pair which can be donated. There are two main classes; classical and non-classical. Classical ligands act as an electron pair donor and forms complexes with metal ions and all types of Lewis acids. Non-classical ligands are formed with transition metal atoms through π-bonding, π-ligands include aromatic hydrocarbons, cyanide, carbon monoxide and unsaturated hydrocarbons. Transition metals possess *d* orbitals with can be used in bonding, the ligand possess both donor and acceptor orbitals. The coordination of a ligand can further subdivide it into a monodentate (A single atom donor) and Multidentate (several donor atoms) (Mahaffy et al. 2014, Cotton and Wilkinson 1988).

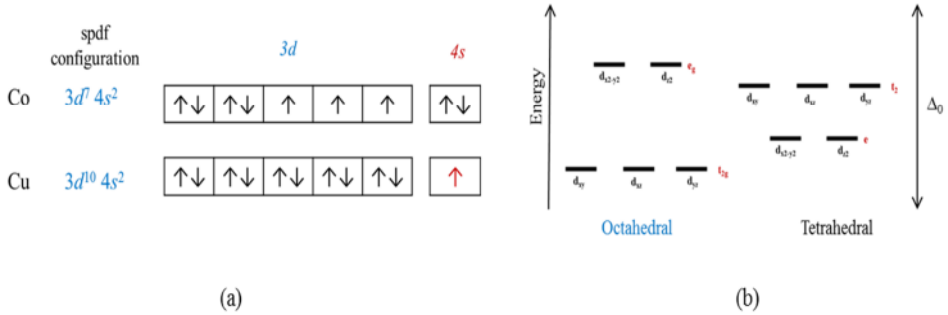

Figure 1.6: (a) Electron configuration of two of the transitional metals; Cobalt (Co) and Copper (Cu), demonstrating the difference in the 4s sub shell, (b) splitting of the 'd' degenerate orbitals in an octahedral and tetrahedral fields.

In transition metals with a perfectly octahedral coordination the five d orbitals are split into three subset orbitals of d_{xy}, d_{yx} and d_{zx}. These three are the basis of the t_{2g} and two orbital subsets named d_{z2} and d_{x2-y2}arethe basis to the e_g orbital. The orbitals of t_{2g} are non-bonding and hence occupy a lower energy level than that of the e_g anti-bonding orbital (Leipoldt and Coppens 1973). In tetrahedral complexes there are also two levels e and t_2, the lower level e is doubly degenerate and the upper level t_2 is triply degenerate, demonstrated in figure 1.6 (b). The energy between the two levels is referred to as Δ_o, this is governed by the nature of the metal ion and ligand, the oxidation state of the metal (Janes and Moore 2004). Electron-electron repulsion is an added consideration in systems containing more than one *d* electron. An example with iron is the addition of six *d* electrons, if the electron to electron repulsion is greater than 10 Dq then the electrons will enter the orbitals in accordance with Hund's rule resulting in a high spin ^5T_2g ($t_{2g}^4 e_{g2}$) ground state, whereas if the repulsion is lower the electrons will pair up in the t_{2g} orbitals resulting in a low spin $^1A_{1g}$ (t_{2g}^6) ground state, this is demonstrated in figure 1.7 (Gütlich and Goodwin 2004).

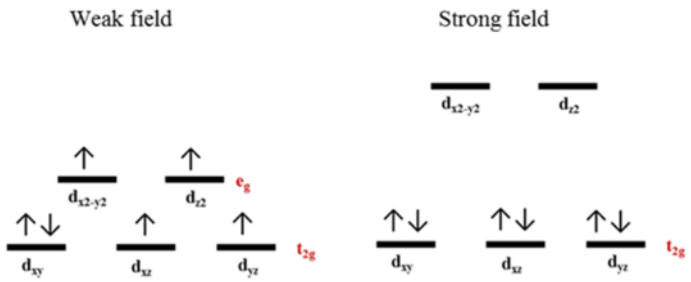

Figure 1.7: Electron configuration of six d electrons of a possible Iron complex in a weak and strong field

In ligand metal complexes back bonding interactions are of a particular importance to ligands with unfilled π* orbitals, these are ideal for secondary $n_M \rightarrow \pi_L^*$ interactions with filled metal *d* orbitals. In these cases the ligand acts as both a strong π- acceptor (acid) and a σ- donor (base) (Weinhold and Landis 2005). An example of back boning is demonstrated in figure 1.8 (b), the metal form a complex with the ligand through π-back bonding of the metal ion to the CO group. Two modes of π-back bonding and two types of π-acceptor ligands are available; longitudinal acceptor e.g. carbon monoxide and perpendicular acceptor e.g. alkynes (Hegedus 1999).

Studies have shown a stabilisation effect on the transition metal in complexes, e.g. copper (I) protection with novel oligotriazole ligands, cyclic voltammetry confirmed the tight attachment of the ligand to copper (I) and stabilising the oxidation state of the transition metal (Chan et al. 2004).

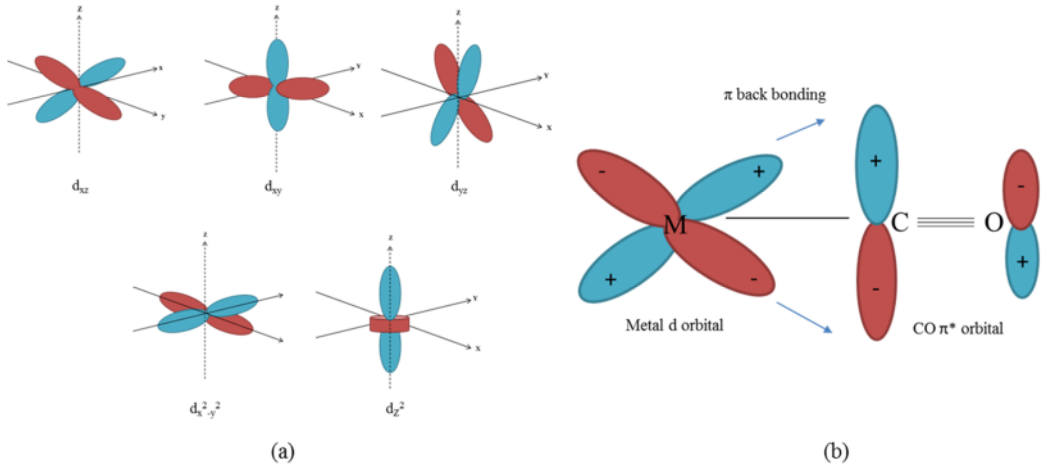

Figure 1.8: (a) d atomic orbitals d_{xz}, d_{zy}, d_{yz}, $d_{x^2-y^2}$ and d_{z^2}, (b) back bonding of metals and ligand (CO) through π bonding.

The metal ion in a complex is under the influence of the electric field from the surrounding ligand which causes changes in the nature of the metal ion and vice versa. For examples if a transition metal ion is placed in a solution with a surrounding negatively charged ligand then an increase in the energy of the five d orbitals will follow due to the repulsion between the metal ions electron density and the negatively changed ligand field (Sathyanarayana 2001). The electronic field can have an effect on the bonding of the ligand and metal complexes either by attraction or repulsion of the two different fields.

1.6.1 Astaxanthin-metal chelates

Interactions of carotenoids with other systems, either atoms or molecules can occur and result in alterations to the bioavailability and/or bio-effectiveness of the astaxanthin. Interactions with proteins are of particular importance in nature, this allows the hydrophobic carotenoids to exist, function and be transported in an aqueous environment. An added feature can be the modification of the carotenoids light absorption and in turn its colour and photochemistry. Examples of these proteins bonding can occur in plants where a chlorophyll-carotenoid-protein complex is used during photosynthesis and astaxanthin binding to the muscle protein in salmon (Britton et al. 2008). Astaxanthin possess two adjacent oxygen atoms in the form of a keto group and hydroxyl group on the cyclohexane rings. These oxygen atoms permit the formation of complexes with the metal ions. The cyclohexane ring structure is similar to that of many hydroxyl quinones and α-hyrdoxy- ketones, these have high biological activity including the capability to form chelate complexes with metal ions (Polyakov et al. 2010). This ability has been proven to be beneficial in some studies, e.g. Astaxanthin protecting porcine lens from oxidative damage by calcium ion-activate protease (Calpain), the astaxanthin interacts with calcium ions thus blocking the activation of the protease calpain (Wu et al. 2006). This chelating ability can modify the physicochemical properties of astaxanthin and can be examined using a wide range of techniques; these include infra-red spectroscopy, nuclear magnetic resonance (NMR) and cyclic voltammetry.

Hernández-Marin et al (2012) studied the interaction of astaxanthin and a number of metals e.g. Ca^{2+}, Pb^{2+}, Zn^{2+}, Cd^{2+} and Hg^{2+} etc. These interactions were coordinated through two oxygen atoms and their presence was crucial for the formation of the astaxanthin-metal complexes. These complexes resulted in a bathochromic (red) shift. The electron acceptor and donor capacity of astaxanthin effect the electron transfer capacity and this in turn alters its free radical scavenging ability. A number of possible configurations of metal chelate complexes are shown below in figure 1.9 with a cobalt salt. These complexes can also play an essential role in the photoprotective action of astaxanthin and they have been shown to broaden the absorption spectra which can provide additional lights absorption in the visible region (Polyakov et al 2010).

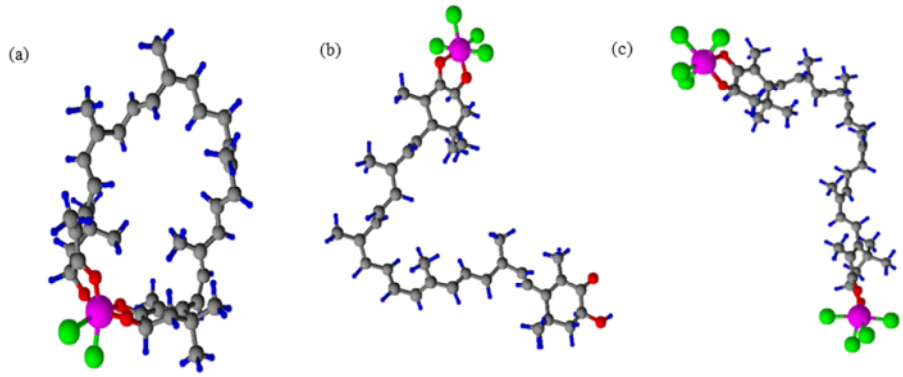

Figure 1.9: Possible structure of astaxanthin metal complexes with cobalt generated using Chemsketch software, **a.** 1:1 ratio in which the astaxanthin chain coils up and the two cyclohexane rings are linked together with a $[ASTA\text{-}CoCl_2]^{2+}$ molecule, **b.** 1:1 ratio of astaxanthin to $[ASTA\text{-}CoCl_4]^{2+}$ through an attachment to the oxygen atoms in the cyclohexane ring on one end of the chain and **c.** 1:2 ratio of astaxanthin to $[ASTA\text{-}2CoCl_4]^{2+}$ through an attachment to the oxygen atoms in the cyclohexane ring at each end of the chain.

The stoichiometry of complexes formed in figure 1.9 represent a number of possible complexes but their actual existence can be confirmed through using a variety of methods, e.g. Job's continuous variation method, Mole ratio method and the Slope ratio method. Job's method involves the preparation of solutions of the metal cations and ligand, both with identical concentrations. The technique involves mixing the two solutions together while keeping the total molarity constant, thus the relative concentration of the metal and ligand are varied. The absorbance of the solution is recorded and is plotted versus the mole ratio (Trimm and Hunter 2011).The slope ratio method differs in that one of the solutions concentrations is held constant while the concentration of the second is varied, a break in the slope of the curve corresponds to the mole ratio of ligand to mole of metal cation (Dash 2011).

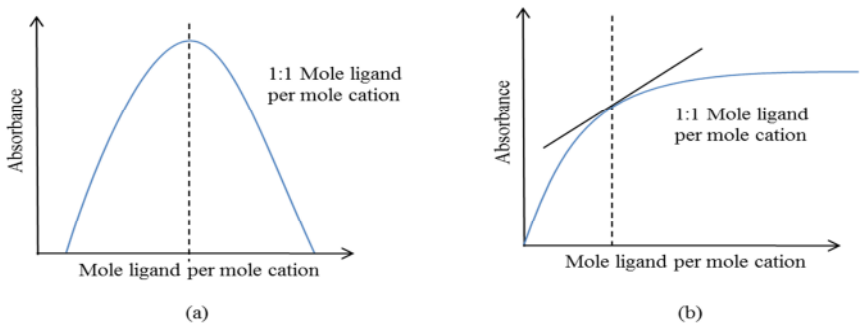

Figure 1.10: Plots investigating the stoichiometry of the astaxanthin chelate complexes using (a) Job's continuous variation method and (b) the Slope ratio method.

Astaxanthin metal chelate complexes have been previously examined using Hydrogen Nuclear Magnetic Resonance (H-NMR). H-NMR spectra of astaxanthin and metal ions (Ca^{2+} and Zn^{2+}) complexes in ethanol revealed a large chemical shift of the 3-CH proton nearest to the hydroxyl (OH) group, a small shift in the 2-CH and 5-CH_3 protons in the cyclohexane ring. Optical studies of astaxanthin in the presence of a metal salts ($Fe(ClO_4)_2$) revealed a large shift in the maximum absorption spectra from 480 nm to 492 nm, this was similarly found with Ca and Zn complexes. The solvent chosen also proved to have an effect on the complexes as the use of acetonitrile decreased the stability of astaxanthin when compared to the use of ethanol. The positively charged metal ion electron withdrawing effect in the complexes decreases the electron density of the cyclohexane ring. The capability of astaxanthin to from metal chelate complexes can prove beneficial in the case of excess metal ions, e.g. Ca^{2+}, Fe^{2+} and Zn^{2+}. These metal ions can prove harmful and have a negative health effect, e.g. Fe^{2+} producing OH radicals (Polyakov et al. 2010).

1.7 Electronic Spectroscopy

1.7.1 Absorption spectroscopy

An obvious characteristic of most carotenoids is the inherent range of colours associated with this class of molecule. Consequently the use of electronic spectroscopy provides a convenient means to probe the underlying electronics of these molecules. Absorption spectroscopy involves electronic transitions from the ground state (low lying state) to an excited state. Electron transitions involve promoting an electron from a low energy orbital to a higher energy orbital or vice versa. The excitation from the ground state occurs through the promotion of an electron from the highest occupied molecular orbital (HOMO) to the lowest unoccupied molecular orbital (LUMO), this transition is subject to selection rules which are determined by symmetry considerations. The absorption of light by carotenoid molecules occurs in the visible region of the electromagnetic spectrum, e.g. astaxanthin, β-carotene and violaxanthin. Absorption of these long chain polyenes in the visible region also accounts for their ability to act as an absorption centre or chromophore in diverse photosynthetic systems. The absorption of yellow, orange and red pigmented carotenoids occur between 400 to 550 nm. These shifts in

the absorption spectra of carotenoids can occur after binding to other molecules and they are the basis of biological coloration, e.g. astaxanthin in the carapace of a lobster (Britton et al. 2008).

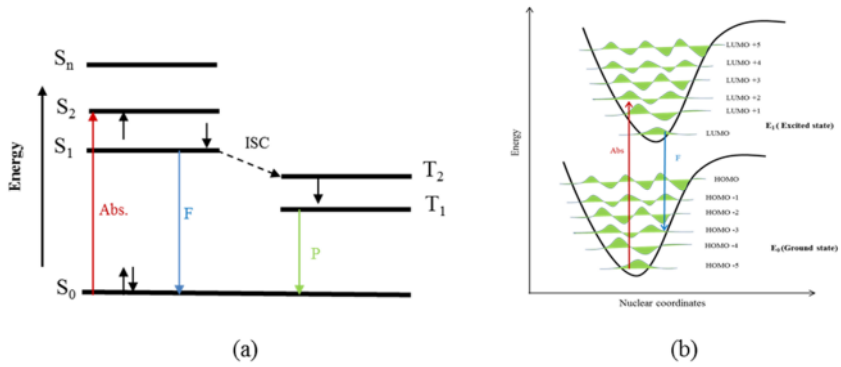

Figure 1.11: (a) Jablonski diagram demonstrating the transitions between the electronic states with intersystem crossing, abs is absorption, F is fluorescence and P is phosphorescence (b) Frank-Codon energy principle diagram demonstrating the change in the vibrational level.

Molecular aggregates have the ability to bridge the gap between the physics of single molecules and structurally ordered crystals. In biological systems molecular self-assembly is highly precise self-directed process and fundamentally important in living organisms for correct functioning (Britton et al. 2008). In 1936 molecular aggregation was first examined by Jelley, E.E., in a study examining dyes. A bathochromic (red) shift was observed upon supramolecular self-organization (aggregation) (Jelley 1936). This red shift to a higher wavelength according to the molecular excitation model is an indication of a loose type association (J- or head to tail), while a hypsochromic (blue) shift of absorption spectral band to a lower wavelength demonstrates a tight association called H-type or card- pack aggregate. These shifts can help gain a better understanding of the conjugation undergone by astaxanthin during complexation with metals centres (Simonyi et al. 2003, Yadav 2005).

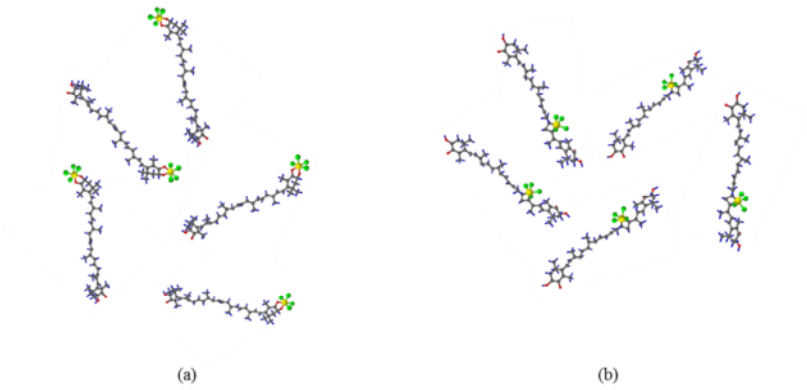

Figure 1.12: (a) J-type aggregate with a head to tail orientation, (b) H-type aggregate involving a face to face arrangement (i.e. parallel)

Absorption bands are designated by the electronic transition type but more than one band may be produced due to the same type of electronic transition thus letters were designated to distinguish between them. There are four bands; K-band (Conjugate) originating from π (bonding orbital) to π*(anti-bonding orbital) transitions in a conjugated system compound (π-π), R-band (radical-like) produced by a single chromophoric group transition from n→π*, B-Bands (Benzenoid) brought about by transitions from π → π* in aromatic or heteroaromatic compounds and E-bands (Ethylenic) originating from ethylenic bonds transition from π → π* in aromatic ring. E-bands are also a characteristic of aromatic and heteroaromatic compounds (Yadav 2005).

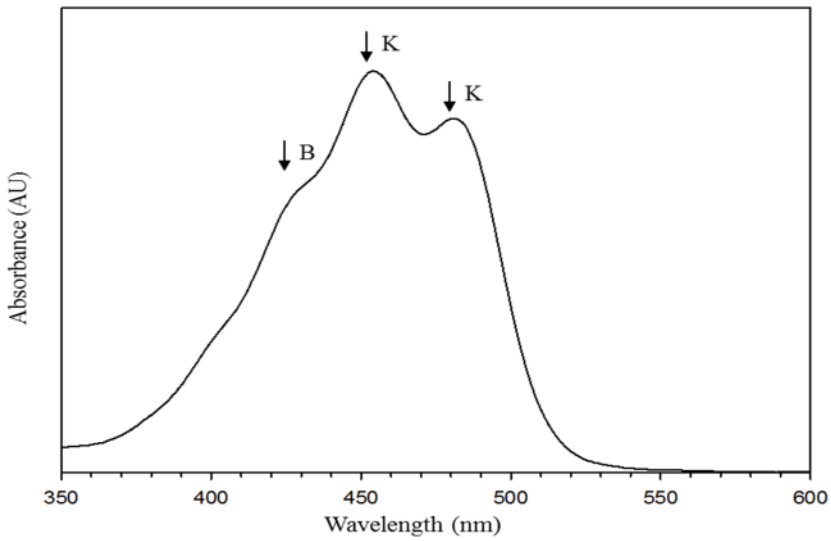

Figure 1.13: Absorbance spectra of β-carotene with the corresponding to their electronic transition bands

Carotenoids are limited by their solubility as they are highly hydrophobic, the majority are lipophilic molecules. Thus majority of studies are carried out using organic solvents or mixtures, e.g. water and ethanol. The solvent chosen can have an effect on the absorption of astaxanthin (Yuan et al. (2012) examined the absorbance spectrum of astaxanthin in methanol and observed four peaks with a maximum absorption at 478 nm, this K-band absorption was attributed to the transition of the large conjugated molecule from $\pi \rightarrow \pi^*$ orbital. The other two K-band absorptions at 203 and 250 nm were produced by the transitions of the C=C and C=O conjugated system from $\pi \rightarrow \pi^*$ in the hexatomic ring and absorption of the hexatomic ring on a whole respectively. The fourth R-band absorption at 295 nm was generated of the carbonyl group transition from $n \rightarrow \pi^*$ and is the carbonyl compound characteristic peak (Yadav 2005). A number of factors influence the maximum absorption of astaxanthin in an aqueous solvent; these include the acidity, the mediums refractive index and salt concentration. An investigation of the effect of added salts with both hard and salt anions on an aqueous ethanolic dispersion of astaxanthin yielded a hypsochromic shift giving a band at around 400 nm (yellow colour) along with the ratio of the absorbance at 407 and 475 nm being more pronounced (Britton et al. 2008).

Structurally different aggregates of different stabilities of astaxanthin may be formed simply through changing either the temperature or the solvent shell. In a mixture of water and acetone astaxanthin forms H-aggregates and these rearrange to J-aggregates with an increase in acetone concentration. When astaxanthin is placed in a 10% acetone and 90% water solvent mixture the maximum absorption occurs at a wavelength of 478 nm and once the acetone concentration is increased to 40% the absorption peak changes into a double peak at 520 and 562 nm. This behaviour demonstrates clearly that the orientation of the hydroxy group is crucial in determining the particular aggregate type and presence of this group is helpful in aggregate formation. Assumption of different free energies of the H- and J- aggregates and the monomers explains the temperature dependence of the formation of aggregate mixtures (Britton et al. 2008). In UV-Visible spectroscopic studies on complexes formed with metals, the maximum absorption band of astaxanthin showed a bathochromic shift towards the red portion of the spectrum. Astaxanthin metal chelates complexes formed with iron (Fe), calcium (Ca) and Zinc (Zn) also demonstrated a bathochromic shift from 480 nm to 492 nm and the

appearance of a new shoulder between 520-600 nm (Polyakov et al 2010). This was also observed by Chen et al. (2007) during studies on the interactions of astaxanthin and calcium complexes. The absorption band at 480 nm shifted to 492 nm possibly suggesting an improvement in the conjugated system of the polyene backbone possibly due to the formation of the metal complex whereas studies with copper ions resulted in a hypsochromic or blue shift from 480 nm to 373 nm in ethanol possibly due to accelerated isomerisation. Absorption spectroscopy can be used to probe the stoichiometry of the astaxanthin and the transition metal complexes and to analyse any band shifts or decreases in oscillator strength thus assisting in the characterisation of the complexes examined in this study.

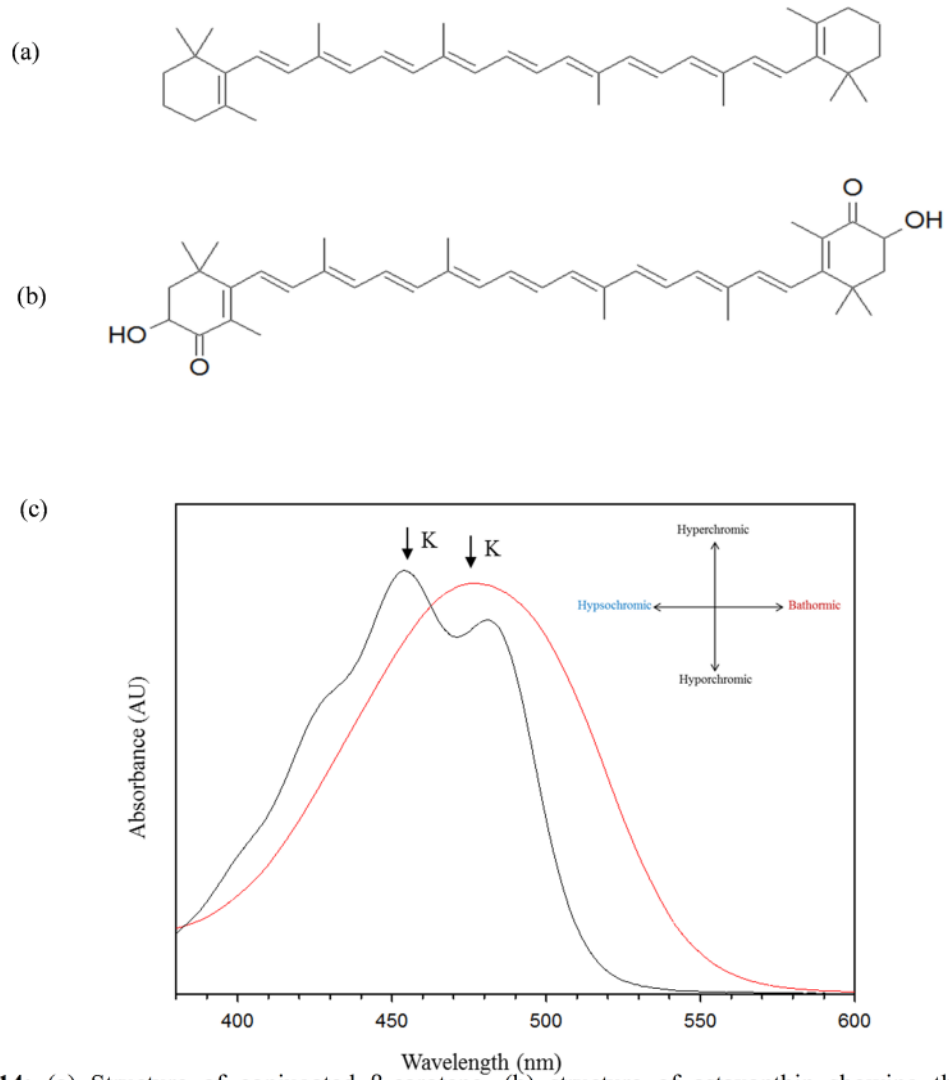

Figure 1.14: (a) Structure of conjugated β-carotene, (b) structure of astaxanthin showing the two functional groups hydroxyl and carbonyl at each end & (c) normalized absorbance spectra of astaxanthin (red) and β- carotene in acetone demonstrating the difference in the maximum K absorption band.

The absorbance spectrum of β-carotene as reported in figure 1.13 reveals the presence of three distinct bands. The first of the transitions, the B- band is a result of the $\pi \rightarrow \pi^*$ transition in aromatic ring at both ends of the molecule. The two K- bands resulted from the large conjugated molecule transition from $\pi \rightarrow \pi^*$ and the transitions of the C=C from $\pi \rightarrow \pi^*$ in the hexatomic ring respectively. β- Carotene and astaxanthin are similar in the polyene chain length (C_{40}) but they differ in the presence of the function al groups hydroxyl and carbonyl functional groups. The presence of these differences alter and shift the absorbance bands but altering the electronic band structure of the molecule.

1.7.2 Fluorescence spectroscopy

Fluorescence spectroscopy is a type of luminescence which involves the emission of light from a substance during its excited state (Lakowicz 1999). Fluorescence emission is accompanied by the electronic transition from LUMO to HOMO (Britton et al, 2008). This technique can be used along with absorption spectroscopy for a better understanding of the character of an excited carotenoid molecule. Fluorescence spectroscopy is inherently sensitive but there are technical difficulties which can prohibit the measurement of molecules fluorescence. These difficulties may be due to small impurities or the inherent low emission from carotenoids and longer polyenes (Valeur and Berberan-Santos 2012). One of the characteristics of emission spectra is that they are Stoke's shifted (difference between position of the maximum absorption band and the maximum emission band) and the emission energies are typically lower than those of the corresponding absorption. Hence emission spectra occur at lower energies and they are independent of the excitation wavelength. They are typically mirror images of absorption spectra and are governed by the Frank-Condon factor. The frank codon principle states that all electronic transitions are vertical, because the electronic transitions occurring mostly without a change in the nuclei position (Lakowicz 1999). The mirror image rule can have exceptions as indicated in figure 1.15, these are due to a different geometric arrangement of the nuclei in an excited state in comparison with the ground state (Lakowicz 1999). Quenching of fluorescence can occur by different mechanisms of which are collisional quenching (contact with another

molecule “quencher” in solution and deactivation of excited-state fluorophore), static quenching (involves the formation of non-fluorescent complexes with quenchers in a grounded state) and a fluorophore attenuation of the incident light (Valeur and Berberan-Santos 2012).

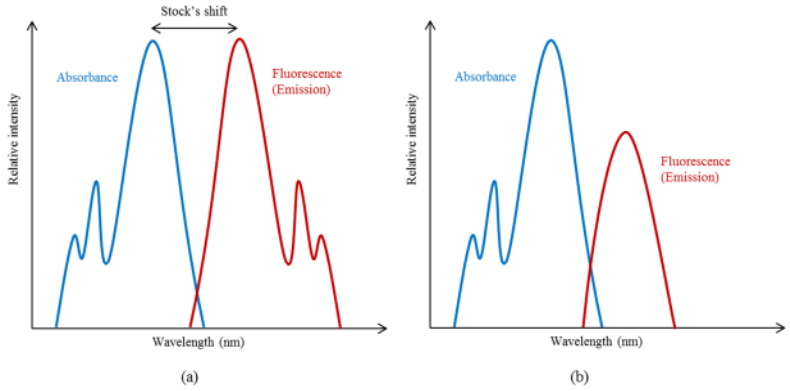

Figure 1.15: Comparison of absorption and fluorescence bands, (a) the mirror image rule applied and (b) exception to the mirror image rule.

Fluorescence bands of carotenoids are often broad and featureless; this can present complications in assigning spectral regions. Gillbro and Cogdell (1989) first demonstrated the fluorescence of carotenoids, a comparison of β-carotene, rhodephin and spheroidene. The results for β-carotene showed an almost identical match between the absorption and excitation spectra, an overlap between the excitation and emission spectra, the emission spectrum is an almost mirror image of absorption along with a small stock’s shift and the fluorescence quantum yield was especially low. The fluorescence of the carotenoid depends on the number of conjugated double bonds rather than its origin from an $S_1 \rightarrow S_0$ or $S_2 \rightarrow S_0$, i.e. chain length. Four all trans-spheroidenes fluorescence spectra containing 7 to 10 conjugated double bonds were compared and it was determined that a systematic crossover occurred from $S_1 \rightarrow S_0$ emission to $S2 \rightarrow S_0$ emission as the π-electron conjugation increased (Britton et al. 2008, Ke 2001).Astaxanthin fluorescence in acetone resulted in a maximum excitation at 350 nm and emission at 570 nm, the emission measurement was found to change to 675 nm intracellularly (*X. dendrorhous*) by Ukibe at el (2008). Fluorescence spectroscopy will assist in understanding the characteristics of the excited state of the astaxanthin metal complex.

1.8 Vibrational spectroscopy

1.8.1 Infra-Red (IR) spectroscopy

The bond between two atom centres can be consider to behave as a spring that oscillates or resonates at particular frequency which is dependent upon the mass of the individual atoms involved in the bond. By changing the mass of one or both of the atoms the frequency at which the two atoms vibrate relative to each other will change. More over these vibrations are characteristics of the type of atom(s) involved in the bond and thus the frequency at which they vibrate can be used as a diagnostic tool to identify the atoms involved in the bond. The amount of energy required to induce a vibration between two atoms is quite small and thus the absorption of energy, as a result of resonance matching between the fundamental harmonic of the bond of to the wavelength of energy from the red region of the spectrum is generally sufficient to induce a vibration. Molecules like astaxanthin contain numerous different bonds which can vibrate in many ways each of which is termed as vibrational mode. For an astaxanthin molecule bond's to be infrared active there needs to be a change in the dipole moment associated with the bond during the vibrate. Infrared spectroscopy is a powerful tool to help identify molecules with in a sample mixture. Smith (2011), Griffiths and De Haseth (2007) have previously used IR spectroscopy for the characterisation of astaxanthin.

The characteristic infrared vibrational modes of astaxanthin are C=O stretching between 1540 cm^{-1} and 1870 cm^{-1}, C=C stretching between 1640 $cm^{-1}$and 1670 cm^{-1}, C-H stretch between 2850 cm^{-1} and 2980 cm^{-1}, OH stretch between 2500 cm^{-1} to 3300 cm^{-1} and ring vibration between 1585 cm^{-1} and 1600 cm^{-1} (sharp) or 1400 cm^{-1} and 1500 cm^{-1} (sharp) (Mahaffy et al. 2014). These assignments were confirmed in the subsequent literature where the C=O stretching mode at 1654 cm^{-1} was confirmed. Additionally the C=C stretching mode in the hexatomic ring was detected at 1552 cm^{-1} and an absorption band at 974 cm^{-1} also indicated the presence of a C-H in C=C conjugate system (Yuan et al 2012). The presence of a methyl group was also confirmed in the aliphatic chain and aromatic rings at 1385 cm^{-1} and bends in the aromatic rings at 572 cm^{-1} and 783 cm^{-1} (Elumalai et al. 2014).Variations were found in the spectra of astaxanthin once placed in an inclusion complex with hydroxypropyl-β-cyclodextrin (HPCD). The mode at 1654

cm^{-1}disappears or shifts to a lower wavenumber indicating the restriction if the C=O stretching vibration following the inclusion complex formation. This was accompanied by a reduction in the band at 1552 cm^{-1} indicating the inclusion of the majority of hexatomic ring in the complex (Yuan et al 2012, Yuan et al 2005).

1.8.2 Raman spectroscopy

Raman is a form of vibrational spectroscopy and is used for the identification of molecular compounds through their inelastic scattering. The raman effect can be described as a change in light frequency of scattered radiation by a monochromatic radiation, which occurs due to an exchange of energy between the photon and the scattering molecule (Frank et al. 1999). Raman scattering involves a series of Raman shifts each corresponding to the characteristic frequencies of the molecules different vibrational modes. These modes correspond to the promotion of an electron from a vibrational energy level in the ground state of the molecule to a virtually excited state induced by the high intensity radiation. Upon relaxation the photo-excited electron returns to either there original vibrational energy or a nearby vibrational energy level wither higher or lower in energy. This provides information on energy spacing in the ground state of the molecule (Landrum 2011). In raman spectroscopy the molecule is irradiated with monochromatic radiation using a laser and the scattered light is measured after passing through a notch filter (Ferraro et al. 2003). There are two types of scattered light, the first is Rayleigh scattering (strong and the same frequency as the incident beam V_o), the other is called raman scattering (very weak and the frequencies $V_o \pm V_m$ [V_m vibrational frequency of molecule]) (Ferraro et al. 2003). Raman scattering is further divided into two types stokes ($V_o - V_m$) and anti-stokes ($V_o + V_m$), stokes raman scattering is the result of the molecule initially in the ground vibrational state whereas anti-stokes scattering is a result of a molecule relaxing back to an energy state lower in energy than the original state and anti-stokes scattering is the relaxation of a molecule back into a higher vibrational energy state (Larkin 2009).

A Raman spectrum of a molecule consists of the combination frequencies and the relative intensities. Raman has been employed in non-invasive detection of carotenoids in living tissue, the energy level structure and optical pumping cycle of a carotenoid

molecule is unique (Landrum 2009). Characteristic Raman bands of carotenoids include C-C and C=C stretching and C-H bending (frequencies) (De Oliveira et al. 2010). The stretching vibration of C=C occurs between 1400- 1600 cm^{-1} and the C-C stretching is between 1100- 1200 cm^{-1} (Withnal et al. 2003). In astaxanthin the C=C and C-C stretching vibrations occur at 1512 cm^{-1} and 1157 cm^{-1} respectively (Kaczor et al. 2011). The C=C stretching bands in carotenoids is reported to be sensitive to the degree of conjugation of the polyene chain. The relationship between the number of conjugated double bonds in the skeletal structure of the polyene chain and the wavenumber of the raman modes can help in providing information on the structure. This can assist in studying the formation of astaxanthin and metal complexes (Sasic 2008). Even though carotenoids are a large family with a diverse number of chemical structures producing extraordinarily similar resonance raman spectra, one of the dissimilarities was found to be the stretching conjugated C=C band as this was found to be dependent on the length of the polyene chain and decreases along with it (Frank et al. 1999). The C=C stretching vibration is a sensitive indicator of the chemical structure of the carotenoid (Kaczor et al. 2011). Aggregates of carotenoids have exhibited a shift in the raman bands, e.g. an astaxanthin J-aggregate shifts the C=C stretching band from 1527 cm^{-1} (monomer) to 1516 cm^{-1} (red shift), whereas the H- aggregates were found to exhibit a lower red shift to 1522 cm^{-1} (Britton et al. 2008). These variations may be a result of either the difference in the geometry of the carotenoid or an alteration in the total molecular force field (Britton et al. 2008).

1.9 Electrochemical analysis

Electrochemistry is a term used to describe the various chemical reactions that are induced by the passage of an electrical current through a system. In electrochemistry the movement or transfer of an electron from one species to another is referred to as an oxidation-reduction reaction or more simply a redox reaction. When a chemical species undergoes oxidation it losses an electron from its outer electron shell. Similarly when a chemical species is reduced it gains an electron into its valence shell. Both of these reactions results in either an increase or decrease to the oxidation state of the element or molecule. In its simplest form an electrochemical cell is a device which utilises this electron transfer between two chemical species to either generate electricity or to drive a

non-spontaneous chemical reaction forward to completion. Electrochemical cells normally comprise of two conductive or semi-conductive electrodes known as the anode where oxidation takes place and the cathode where reduction of the chemical species takes place. The electrodes joined together by an external wire are immersed in a conductive electrolyte. This electrolyte contains ions which can move freely and thus prevent charge build-up on the respective anode and cathodes. These electrochemical cells form the basis for more complex electrochemical techniques like cyclic voltammetry that can be used to characterise various physical chemical systems.

1.9.1 Cyclic Voltammetry

Cyclic voltammetry involves the application of a potential to the working electrode which varies with time. The current flowing between the working electrode and the counter electrode is recorded and plotted as a function of the applied potential. A typical cyclic voltammetry setup consists of an electrochemical cell comprising of three electrodes; a working, reference and counter electrode. These are connected to a potentiostat and are immersed in a liquid containing a supporting electrolyte. The potential difference between the reference and working electrode is controlled by the potentiostat while current flow between the working electrode and the counter electrode is monitored.

The selection of the starting voltage depends on the oxidation and reduction of the analyte. The potential is swept from the start voltage (E_1) to the end voltage (E_2) in a linear manner at which the direction of the scan is reversed back. There are practical considerations when performing cyclic voltammetry, one of which is the selection of the potential range (E1 to E2) across which the scan is measured. It is important to ensure that within this range all the features of the analyte are recorded for analysis; this is determined by comparison with previous literature works and experiment investigation. Another consideration is the choice of electrodes, most common reference electrodes are a silver/silver chloride (Ag/AgCl) or calomel half-cell, a counter electrode which ideally possess a large non-reactive surface area (e.g. platinum wire) and a working electrode commonly used are inlaid disc electrode (e.g. gold, graphite, glassy carbon etc.) (Scholz and Bond 2005, Compton and Banks 2011). Astaxanthin is known for its

powerful antioxidant activity, this can be electrochemically examined using cyclic voltammetry. This is an efficient technique in determining redox potentials and assessing the kinetics of electron transfer within the molecule.

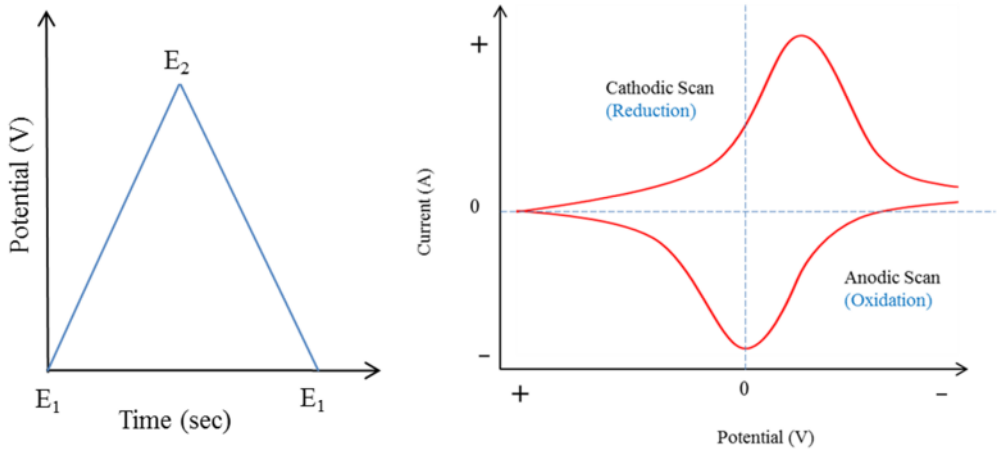

Figure 1.16: (a) A Cyclic voltammetry waveform between the start (E_1) and end (E_2) potential, (b) Cyclic voltammogram demonstrating the cathodic scan and the anodic scan.

Carotenoids possess low oxidation potentials which makes them good electron donors. Changes in the structure of carotenoids can lead to variations in redox potentials, e.g. the electron withdrawing strength depends on the difference in oxidation potentials, an increase in the electron withdrawing strength in turn increases the separation between oxidation waves. Reversible cyclic voltammetry can be difficult with carotenoids, this is due to the formation of less stable radical cations and dications. The type of electrolyte and working electrode influence the reversibility along with moisture and air. In previous electrochemical studies of the carotenoid astaxanthin by Focsan et al. (2014) two peaks appear in each of the anodic and cathodic scan, which reveals a two electron transfer oxidation. In the anodic scan the astaxanthin carotenoid is oxidised and radical cations and dications are formed, these two peaks correspond to the oxidation of neutral carotenoid species and radical cations. In the cathodic scan the radical dications and cations are reduced. Ferrocene was used as a reference for the potentials and the potentials were further standardised to 0.528 V. The normalized oxidation potential of astaxanthin cations, dications and neutral radicals were found to be 0.7678 V, 0.9828 V and 0.0792 V respectively (Britton et al. 2008).

Cyclic voltammetry can also be implemented in measuring the effect of metal chelate complexes on astaxanthin. The stability of the astaxanthin metal chelate compounds have been studied using cyclic voltammetry, e.g. Polyakov et al. (2010) and from their finding it thought that the stability constant of an astaxanthin Ca^{2+} complex decreases by a factor of eight in acetonitrile compared to ethanol. This ascribed to the solvent incorporation into the complex. The presence of the salt $Ca(ClO_4)_2$ lowered the oxidation potential of astaxanthin thus lowering its radical scavenging capability (i.e. antioxidant activity). The metal salt also affects the stability of the astaxanthin radical cations and dications negatively by decreasing it and increasing the neutral radicals' lifetime.

1.10 Conclusion

The xanthophyll astaxanthin possess a wide range of electronic, vibrations and electrochemical characteristics. Its long hydrocarbon chain and functional ketone and hydroxyl groups in the cyclohexane rings at both ends attribute to its increasing popularity. The recent growth in the nutraceutical industry has increased it demand due to its proven powerful antioxidant activity (Shimidzu et al. 1996 and Bagchi 2001). There are numerous sources as previously mentioned including crustaceans, echinoderms and algae, the waste generated by consumption of these organisms can be used as a given possible source, however in this project only crustaceans will be examined. The possibility of this carotenoid reacting with other molecules within the body are high, its structure makes it perfect candidate to perform as a ligand in complexes, e.g. with transition metals. These interactions can incur an effect on its electronic and vibrational characteristics and in turn it's potential. These interactions will be further examined using a wide range of techniques within this project to diagnose the changes on a molecular and electronic level.

Chapter 2
Experimental Methodology

2.0 Introduction

The purpose of this chapter is to detail the various methodologies used during this work. A range of different techniques were utilised ranging from solvent extraction to spectroscopic characterisation. The initial stages of the project involved the isolation and purification of the carotenoid molecule, astaxanthin from brown crab (*Cancer pagurus*). Astaxanthin is then subjected to a number of spectroscopic and electrochemical characterisation techniques. Astaxanthin is one of the most powerful antioxidants (Baghi 2001, Shimidzu et al. 1996), its effectiveness can vary considerably with reactions carried out within the human body following consumption. The structure of astaxanthin nominates it as a suitable ligand candidate promoting complex formation. Within the digestive system are transition metals, these are renowned for their affinity to form metal chelate complexes. The formation of these ligand metal complexes can

incur a negative effect on the radical scavenging activity of the astaxanthin thus negating its intake.

2.1 Chemicals and materials

All chemicals were used as purchased without further purification. The following is a list of the chemicals used throughout the research: acetone (Sigma Aldrich), acetonitrile (Fisher Scientific), ethanol (Sigma Aldrich), methanol (Sigma Aldrich), glacial acetic acid (Sigma Aldrich), diethyl ether (Fisher Scientific), sodium hydroxide (Fisher Scientific), ammonium acetate (BDH, AnalaR), cobalt chloride hexahydrate ($CoCl_2.6H_2O$) (Sigma-Aldrich), copper chloride dihydrate ($CuCl_2.2H_2O$) (Sigma-Aldrich), astaxanthin standard 98.5% (Dr.Ehrenstorfer GmbH, Germany), tetrabutylammonium tetrafluoroborate (TBA TFO, Sigma-Aldrich) and brown crab (*Cancer pagurus*, LYIT).

2.2 Instruments

A wide range of instruments were used throughout this project for preparation purposes, these include: analytical scales (Sartorius AG TE214S, Germany), ultrasonic Cleaner (VWR), Orbital incubator (Stuart S1500, United Kingdom), Concentrator Plus (Eppendorf), Centrifuge 5810 (Eppendorf) Hotbox oven (Gallenhamp, UK), Heating block (TechneDri-block DB-3D, UK), Dessicator (Jencons Hemel Hempstead,England), Heating mantel (BI Barnstead electro thermal, UK), Masterflex console drive 7518-00 (Cole-Parmer Instruments, USA), Osciallting electric fan G12DFAN (GET, UK), AstecMonair recirculating fume cabinet (AGB scientific ltd., Ireland) and Chemflow CSC fume hood (Chemical systems control ltd., Ireland).

2.3 Astaxanthin solvent extraction

2.3.1 Brown Crab (*Cancer pagurus*) Shell

The method used for the extraction of astaxanthin from the crab shell was adapted from a method by Sachindra et al. (2006). The solvent extraction was performed using glacial acetic acid (100%) in a fume hood. The brown crab shell was weighed out and

glacial acetic acid was added at a ratio of 2.5ml to 1g. The extraction was allowed to take place over 24 hrs in an orbital incubator (200 RPM) at room temperature (22°C).

Subsequently the sample was centrifuged at 4000 RPM for 3 mins to separate the pigmented glacial acetic. Given the corrosive nature of glacial acetic acid the extract required separation into a second non-corrosive different solvent, in this case diethyl ether was chosen for this task. An equal amount of Diethyl ether was added to the coloured glacial acetic acid. Next an equal amount of 5M Sodium Hydroxide was added, this was performed in an ice bath due to the exothermic reaction between the acetic acid and the 5M NaOH as astaxanthin is temperature sensitive (Pacheco et al. 2009). The mixture was then centrifuged at 4000 RPM for 3 mins to help the different layers settle into place as shown in figure 2.1, the colour had transferred into the diethyl ether top layer. The coloured diethyl ether was then collected.

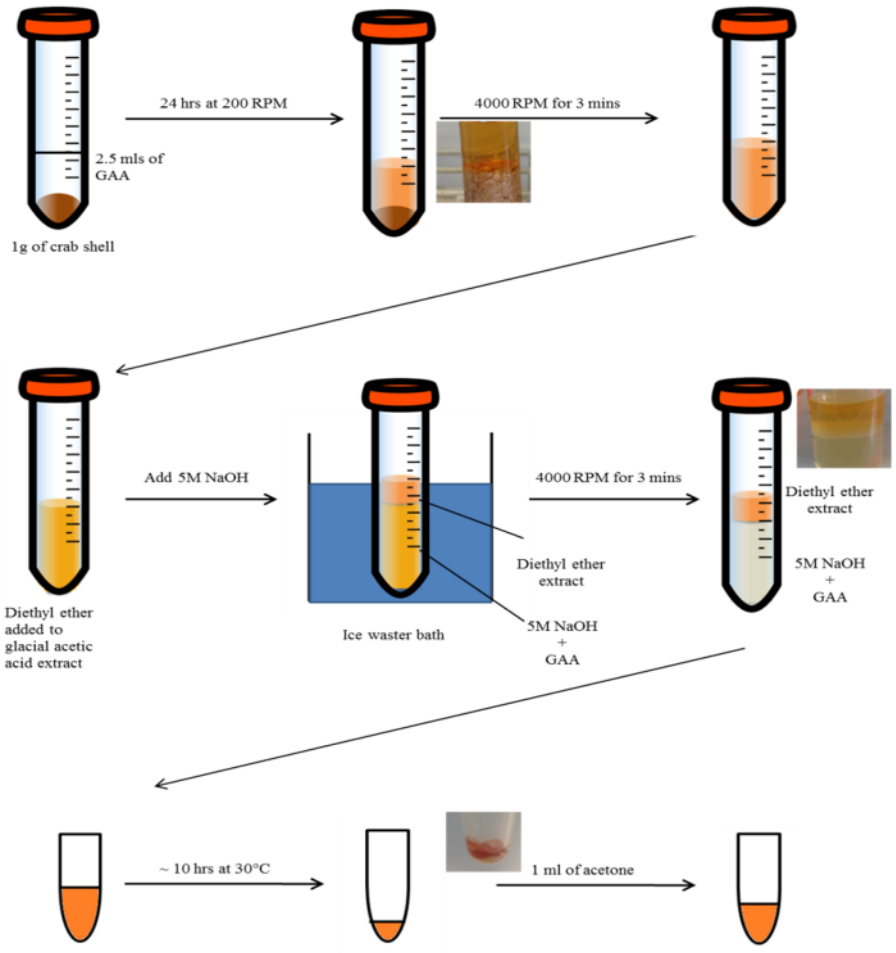

Figure 2.1: A flow diagram outlining the steps involved in the solvent extraction procedure of astaxanthin from brown crab using glacial acetic acid (GAA).

The extract was then transferred into a 1.5 ml micro-centrifuge tube. The extract was concentrated at 30 °C for approximately 10 hrs. A flow diagram representing the different steps is demonstrated in figure 2.1, this includes acid extraction to release the xanthophyll from the crab shell, transfer into diethyl ether and concentration into a dry powder. The concentrated extract was then weighed, suspended in 1 ml of acetone, filtered through a 2 micron filter and sonicated for HPLC detection.

2.4 Astaxanthin detection

2.4.1 High Performance Liquid Chromatography (HPLC)

A HPLC (Shimadzu, Japan) system was used in this project and consisted of a number of components. The system was controlled by a shimadzu SCL-10Avp with parameters of a time program of 0.01- 9999.9 min, analysis of 20 files and a fraction collector of 10 files. Setting files include an auto injector sequence, sample and pre-treatments. A SIL-10ADvp shimadzu auto injector was used to load the sample, this consists of a sample injection system with a range of 1- 500 µl. The pump used to control the mobile phase flow was a shimadzu LC-10ATvp pump with dual piston tandem flow providing consistent solvent delivery from 0.001- 9.9999 ml/min, a flow range of 0.001-5.000 mL/ min A FCV-10ALvp mixing chamber was used with an inbuilt fan preventing overheating of switching valve. A DGU-14A shimadzu degasser was used, this provided a capacity of up to four solvents, this four in-line channel in line degasser maintains a strong vacuum and maintains a dissolved oxygen concentration of <2 ppm at flow rates up to 3 ml min^{-1} and a maximum flow rate of 20 ml min^{-1} per flow line. To control the temperature of the column a CTO-10ACvp shimadzu column oven was used, it is a forced air circulation type oven, temperature control range of -10 – 80 °C and a control precision of ± 0.1 °C. the detector chosen was a shimadzu SPD-M10AV diode array detector, the light source consisted of a deturertium lamp. The wavelength ranged from 190- 800 nm, with an accuracy of ± 1 nm and a reproducibility of ± 0.1 nm. The cell optical path length was 10 mm with a pressure of 4.9 MPa. An XTerra MS C18 column (Waters, Ireland) was used for analysis, the column held a carbon load of 15.5 %, an inner diameter of 4.6 mm, length of 150 mm, a revered phase mode, a

particle size of 5 µm, a pore size of 125Å and a pH range of 1- 12.The detection and quantification of astaxanthin in the extracts was performed using the aforementioned HPLC instrument. The method used was adapted from different methods as follows: two mobile phases were used and prepared; Mobile phase A: 50:50 0.5M Ammonium acetate and Methanol, Mobile Phase B: 20:20:60 Methanol, Acetone and Acetonitrile (Schmid and Stich 1995, Li et al. 2002, Vidussi et al. 1996, de Azevedo-Meleiro and Rodriguez-Amaya 2009). The instrument parameters were set to: a flow rate of 1ml/min, mobile phase A: mobile Phase B (35:65), oven temperature 35°C, detection at 470 nm and run time 20mins. The Astaxanthin standards were prepared in acetone using astaxanthin Standard (98.5%). The standards were filtered, sonicated and run on the instrument, retention times were expected between 9-10 mins. Next the astaxanthin extracts (in 1ml of Acetone) were run on the instrument, retention time and peak area measured.

2.5 Preparation of Ligand metal complexes:

2.5.1 Preparation in solution at room temperature

In order to prepare the complexes Jobs method of continuous variation was employed. This involves the preparation of solutions of the metal cations and ligand, both with identical concentrations (Trimm and Hunter 2011). The two solutions are mixed together varying the concentration of the metal and ligand while holding the total molarity of the mixture constant at 0.04 mM. The metal chloride salts cobalt chloride hexahydrate ($CoCl_2.6H_2O$) and copper chloride dihydrate ($CuCl_2.2H_2O$) were placed in an oven at 100°C overnight to remove moisture. Stock solution of 0.04 mM copper chloride was prepared in ethanol at room temperature and five solutions of varying metal ligand ratios were prepared as per table 2.1.

Table 2.1: Sample preparation of astaxanthin and copper chloride complexes in ethanol

Ratio (ligand: metal)	1:3	2:1	1:1	1:2	3:1
Astaxanthin Concentration (mM)	0.010	0.015	0.020	0.025	0.030
Copper chloride concentration (mM)	0.030	0.025	0.020	0.015	0.010

Initial testing revealed a high difference in absorption between astaxanthin and cobalt chloride, hence the method used for this metal was changed to Benesi-Hildebrandt as used by Polyakovet al (2010). Stock solution of 8 mM Cobalt chloride and 0.04 mM astaxanthin were prepared in ethanol as per table 2.2. This method involved the preparation of solutions with one component increasing awhile the next is held constant across the dilutions.

Table 2.2: Sample preparation of astaxanthin and cobalt chloride complexes in ethanol

Solution no.	1	2	3	4	5
Astaxanthin Concentration (mM)	0.010	0.012	0.016	0.020	0.024
Cobalt chloride concentration (mM)	3				

2.5.2 Reflux of complexes

Following initial testing at room temperature the astaxanthin and metal complexes were refluxed at 37°C and 78°C. Initial refluxes on cobalt chloride and astaxanthin were carried out using the traditional setup as in figure 2.2 (a). This was then later changed due to the large number of samples and time constraints; the set-up is demonstrated in figure 2.2 (b). Polypropylene PP conical centrifuge flasks were used as the reaction vessel, volumetric pipettes (20 ml) used as the condenser, alcohol thermometer for temperature control and the use of a fan as an air condenser.

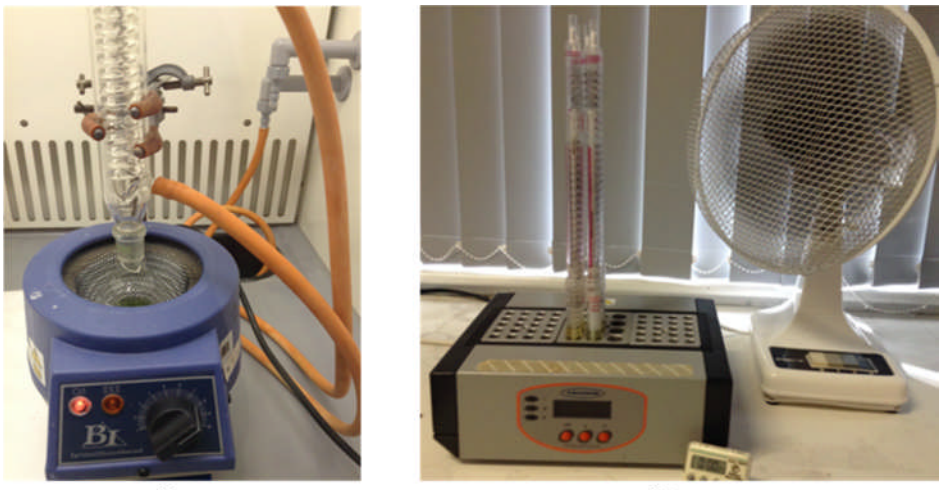

(a) (b)

Figure 2.2: (a) Traditional Reflux set up in a round bottom flask on a heating mantle (Barnstead Electro thermal, U.K.) with a water condenser, (b) reflux set up in Polypropylene PP conical centrifuge flasks (15 ml) using a heating block (Techne, U.K.), volumetric pipette (20 ml), alcohol thermometer and a Fan. The fan acts as an air condenser recycling back the evaporated solvent back into the reaction tube.

2.6 Electronic spectroscopy

2.6.1 UV- Vis spectroscopy

All electronic spectra were recorded using a Shimadzu UV-Vis spectrophotometer UV-2450 (Shimadzu, Japan) double beam instrument with a direct ratio system. The wavelength of the instrument is from 190 – 900 nm, accompanied by a wavelength accuracy of ± 0.3 nm, a repeatability of ± 0.1 nm and a scan rate of about 900 ~ 160nm/min. The available excitation sources include a 50 W halogen lamp and a deuterium lamp, interchangeable at a wavelength between 282-393 nm. This instrument employs a single monochromator with a high-performance blazed holographic grating in aberration corrected Czemy Turner mounting. A detector consisting of a photomultiplier R-928 with a red sensitive spectral range of 185- 900 nm was used.

The absorbance spectra of the complexes were both measured at room temperature and refluxed at 37 °C and 78 °C. The instrument was set to scan a range of between 900 to 200 nm, using a medium scan speed and a 1 nm sample interval with a slit width of 1 nm. Sample absorbencies were recorded using loaded into quartz cuvette (10 mm). Using Jobs method of continuous variation the mole fraction versus the absorbance was plotted and the maximum absorbance point corresponds to the combining ratio of the complex.

Using the Benesi- Hildebrand method a plot of $1/[A_0]$ versus the D_0 /Abs was generated. Where D_0 is the concentration of donor (fixed) and A_0 is the concentration of the acceptor (varied) (Benesi 1949). The shape of the plot determines the ratio of the complex. A straight line plot represents a 1:1 ratio and a two line intersection represents a 2:1 ratio (Polyakov et al. 2010).

2.6.2 Fluorescence spectroscopy

All fluorescence spectra were recorded using a Perkin Elmer flourescence spectrometer (Perkin Elmer LS45, USA) was used, this is a computer controlled luminesce spectrometer with the capability of measuring fluorescence, phosphorescence, chemiluminescence and bioluminescence. The source of the instrument consisted of a

Xenon discharge lamp (equivalent to 20 KW for 8 µs duration) with a pulse width at half height < 10 µs. A gated photomultiplier detector is employed with a modified S5 response for operation up to around 650 nm, the reference electrode consist of a photodiode (operates up to 900 nm). Monochromator included a Monk- gillieson type monochromators covering the different ranges as follow: excitation 200-800 nm (zero order selectable), emission 200-658 nm (standards photomultiplier with zero order selectable) and 200- 900nm (with optional R928 photomultiplier). Synchronous scanning is available with constant wavelength, wavelength accuracy of ± 1.0 nm and reproducibility of ± 0.5 nm. The excitation and emission slits are pre-set to a nominal of 10 nm. A scanning speed in increments of 1 nm can be selected for 10- 150 nm/ min. The sensitivity of the instrument is 500:1 r.m.s. (raman band of water, excitation at 350 nm, excitation and emission bandpass 10 nm).

A Pre scan on the full range was run and from it the maximum excitation and emission scans were recorded. An emission scan was run to measure the fluorescence of the astaxanthin complexes at the maximum excitation wavelength.

2.7 Vibrational spectroscopy

2.7.1 Infrared spectroscopy

All Infrared vibrational spectra were recoded using a Perkin Elmer (Spectrum BX). This instrument can operate in ratio, single, beam or interferogram mode. It possess an optical system that gives data collection over a total range of 7800 to 100 cm^{-1}, with a max OPD resolution of 1 cm^{-1}. It includes a dual level optical module that is sealed and desiccated. The system uses a mid-infrared detector of DTGS (deuterated triglycine sulphate) and uses spectrum software to allow the control and manipulation of data.

The ligand metal complexes were drop cast onto the surface of a sodium chloride (NaCl) window (~500 µl) and allowed to dry at room temperature in the dark. The instrument recorded the percent transmittance across the a wavelength range of 4000-350 cm^{-1}, using an average of 3 scans with a 2 cm^{-1} resolution and a 1 cm^{-1} data interval. A blank NaCl window was used to run a background scan.

2.7.2 Raman spectroscopy

All raman spectra were recorded using a Raman systems R-3000. This features an fully integrated system including an all a diode laser, CCD-array spectrometer, fiber optic probe and operating software. The attached fibre optic probe is flexible class 3b laser with interchangeable accessory caps for different samples. The R-3000 a 500 mW solid state diode laser with a 785 nm excitation wavelength. The instrument allows for collection of multiple spectra across a wavelength range of 200- 2700 cm^{-1}. The laser emerging from the laser output probe is a class 3b laser; this produces visible and invisible laser radiation.

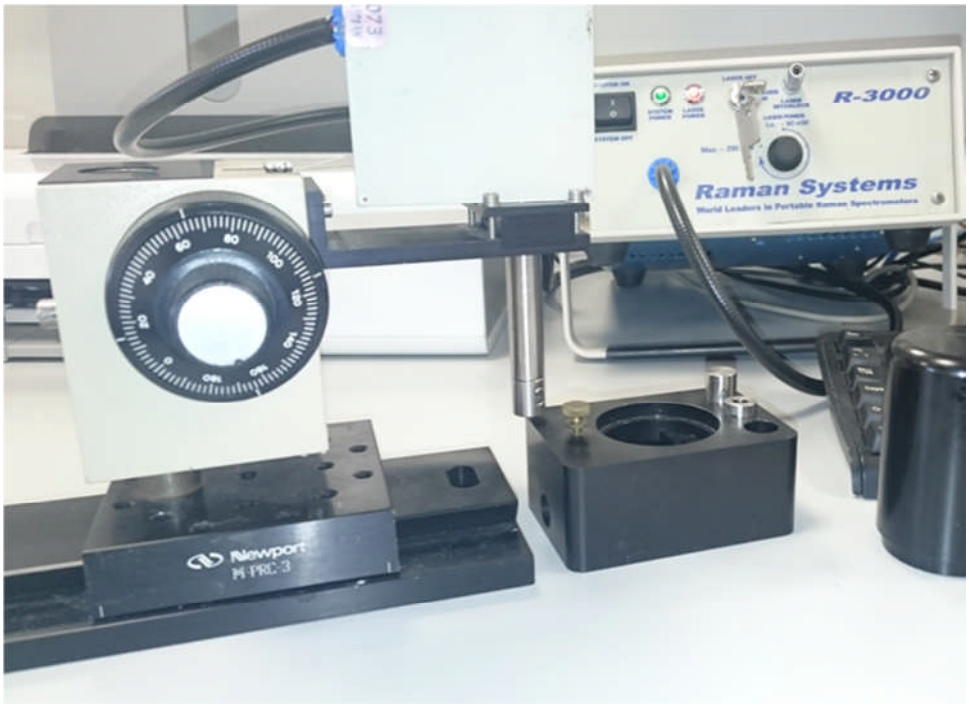

Figure 2.3: Raman system R-3000 setup including the laser mounted onto the holder (allowing repositioning) and the sample mount.

For all raman measurements a quartz supersil window was used. In general 500 µl of the samples complex in acetone was dropped onto the surface and allowed to dry at room temperature in the dark. The laser was pre-set to 90 mW excitation (allowed to warm for 10 mins). All spectra were recorded using an integration time of 90 sec and a frame size of 30 sec.

2.8 Electrochemical analysis

2.8.1 Cyclic Voltammetry

All cyclic voltammetry measurements were performed using an electrochemical analyser 600A (CH instruments, US) and a Picoamp booster and faraday cage (CH instruments, US). The potential control range is ±10 V with a sampling rate of 5 MHz and a scan rate of 20,000 V/s. The current range is ±250 mA, with a low current measurability of 1 pA. The high speed and high resolution data acquisition channels allow a simultaneous sampling of both current and potential at a rate of 1 MHz. The instrument is dynamic and offers a wide range of experimental time scales, with cyclic voltammetry for example a scan rate of up to 1000 V/S with a 0.1 mV potential increment or 5000 V/s with a 1 mV potential increment. It is designed to work with a three electrode cell, ensuring all current flow between the counter and working electrodes while controlling the potential of the working electrode with respect to the reference electrode. Figure 2.4 demonstrating a schematic of the three electrode setup connected to the potentiostat.

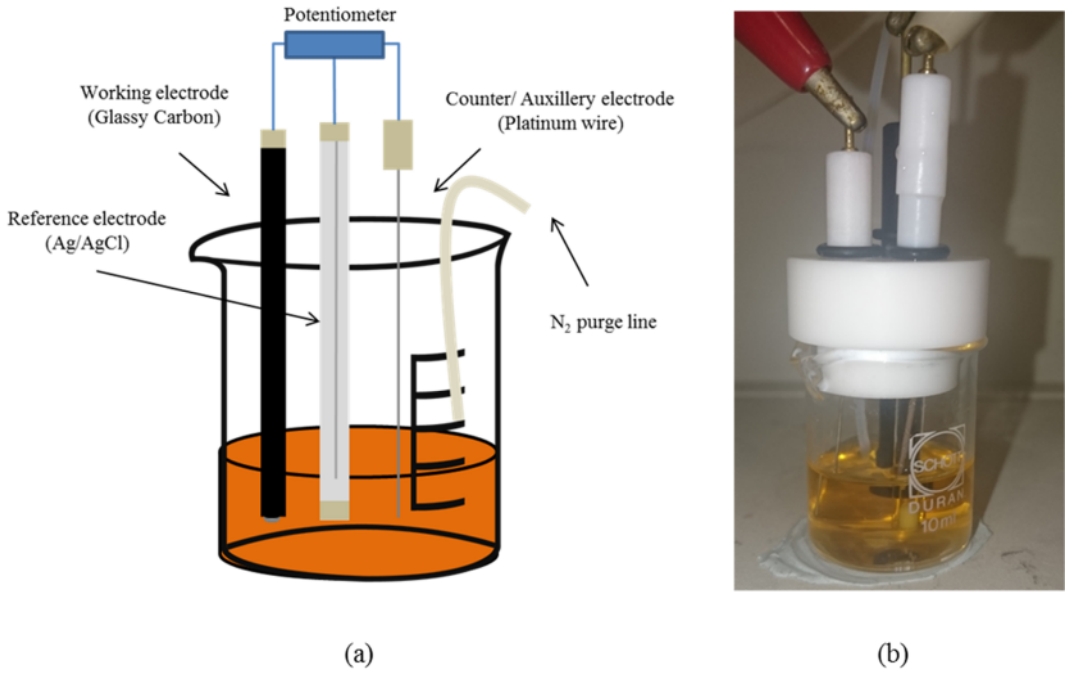

Figure 2.4: (a) Schematic of a three cell voltammetry system consisting of a working (Glassy carbon), reference (Ag/ AgCl) and a counter (platinum wire) electrode with a nitrogen purging line, (b) cyclic

voltammetry set up with a reference Ag/ AgCl electrode, a glassy carbon working electrode and counter platinum wire electrode immersed in electrolyte solution with an N_2 purge line for degassing purposes.

The working electrode chosen was a standard glassy carbon electrode (working electrode) with a surface internal diameter of 3 mm (ALS, Japan). A platinum wire with a diameter of 0.5 mm and a length of 50 mm (ALS, Japan) was selected as a counter electrode. The role of the reference electrode was carried out using silver silver chloride saturated sodium chloride (Ag/AgCl/ saturated KCl, ALS, Japan) was chosen with a ceramic junction and a diameter of 6 mm.

An adaptation of Focason et al (2014) was employed, following initial tests the best electrolyte and supporting electrolyte was concluded to be acetonitrile and 0.1 M tetrabutylammonium tetrafluoroborate. The complexes were reduced at 45 °C and re-suspended in 0.1 M TBA TFO Dichloromethane. The glassy carbon electrode was polished using 0.5 micro aluminium powder on a damp polishing pad and the sample was purged with nitrogen. The potentiometer was set a scan rate of 0.1 (V/s), segments of 10 and a sample interval of 0.01 (V). Alterations to the potential range and sensitivity with the different complexes were applied; copper complex at -0.5- 1.5 (V) & sensitivity of 1×10^{-6} and cobalt complex at a potential range of -1 to 1.5 (V) & a sensitivity of 2×10^{-5}.

Chapter 3
Astaxanthin extraction and characterisation

3.0 Astaxanthin characterisation

This chapter provides an insight into the extraction and subsequent spectroscopic and electrochemical characterisation of astaxanthin. A combination of cyclic voltammetry and various electronic and vibrational spectroscopic techniques were employed to help understand the unique properties of this molecule. The characterisation of the astaxanthin molecule will not only assist in identifying the xanthopyll in the crustacean waste extract but also help understand it properties and behaviour under experimental conditions. This in turn will aid in gaining a better understanding of the changes in the dynamics of the molecule incurred during the synthesis of novel astaxanthin and metal complexes. The difficulties associated with the stability of astaxanthin have hindered

the characterisation of this molecule in previous studies. Its sensitivity to a wide range of factors including high oxygen levels and excessive temperatures can result in a reduction in the stability of astaxanthin esters (Miao et al. 2013, Ahmed et al. 2015).

3.1 Astaxanthin extraction and detection

3.1.1 Solvent extraction of Astaxanthin from brown crab (*Cancer pagurus*)

In order to extract the astaxanthin from the crab shell waste a number of organic solvents were assessed for their suitability for the extraction procedure. These solvents were chosen so as to cover both extremes of the eluotropic series and they ranged in eluotropic strength from the non-polar hexane to the polar glacial acetic acid. The extractions into non polar hexane resulted in poor recoverable yields whereas the trial extractions into glacial acetic acid proved to be the most effective in terms of recoverable yield of the crustacean astaxanthin. This visually can be seen in figure 3.1 as the fraction with the greatest pigmentation. This solubilising preference for a more polar solvent can be understood in terms of the chemical structure of astaxanthin which possesses a number of polar functionalities on both ends of the molecule which act to solubilise the molecule. Aside from the inherent polar nature of glacial acetic acid the corrosive nature of the acid may also have helped in releasing the bound astaxanthin from the protein-calcium carbonate matrix by dissolving the calcium carbonate thus releasing the astaxanthin.

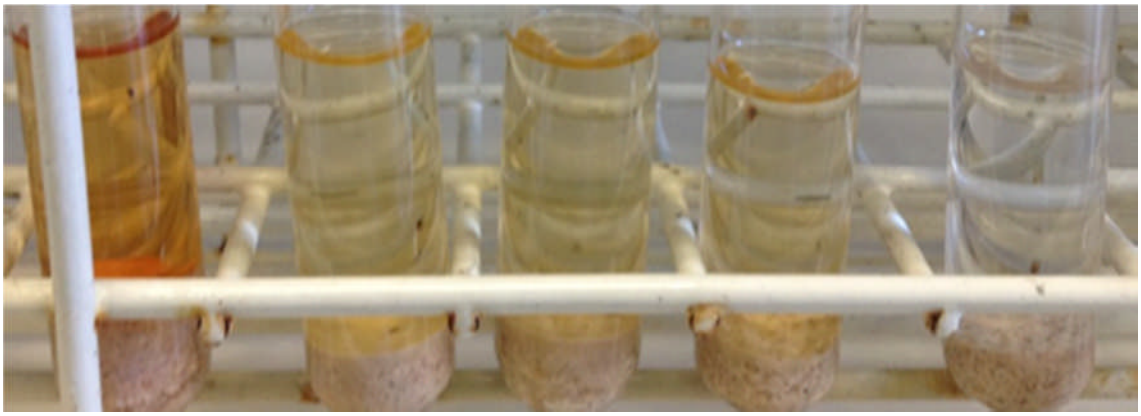

Figure 3.1: Brown crab shell in organic solvent (72 hrs at room temperature), from left to right glacial acetic acid, methanol, Isopropanol/ hexane (50:50), acetone & hexane.

Due to the high acidity associated with glacial acetic acid the extract was then transferred in diethyl and neutralised using sodium hydroxide, which was then followed by concentration of the extract. This orange concentrated extract is identified and quantified using HPLC.

3.1.2 Astaxanthin detection in brown crab (Cancer pagurus) extract using HPLC

An extremely useful technique in the separation and detection of carotenoids is high performance liquid chromatography, (HPLC), which can be used for both qualitative and quantitative purposes. A series of astaxanthin standards 98.5% (Dr. Ehrenstorfer GmbH, Germany) were prepared for chromatographic calibration curve. The astaxanthin standard elutes from the column after 9.7 minutes. Due to the environmentally sensitive nature of astaxanthin, degradation products can from on exposure to sunlight and oxygen (Ahmed et al 2015). The presence of these breakdown products can be easily detected as monoester and diesters which elute from the column at a later time.

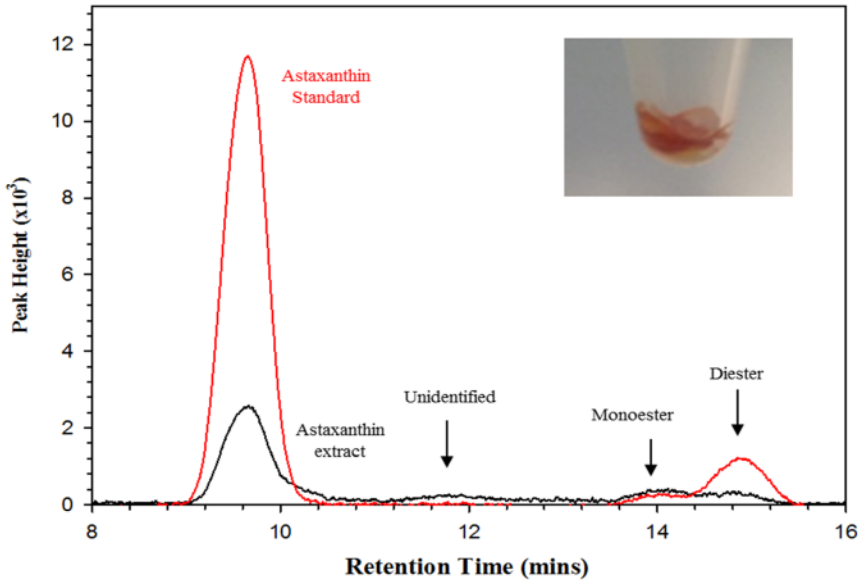

Figure 3.2: HPLC chromatogram of astaxanthin standard 5 µg/ml (red) and astaxanthin extract from brown crab (*Cancer pagurus*) (black) in acetone at a flow rate of 1 ml/min. Inset concentrated pigment after extraction showing a pink/red pigmentation matching that of the carotenoid astaxanthin, 1 in 2.5 dilution.

These breakdown products also result decrease the total peak area associated with the astaxanthin standard. The astaxanthin monoesters degrade at a faster rate than diesters (Miao et al 2013) and the two peaks between 14-15 minutes were identified as the astaxanthin diesters and monoesters respectively.

Once calibrated the system it was utilised to both confirm the presence of astaxanthin in the extract and also to quantify the amount of astaxanthin present. Inspection of the extracts chromatogram shows the presence of both the monoester and diester breakdown products which are identical to those found in the commercial standard. Also present in the extracted sample is the presence of an as yet unidentified component at 11.7 minutes

From the chromatographic analysis there is a strong correlation between the increase in concentration of the astaxanthin standard and the increase in each standards integrated peak areas. This was in close agreement with Beer's law and the inset of figure 3.3 shows the astaxanthin linear calibration curve which was used to determine the concentration of astaxanthin in the extracts from the marine source.

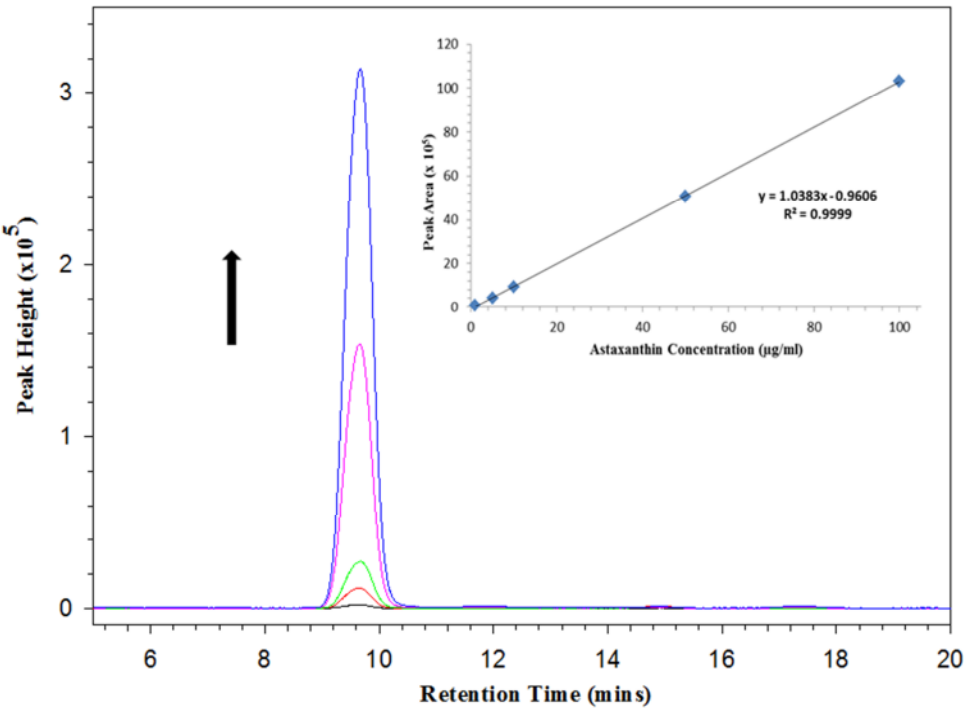

Figure 3.3: HPLC chromatogram of astaxanthin standards in acetone at 470 nm and a flow rate of 1 ml/min, inset astaxanthin calibration curve in acetone.

From the standard calibration data the astaxanthin concentration is determined to be 18.5 mg/100g of brown crab shell. This yield of the extractable astaxanthin obtained is at a much higher concentration than those previously reported by Vilasoa-Martínez et al. (2008), which utilised acetone solely as the extracting solvent. Although vilasoa ultilised a different species of crab (*Chionoecetes opilio*) as the source material they only reported and extraction efficiency of 1.79±1.03 mg/100 g of crab. Thus in comparison the small increase of 16 mg in recoverable material may prove to be attractive enough in terms of profitability for future commercial interest.

3.2 Astaxanthin characterisation

3.2.1 Electronic spectroscopy

The electronic spectrum of the long polyene chain astaxanthin exhibits three peaks with the maximum absorption occurring at a wavelength of 478 nm. Inspection of figure 3.4 shows the highest K-band absorption is generated by the transition of the large conjugated molecule from the π bonding orbital to the π* anti-bonding orbital. The R-band absorption at 294 nm is a characteristic carbonyl peak, which is generated by the transition of the carbonyl group from n→ π* (Yuan et al. 2012).

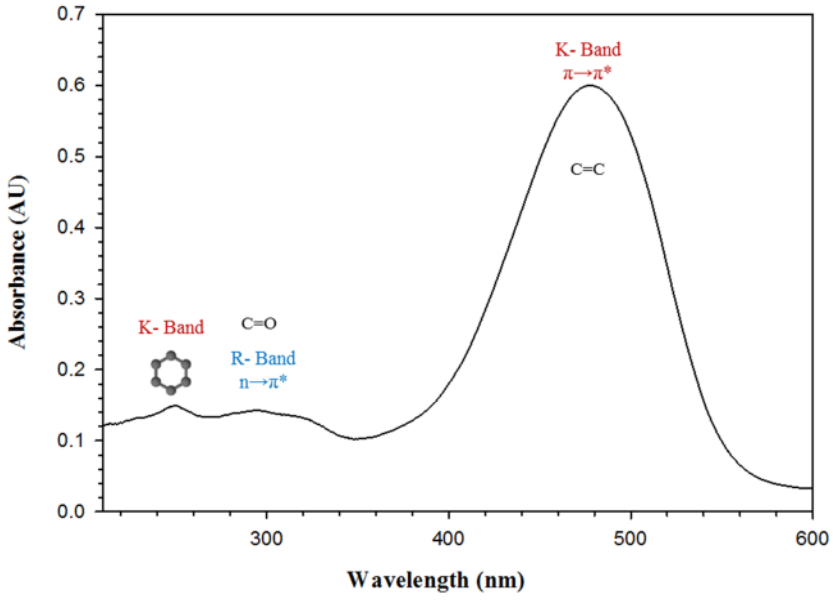

Figure 3.4: Electronic spectrum of astaxanthin standard (0.04 mM) in ethanol with the maximum absorbance K_0 band at 478 nm.

The third K- band absorption at 249 nm from the hexatomic ring absorption (Yuan et al. 2012, Yadav 2005). From literature it is known that this maximum absorbance band can shift depending on the solvent effects and the K-band reveals different maximum absorption peaks in several different organic solvents and mixtures. To examine these shifts of the maximum absorption band the xanthophylls was prepared in different solvent of acetonitrile, dichloromethane, ethanol, methanol and acetone, as shown in figure 3.5.

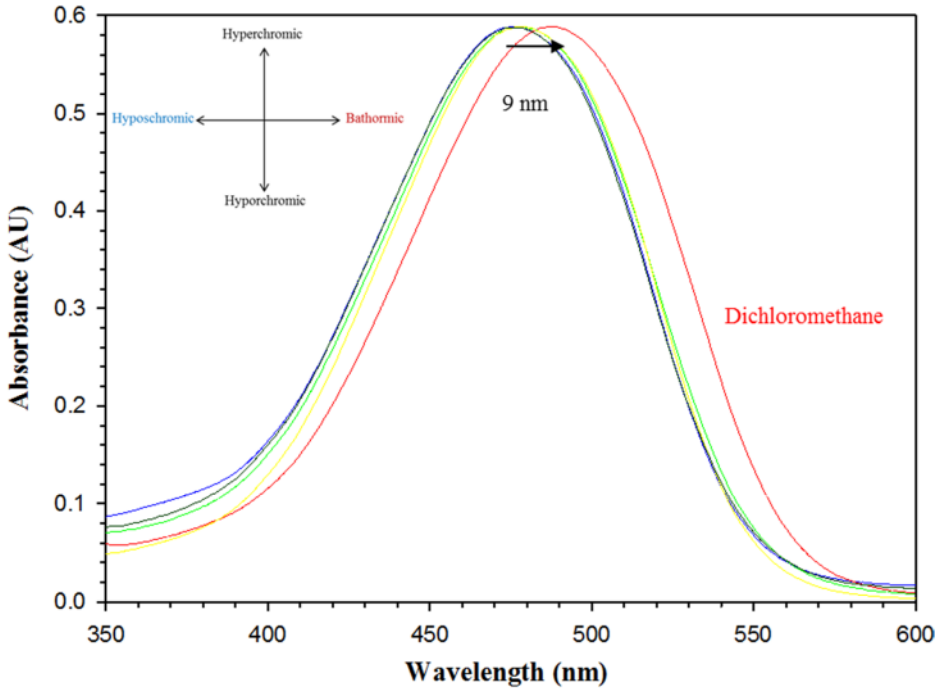

Figure 3.5: Astaxanthin normalized in different organic solvents: acetonitrile (blue) at 475 nm, dichloromethane (red) at 487 nm, ethanol (green) at 478 nm, acetone (yellow) at 470 nm, and methanol (black) at 476 nm

The maximum K- band absorption of astaxanthin shifted in both the hypsochromic and bathormic directions. In dichloromethane the astaxanthin maximum absorption peak shifted in the bathormic (red) direction to a higher wavelength of 487 nm, the 9 nm shift was caused by the attachment of an auxochrome (a covalently saturated group) to the C=C conjugated system (Mohan 2004, Yadav 2005). The organic solvent acetonitrile, acetone and methanol caused a hypsochromic (blue) shift to a lower absorption of 475, 470, and 476 nm respectively. The blue shift is caused by either a change in the polarity

of the solvent or the removal of conjugation (Yadav 2005). The 2 nm shift in methanol can be attributed to the increased polarity of the solvent and n→π* transitions undergoing a hypsochromic shift (Mohan 2004).

In order to fully characterise the electronic states of astaxanthin metal complexes it was necessary to choose a suitable solvent, one which would provide both a high degree of solubilisation and also offer a wide spectral window. The solvent ethanol was deemed to meet these requirements and was subsequently use for all the electronic spectroscopic work on the astaxanthin metal complexes.

3.2.2 Infrared spectroscopy (IR)

Probing the unaltered vibrational structure of astaxanthin was essential so as to provide reference against which the as formed complexes could be compared to. To facilitate this comparative analysis it is important to identify the functional groups involved in the formation of the complexes. Solid astaxanthin samples were prepared in potassium bromide (KBr) and the characteristic functional groups were assigned in the infra-red spectrum as shown in figure 3.6. As described in chapter 1 the characteristic functional groups associated with astaxanthin are with carbonyl and hydroxyl groups located on the hexatomic rings at both ends of the molecule.

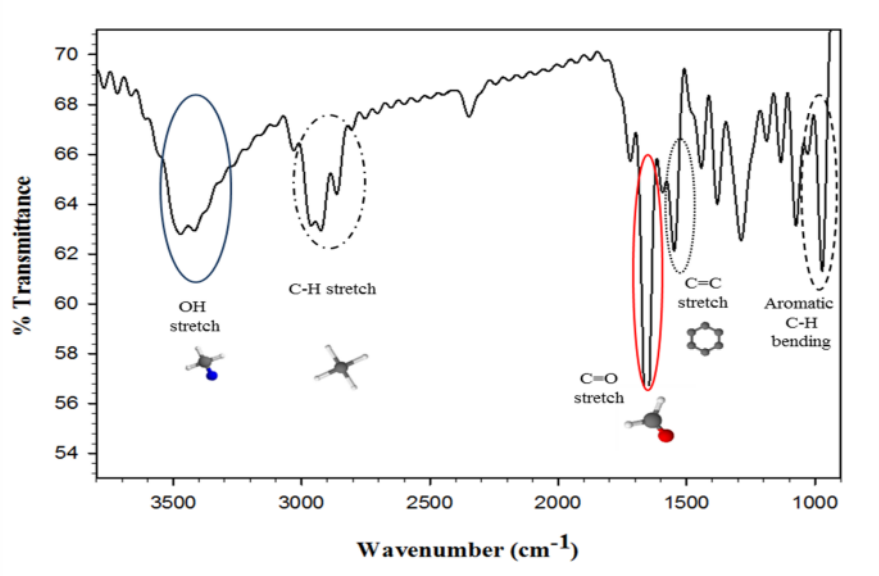

Figure 3.6: Infra-red spectrum of astaxanthin in KBr at a resolution of $2cm^{-1}$ measuring percent transmittance and the vibration of the functional groups.

These two groups allow astaxanthin to perform its functional abilities, e.g. antioxidant activity and solubility in both aqueous and non-aqueous solvents. Inspection of the infra-red vibrational spectra reveals the presence of both functional groups with a sharp vibrational mode at 1660 cm^{-1} which is a result of the C=O stretching and the mode at 3470 cm^{-1} is the result of the OH stretching. The hexatomic ring frequency at 1560cm^{-1}, changes during the synthesis of complexes which can be an indication of the inclusion of the ring in the complex formation (Yuan et al. 2005). The vibration mode at 971 cm^{-1} indicates aromatic C-H bending and the mode at 2920 cm^{-1} band is a result of a C-H stretch (Mahaffy et al. 2014, Yuan et al. 2005). The presence of the aforementioned modes agrees with the literature sources and the structure of the molecule.

3.2.3 Raman spectroscopy

In addition to the vibrational information afforded by the infra-red spectroscopic analysis the interpretation of the raman spectra of astaxanthin offers another source of information which complements the infra-red and aids in the complete characterisation of the molecule. Exposure of astaxanthin to the high intensity laser radiation perturbs the vibrational states of the molecule and results in Raman scattering involving a series of shifts, each of these shifts corresponding to characteristic frequencies.

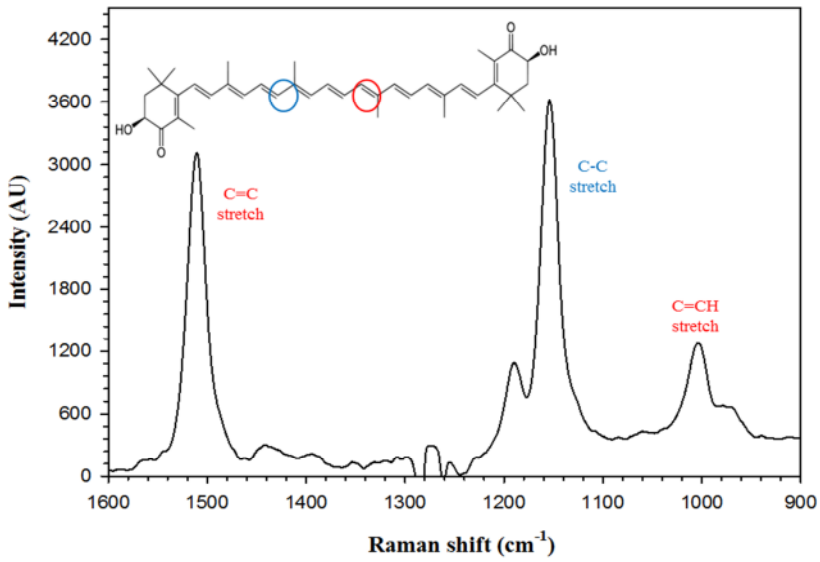

Figure 3.7: Raman spectra of astaxanthin vibrational Raman shifts, each frequency corresponding to functional group.

In carotenoids the characteristic Raman frequencies that are observed are those of the C-C stretching at 1100- 1200 cm^{-1} and C=C stretching at 1400- 1600 cm^{-1}(De Oliveira et al. 2010). Inspection of figure 3.7 clearly confirms the presence of these aforementioned modes. The Astaxanthin Raman spectra were recorded on dry using the lowest power setting of 90 mW from a 785 nm laser. The spectra in figure 3.7 reveals the presence of the Raman modes at frequencies of 1155 and 1510 cm^{-1}, the two peaks are a product of C-C and C=C stretching respectively. A third peak at 1004 cm^{-1} is a C=CH stretch corresponding the polyene chain (Parab and Tomer 2012). The aforementioned three bands are common among carotenoids and will be examined closely in the synthesised ligand and metal complexes to determine the changes in the structure and help gain knowledge on the groups involved in the complex formation.

3.2.4 Cyclic voltammetry

Cyclic voltammetry is a widely used technique for the detection of the antioxidant activity and it allows for the determination of the redox potentials and can also be used to assess the electron transfer kinetics. The reversibility of the cyclic voltammograms has previously proven difficult when studying carotenoids.

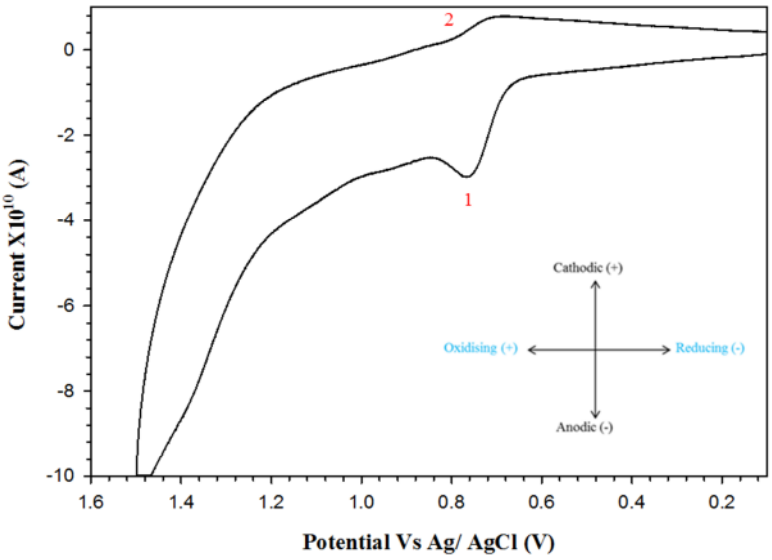

Figure 3.8: Cyclic voltammogram of astaxanthin in 0.1 M TBA TFO dichlormethane at a scan rate of 0.1 V/s and a sensitivity of 1x 10^{-6} A/V

These difficulties are a result of the less stable radical cations and dications being produced. Reproducing a reversible cyclic voltammogram requires careful control of solvent moisture content. The choice of solvent, electrolyte and working electrode were also essential in detecting astaxanthin as initial tests revealed dichloromethane, Tetrabutylammonium tetrafluoroborate (TBA TFO) and a glassy carbon electrode yielded the best results. The cyclic voltammogram in figure 3.8 reveals a single peak on each of the anodic and cathodic scans. The initial peak at a potential of 0.76 V, corresponding to the oxidation of the neutral astaxanthin species and the return cathodic scan a single peak is observed at a 0.72 V, identified as the radical cations (Focsan et al. 2014). The voltammogram reveals a one electron transfer oxidation as opposed to the literature revealing a two electron transfer oxidation, as mentioned previously in chapter 1the stability of the radical cations and dications proves problematic. In order to obtain a double peak stronger controls are needed including moisture control. The choice of the solvent and electrolyte may also be a factor as they may be the best available at hand but may be presenting a non-stable environment.

The solvent used is altered to acetonitrile to observe the changes brought about as studies have revealed the destabilisation of complexes including astaxanthin due to the incorporation of the solvent within complexes (Polyakov et al. 2010).

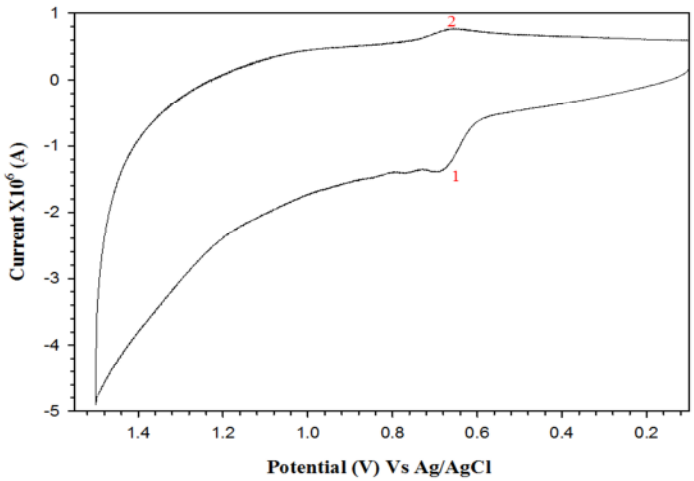

Figure 3.9: Cyclic voltammogram of astaxanthin in 0.1 M TBA TFO acetonitrile at a scan rate of 0.1 V/s and a sensitivity of 5x 10^{-7} A/V

One of the significant differences between the two cyclic voltammograms is the increased gap between the two scans even with the sensitivity increase. The one

electron transfer oxidation remained with a single peak remained present on each of the scan. In the anodic scan an oxidation peak of the neutral astaxanthin species at 0.70 V and a reduction peak of the radical cations at 0.65 V (Focsan, et al 2014). The difficulties in detecting these peaks are a result of the sensitivity of the molecule. Stronger moisture controls are required but due to the lack of equipment available this was unfeasible.

The astaxanthin molecule was characterised using a range of techniques, this was carried out in order to determine the changed brought about through complexation with molecules in the surrounding medium. In this case metal chloride salts are used. The changes are examined on an electronic, vibrational and electrochemical level. Electronic in order to examine the shifts caused through the aggregation of the complexes, vibrational to identify the responsible functional groups for complexation and electrochemical to examine the effect on the significant antioxidant activity of the molecule.

Chapter 4
Copper chloride and astaxanthin complex

4.0 Introduction

As discussed in chapter 1 copper differs from most other transition metals in the possession of one electron in the *4S* orbital as opposed to two. This electronic arrangement results in it being one of the strongest binding transition metals and copper binds to many different chelating agents and ligands both natural and synthetic (Cornelias et al. 2005). The polarizability and outer shell asymmetry of copper allow the metal to interact with most ligands (Martell and Smith 1974). This metal is a perfect candidate for the formation of metal chelate complexes with astaxanthin and this in turn can disrupt the efficacy of the xanthophyll upon intake and negating its powerful antioxidant activity. Copper can be introduced to the digestive system through a number of dietary intakes including dried fruit, meat, nuts, mushrooms, clams, legumes and grains (Kamberg 2010). The synthesis of astaxanthin and a copper salt and its

characterisation will be examined using a number of spectroscopic and electrochemical techniques. Also in order to replicate possible processing conditions, the complexes mixtures were subjected to higher temperature regimes.

4.1 Synthesis of astaxanthin and copper chloride complexes

During the initial study utilising Job's method, the reaction mixtures were maintained at room temperature. It is apparent that little or no complexation had taken place due to the slight changes in the absorbance bands as indicated in figure 4.2. In order to mimic the possible reaction conditions experienced during the metabolism of astaxanthin following consumption, the complexes were refluxed at a temperature of 37 °C. In additionally as means of ensuring sufficient activation energy in addition to body temperature refluxes, a series of mixtures were also refluxed the boiling point of ethanol at 78 °C

In order to prepare the stable copper chloride and astaxanthin complexes job's method of continuous variation is utilised. The method involves maintaining the molarity of the solution mixture at 0.04 mM while systemically changing the concentration of each. As a general observation the astaxanthin and copper complexes did not exhibit a colour change upon complexation at room temperature. However upon refluxing at 37 °C there is an observable increase in the intensity of the astaxanthin orange pigmentation while at 78 °C the mixture changed dramatically, this can be observed in figure 4.1 (c). At lower astaxanthin concentrations the solution transformed into a pale green and at higher concentrations a yellow/pale green colour. The refluxed complexes also exhibited no noticeable thermochromism effect across all three reaction temperatures.

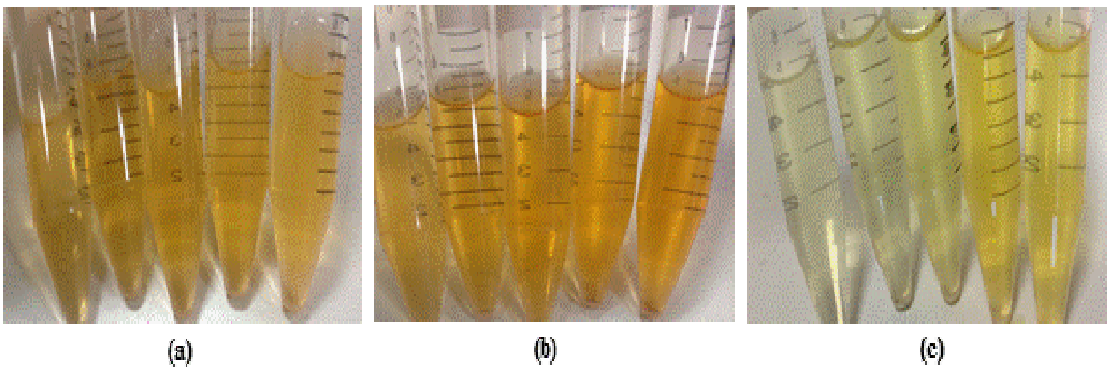

Figure 4.1: Astaxanthin increase & $CuCl_2$ decreasing from left to right, (a) at room temperature (20 °C), (b) refluxed at 37 °C for 30 mins and (c) refluxed at 78 °C for 30 mins.

4.2 Characterisation of astaxanthin and copper chloride complexes

4.2.1 Electronic spectroscopy

4.2.1.1 Absorption spectroscopy

The complexes were initially synthesised at room temperature in ethanol and the electronic spectra revealed no shift in the maximum absorption peak of astaxanthin at 478 nm, as revealed in figure 4.2. At lower concentrations of copper chloride an absorption peak is observed at 277 nm, following the complex formation the metal chloride peak shifted slightly to 279 nm, this bathormic shift may have been a result of the complex formation. In accordance with the molecular excitation model this is an indication of loose type association (J- or head to tail) (Yadav 2005).

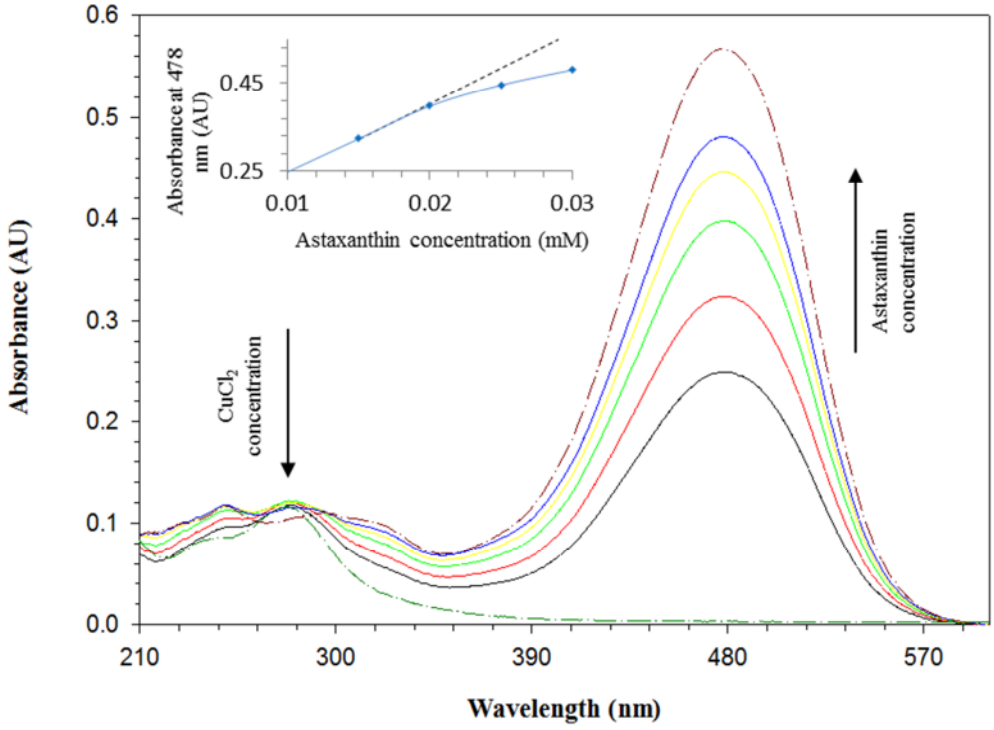

Figure 4.2: Electronic spectra of astaxanthin and $CuCl_2$ complexes synthesised at room temperature 20 °C in ethanol (normalized), astaxanthin (0.04 mM) (dashed dark red) and $CuCl_2$ (0.04 mM) (dashed dark green). Inset of astaxanthin concentration (mM) versus absorbance at 478 nm demonstrating a deviation of beer lamberts law.

J- type aggregates are a one dimensional molecular assembly involving the individual monomers dipole moments aligning parallel to the line joining their centres (end – end arrangement) (Johal et al. 2011). In J- aggregates the arrangement of the monomers to

each other extends the chain length, assuming that the motion of the electron is along the dipole then the motion is considered delocalised along the entire length of the aggregate. The length of the aggregate is greater than the individual monomer, hence ΔE is small and inversely proportional to the wavelength resulting in a higher wavelength in comparison with the monomer (Johal et al. 2011).

In figure 4.2 the maximum K- band absorption peak ($\pi \rightarrow \pi^*$) of astaxanthin increases constantly up to the higher concentrations of 0.02 and 0.025 mM, at which the absorption peaks increase at a slower rate causing a dip in the curve and a deviation of beer law (figure 4.2 inset). The deviation from the linear relationship can be attributed to one of either the interference of the metal salt at higher concentrations (chemical deviation) or the decreases solubility of astaxanthin at higher concentrations in ethanol at room temperature. The change in the $CuCl_2$ absorption can be observed in job's plot in figure 4.3.

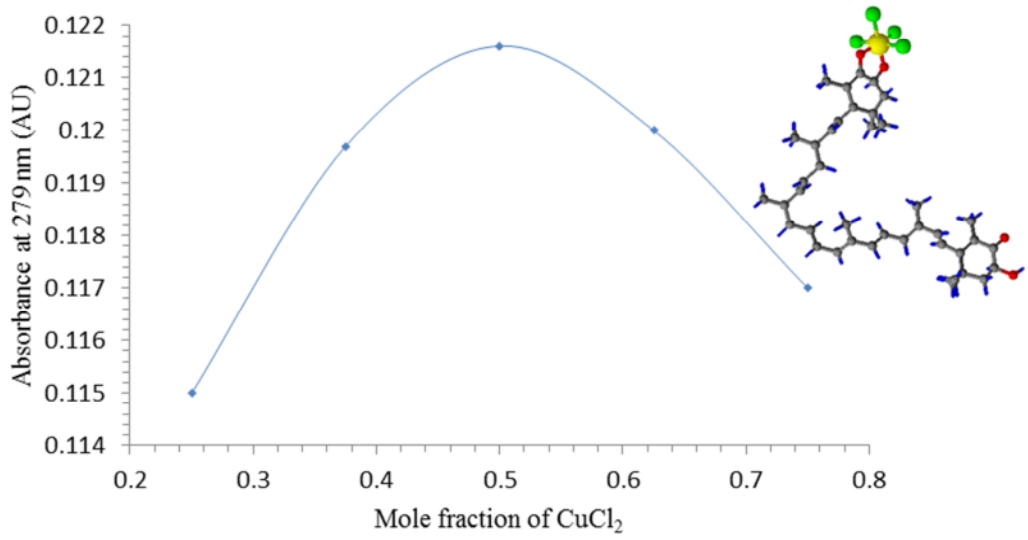

Figure 4.3: Job's plot of $CuCl_2$ in the astaxanthin metal chloride metal complex in ethanol at room temperature (20 °C). Inset of predicted astaxanthin and copper chloride complex generated at room temperature.

The maximum absorption of the $CuCl_2$ occurs at a mole fraction of 0.5 and this corresponds to the combining ratio of 1:1 (metal: ligand). From the plot we can determine the binding ratio of metal to ligand at 1:1 and a J-type aggregate, (head to tail) this can suggest an attachment of the copper chloride molecule (head) to the tail of

the astaxanthin molecule. The Bathormic shift indicates a loose J- type association hence inspection of the electronic spectra determines that the structure of the astaxanthin and copper chloride complex synthesised at room temperature is off an astaxanthin polyene chain with a copper chloride attachment at either end of the molecule through the carbonyl and hydroxyl groups (figure 4.3 inset).

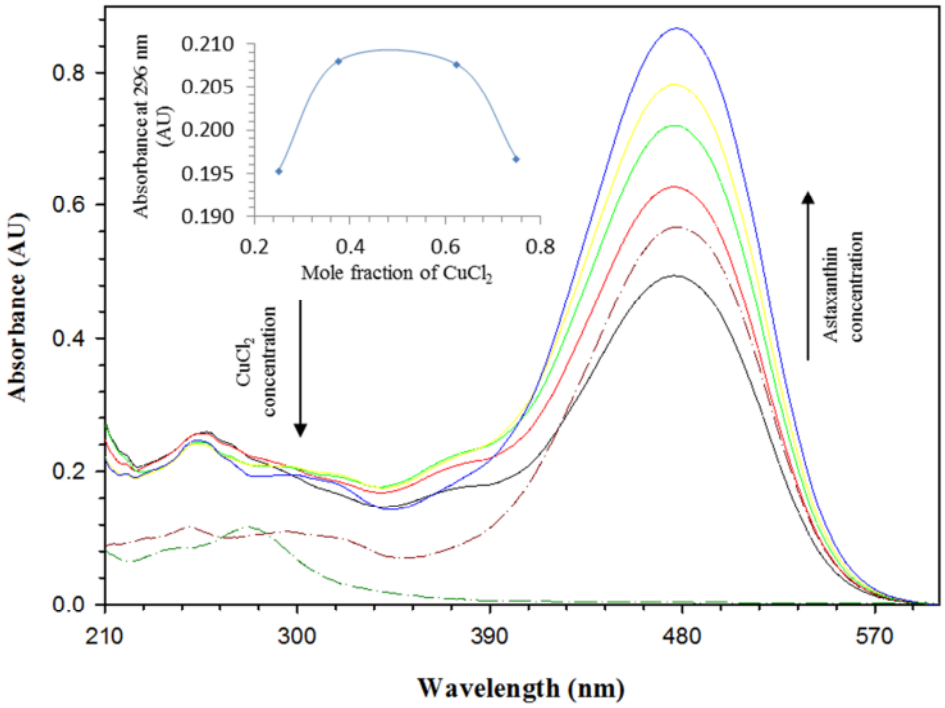

Figure 4.4: Electronic spectra of astaxanthin and $CuCl_2$ complexes refluxed at 37 °C in ethanol (normalized), astaxanthin (0.04 mM) (dashed dark red) and $CuCl_2$ (0.04 mM) (dashed dark green). Inset Job's plot of $CuCl_2$ in the astaxanthin metal chloride metal complex refluxed at 37 °C.

In spectra of the complexes refluxed at 37 °C revealed that there is a large increase in the maximum absorption band of astaxanthin (hyperchromic shift) and the elevated temperature also increased the solubility of the carotenoid in ethanol. This accompanied a small hypsochromic shift of 1 nm to 476 nm. A large hypochromic effect had been exhibited on the $CuCl_2$ peak originally centred at 277 nm and a bathormic shift to a higher wavelength of 296 nm. A red bathormic shift is an indication of a loose type association (head to tail) (Yadav 2005) as seen with the complex synthesised at room temperature. The inset of figure 4.4 show job's plot of $CuCl_2$. The overall shape of the curve leads to an estimation of 0.5 mole fraction and in

turn a 1: 1 ratio of astaxanthin to copper chloride as with the synthesis at room temperature.

The final set of reaction complexes were refluxed at 78 °C (boiling point of ethanol), these complexes experienced large changes in the maximum absorbance peak. In figure 4.5 the astaxanthin K-band shifted largely in the blue region (hypsochromic) to 369 nm, this shift of 109 nm proves a more tight association called a card- pack aggregate or H-type (Simonyi et al. 2003).

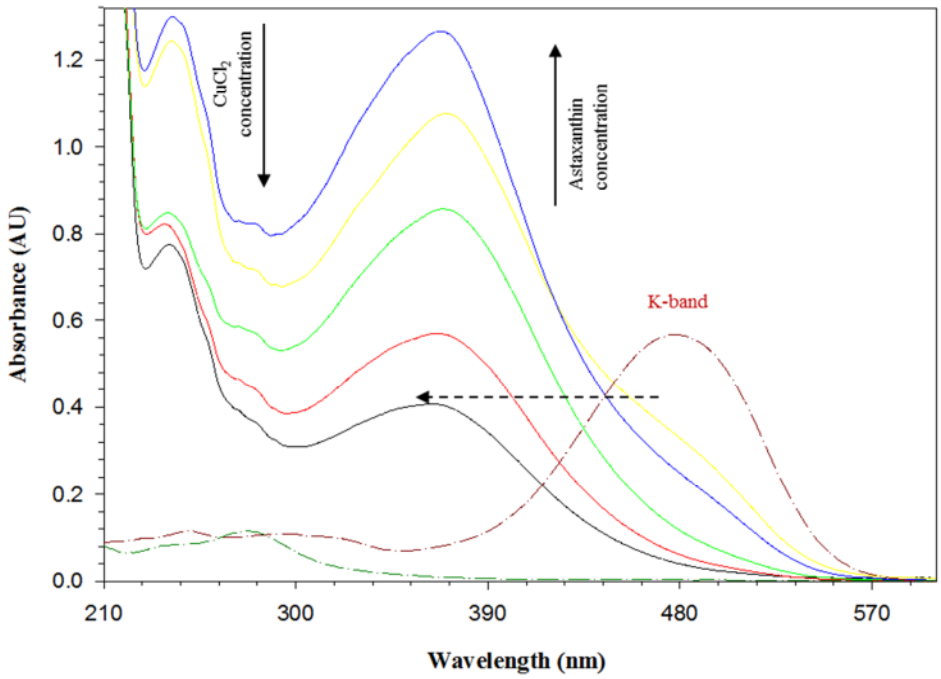

Figure 4.5: Electronic spectra of astaxanthin and $CuCl_2$ complexes refluxed at 78 °C in ethanol, astaxanthin (0.04 mM) (dashed dark red) and $CuCl_2$ (0.04 mM) (dashed dark green).

H-type aggregates are also a one dimensional array, these involve the parallel alignment of the dipole moments to each other but as opposed to the J- type aggregates these are perpendicular to the line joining their centres (face to face arrangement) (Johal et al. 2011). H-aggregates possess a shorter conjugation length and hence a larger ΔE which in turn leads to the blue shift into a shorter wavelength than the monomer (Johal et al. 2011). The copper chloride peak reverted back to the original wavelength of 277 nm and increased with astaxanthin concentrations. Determination of the ratio of complex formation proved difficult as the astaxanthin absorbance appeared to mask that of the copper chloride. The tight H- type aggregates may be a cause of interference in the

copper chloride absorption bands. Due to the previous synthesis results of a 1: 1 ratio complexes it will be assumed that a similar ratio occurred at the elevated temperature of 78°C but with a different packing of H-aggregates.

A comparison of the absorbencies varying with the different complexes is listed in table 4.1. These were plotted in the previous figures versus the copper chloride mole fraction. The increase and decrease pattern is consistent with the first two synthesised complexes at 20 °C and 37 °C whereas the final complex synthesised at a higher temperature is found to increase consistently.

Table 4.1: Absorbencies of copper chloride in metal and ligand complexes synthesised at different temperatures.

Synthesis temperature (°C)	**20**	**37**	**78**
$CuCl_2$ mole fraction	**Absorbance at 279 nm (AU) ± 0.001**	**Absorbance at 296 nm (AU) ± 0.001**	**Absorbance at 277 nm (AU) ± 0.001**
0.250	0.115	0.195	0.824
0.375	0.120	0.208	0.722
0.500	0.122	0.206	0.578
0.625	0.120	0.208	0.451
0.750	0.117	0.197	0.376

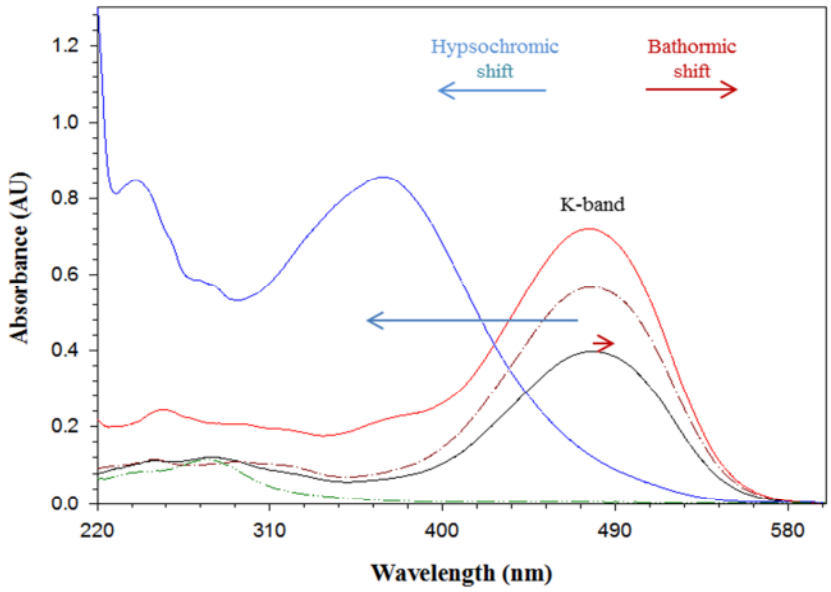

Figure 4.6: Electronic spectra comparing shift between complexes of astaxanthin and copper chloride (normalized) astaxanthin (0.04 mM) (dashed dark red), $CuCl_2$ (0.04 mM) (dashed dark green), astaxanthin and $CuCl_2$ complexes (1:1) synthesised at 20 °C (black), astaxanthin and $CuCl_2$ complexes (1:1) refluxed at 37 °C (red), astaxanthin and $CuCl_2$ complexes (1:1) refluxed at 78 °C (blue).

A more clear demonstration of the shift of the maximum astaxanthin k-band can be seen in figure 4.6. A ratio of 1:1 is used as an example of the synthesised complexes at the three varying temperature of 20 °C, 37°C and 78 °C as this is found to be the binding ratio of the ligand and metal in complexes.

Refluxing the metal ligand complex at 78°C resulted in a more tight packed assembly as opposed to the previous two syntheses at room temperature and 37 °C. The characteristic high absorption of astaxanthin presented difficulties in detecting the changes of the metal chloride salt, to perform job's plot of continuous variation the overall molarity of the solution is to remain constant, the low absorption of the metal chloride salts at these concentrations proved problematic. The electronic spectra of the synthesised complexes at room temperature, refluxed at 37 °C and 78 °C helped gain a better understanding of the changes incurred by the complex formation and the optimum ratio for the astaxanthin and copper chloride binding. These interactions induced changes in the distinct absorption characteristic of astaxanthin.

The interest into the carotenoid astaxanthin is driven by its powerful antioxidant activity; this involves a direct reaction between the radical and antiradical. The assumption of the bioassimilation of astaxanthin in the body is supported by the results, copper can be found in many components of a diet, e.g. metal and dried fruit. The interaction to form a metal ligand complexes can cause interferences in the antioxidant activity thus defeating its purpose of ingestion. The normal body temperature at rest is 37 °C (Goyal 2013), at which refluxing astaxanthin and the metal chloride complex resulted in complex formation (J- aggregates).

The electronic studies of the complex in solution were followed by the concentration of the complexes at 45 °C; the complexes were examined for crystal precipitate on a quartz window at a magnification of 10x. The complex precipitate revealed a separation between the astaxanthin and copper chloride. The increase in astaxanthin concentration is accompanied by an increase in the crystallisation of the carotenoid at the edge of the quartz window. The centre exhibited a more green hue; this is attributed to the copper chloride. Crystallization of the astaxanthin and copper chloride complex is not observed.

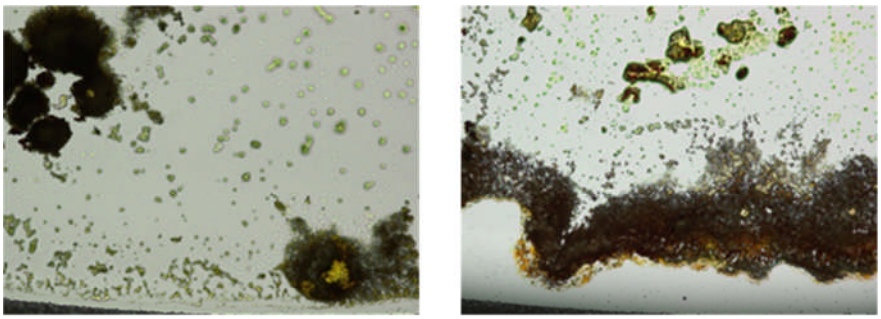

(a) (b)

Figure 4.7: Solid state astaxanthin and $CuCl_2$ complex refluxed at 37°C on quartz window at 10x (edge), (a) astaxanthin and copper chloride in a 3:1 ratio and (b) a reversed 3:1 ratio.

The precipitate of the complex refluxed at 78 °C revealed a more unified pattern, with the increase in astaxanthin the orange pigmentation intensified. Crystallisation of the complex is not observed in the dry state. Larger quantities may have been required of the complex to observe a detectable crystallised structure.

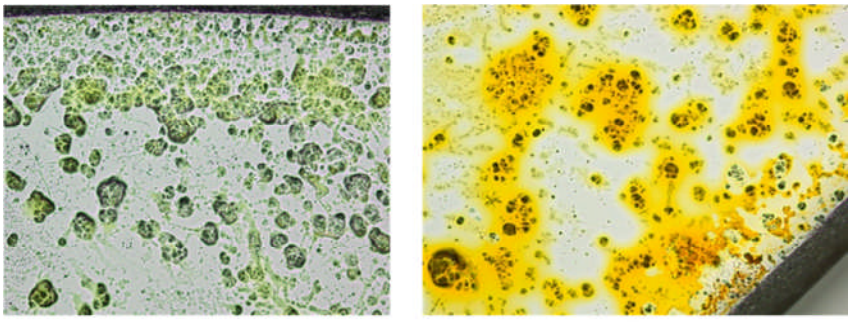

(a) (b)

Figure 4.8: Solid state astaxanthin and $CuCl_2$ complex refluxed at 78°C on quartz window at 10x (edge), (a) astaxanthin and copper chloride in a 3:1 ratio and (b) a reversed 3:1 ratio.

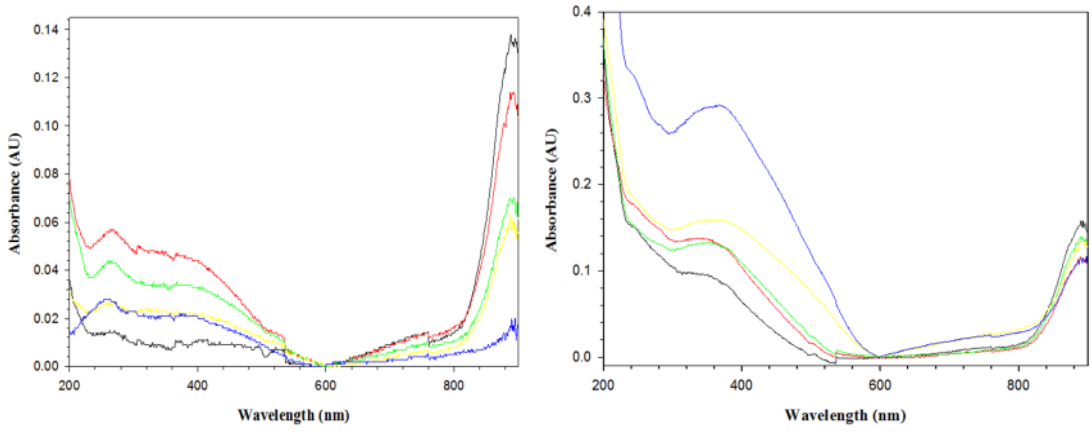

(a) (b)

Figure 4.9: Electronic spectra of solid state astaxanthin and $CuCl_2$ complexes on quartz window (normalized), (a) refluxed at 37 °C and (b) refluxed at 78 °C (normalized). Astaxanthin and copper chloride concentrations: 1:3 (black), 1:2 (red), 1:1 (green), 2:1 (yellow) and 3:1 (blue).

Electronic spectra were recorded on both dry state complexes and a large shift in the baseline is observed which presented difficulties in determining the pattern of changes in absorption even following normalization. The maximum absorption bands of copper chloride are present at 890 nm in both refluxed complexes, whereas the astaxanthin peak shifts. In the complex refluxed at 37 °C and 78 °C the absorption maximum occurred at 258 nm and 355 nm respectively. The maximum absorption of astaxanthin on quartz is detected at a wavelength of 509 nm.

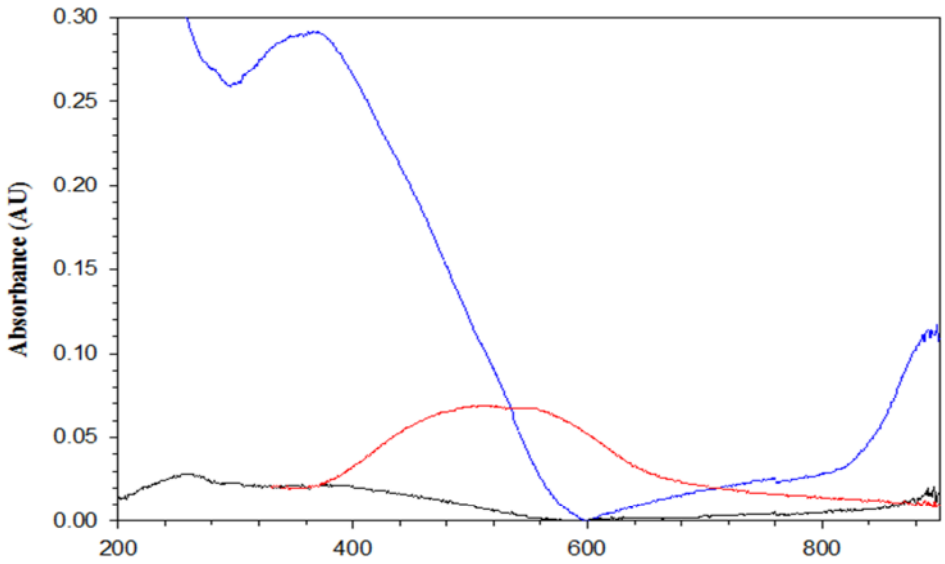

Figure thin and copper chloride complex refluxed at 37 °C (black) and refluxed at 78 °C (blue) (normalized), the ratio of astaxanthin and copper chloride in complexes (3:1).

The maximum absorption band of astaxanthin in the dry state refluxed complexes shifted in the hypsochromic (blue) direction to a shorter wavelength suggesting H- type aggregation. In both the solution and solid states electronic spectra a large hypsochromic shift of over 100 nm is observed. In contrast the corresponding shift of the refluxed complex at 37 °C is in an opposite direction, as in solution it exhibited a bathormic shift as opposed to the hypsochromic shift of the solid state over 200 nm. The result of the electronic spectra of the solid state complex proved inconclusive and further investigation is required.

4.2.1.2 Fluorescence spectroscopy

Since the fluorescence lifetimes of carotenoid like molecules occur in the picosecond range (Bautista et al. 1999), instrumental limitations restricted the fluorescence spectroscopic analysis to as formed complexes. The fluorescence spectra of the astaxanthin and copper chloride complexes produced at room temperature and refluxed at 37 °C in ethanol revealed no observable fluorescence indicating that in fact at these temperatures no true bonding occurs between copper and the astaxanthin. However the copper and astaxanthin complexes formed at 78 °C did fluoresce when excited at 498 nm.

This is not the case with the complexes refluxed at 78 °C as fluorescence spectra obtained at an excitation wavelength of 498 nm revealed a double peak absorbing at 587 and 607 nm. The captured fluorescence indicates an alteration in the characteristics of the astaxanthin molecule as the lifetime measurement speed decreases into detectable milliseconds. Due to the absence of the fluorescence spectra of the astaxanthin a band shift is undetermined.

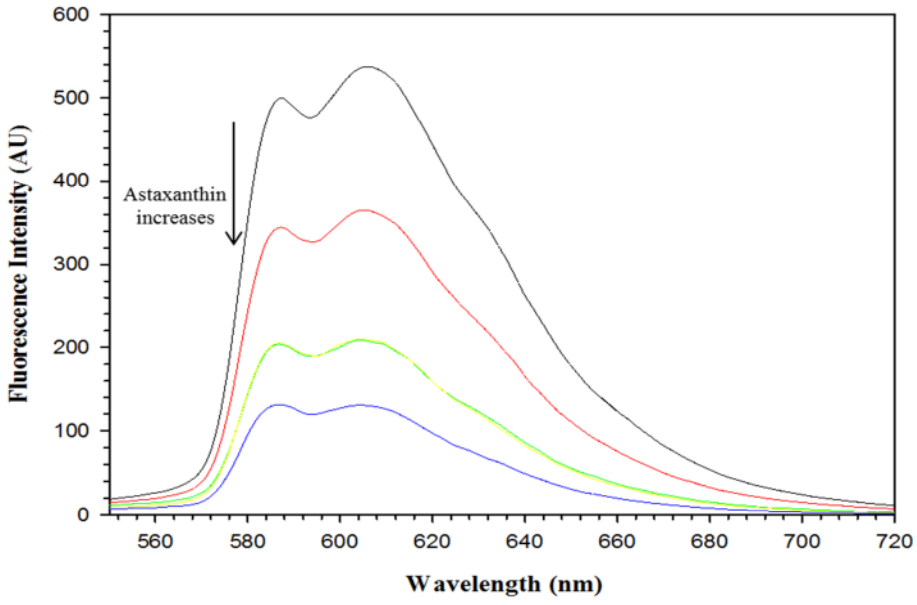

Figure 4.11 at 78 °C in ethanol, Astaxanthin and copper chloride concentrations: 1:3 (black), 1:2 (red), 1:1 (green), 2:1 (yellow) and 3:1 (blue).

Fluorescence spectra proved the formation of a complex which can be detected at a slower speed of milliseconds, the metal ligand complexes appeared to have an impact

on the speed of the fluorescence lifetime measurements further proving complexation with an increased activation energy.

Table 4.2: fluorescence intensity of astaxanthin in ligand copper chloride complexes synthesised at different temperatures.

Synthesis temperature (°C)	**78**
$CuCl_2$ mole fraction	**Fluorescence intensity at 607 nm (AU) ± 0.001**
0.250	336.9
0.375	247.6
0.500	286.2
0.625	341.7
0.750	466.6

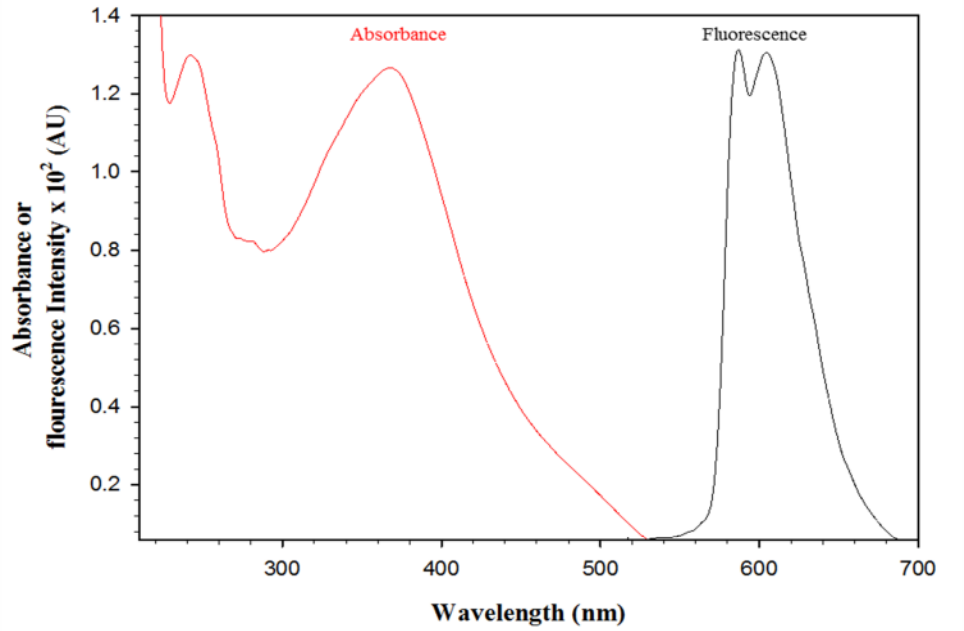

Figure 4.12: Electronic and flourescence spectra of refluxed astaxanthin and copper chloride complex refluxed at 78 °C, ratio of ligand to metal 3:1.

A comparison of the absorbance and fluorescence spectra reveals an exception to the mirror image rule, this in accordance with the literature is due to geometric changes of the nuclei in the excited state when compared with the ground state (Lakowicz 1999). The shape of the peaks differ, as the fluorescence band is a double peak whereas the absorbance is separated into two individual peaks. The maximum absorbance band occurs at 369 nm and the reverse fluorescence occurs at 607 nm, separating the peaks by a distance of 238 nm.

4.2.2 Vibrational spectroscopy

4.2.2.1 Infrared spectroscopy

To gain insight into the changes in the type of bonding between the astaxanthin and copper, the vibration spectra of formed complexes were examined using infrared spectroscopy. The complexes were dried onto sodium chloride windows and run on the infrared for % transmittance measurements at a resolution of 2 cm-^{1} with interval of 1 cm^{-1}and between 4000- 350 cm^{-1}. The low concentration of the complexes proved problematic in the detection of the vibrational changes.

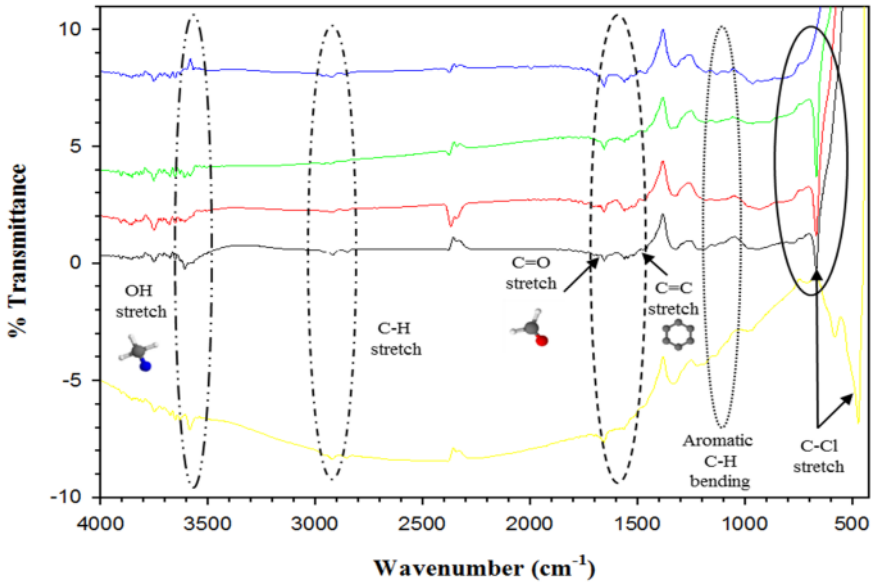

Figure 4.13: Infrared spectra of astaxanthin and complexes formed with copper chloride (normalized), Astaxanthin and copper chloride concentrations: 1:3 (black), 1:2 (red), 1:1 (green), 2:1 (yellow) and 3:1 (blue). Corresponding functional groups labelled.

Characteristic frequencies of astaxanthin are at 980 cm^{-1} , 1680 cm^{-1} and 3050 cm^{-1} , these correspond to aromatic C-H bending, C=O stretching and OH stretching, respectively (Mahaffy et al. 2014, Yuan et al. 2005). In figure 4.13 of the Infrared spectra it is evident that the complex concentration is too low and close to the detection limit, this required a further magnification to examine the spectra closely and identify the peaks. The C=O stretch at 1640 cm^{-1} shifted largely from it original frequency of 2860 cm^{-1} (chapter 3), this is an indication of the involvement of the carbonyl functional

group in the complex. The hexatomic ring at 1280 $cm^{-1}$and aromatic C-H bending at 820 cm^{-1} were present. The OH stretch at 3400 cm^{-1} is also detected with a large decrease. A peak at 680 cm^{-1} appeared in three of the complexes and shifted to 480 cm^{-1}, these peaks in accordance with literature correspond to C-Cl stretch (Varsányi 2012), this peak shifted at an increased ligand to metal ratio and is not detected at the highest ratio confirming that decrease in the copper chloride concentration. Although the C-Cl peak appeared to increase with the decreasing metal chloride concentrations before its absence in the final ratio of 3:1 (ligand to metal). The small peaks proved problematic in examining a decrease pattern while examining the spectra as the determination of the changes in the vibration of the functional group is difficult. The involvement of the carbonyl group in the astaxanthin and copper chloride complex is confirmed.

4.2.2.2 Raman spectroscopy

The vibrational changes associated with the functional groups involved in the complexation were also probed using raman spectroscopy. The complex intensity is measured at an integration time of 90 sec and frame size of 30 sec. Of particular note are the characteristic carotenoid bands centred at 1150 cm^{-1} associated with the C-C stretching and the C=C stretching between 1400- 1600 cm^{-1}(De Oliveira et al. 2010, Parab and Tomar 2012).

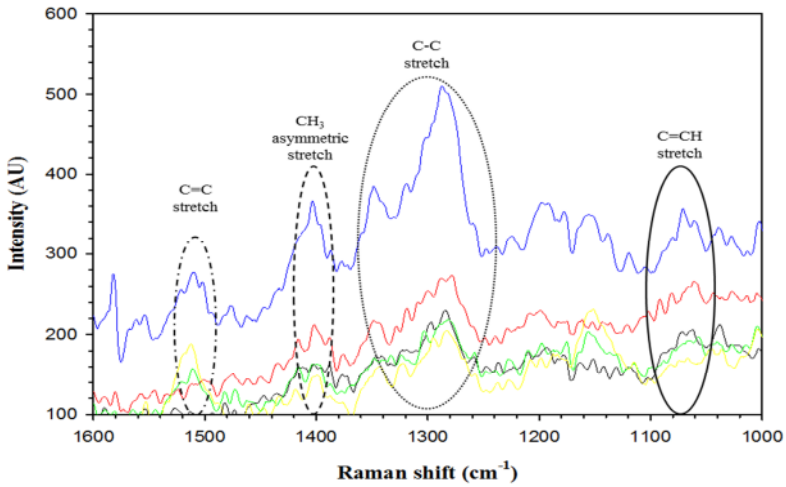

Figure 4.14: Raman spectra of solid state astaxanthin and copper chloride complex (normalized), Ratio of astaxanthin and copper chloride in complexes 1:3 (black), 1:2 (red), 1:1 (green), 2:1 (yellow) and 3:1 (blue). Astaxanthin (98%) (dashed dark red).

Astaxanthin raman bands were found at frequencies of 1155 cm^{-1} and 1510 cm^{-1}, the two peaks are a product of C-C and C=C stretching respectively. A third peak present at 1010 cm^{-1} is a result of the C=CH stretch (Parab and Tomar. 2012). The complexes exhibited the three characteristic frequencies of C=C, C-C and C=CH at 1550 cm^{-1}, 1284 cm^{-1} and 900 cm^{-1} respectively. The modes were at a rather low intensity, the highest intensity corresponding to the highest concentration of 0.03 mM.

The raman signal obtained proved poor this is again reflective of the lower concentrations of the complexes. The C-C stretch frequency had shifted to 1280 cm^{-1}, this shift can be an indication of the involvement of functional group in the binding of the ligand and metal. A CH_3 asymmetric stretch is detected at a frequency of 1410 cm^{-1}, this new feature may have been detected due to the lower intensity of the peaks. The C=CH and C=C stretch at 1010 and 1510 1410 cm^{-1} respectively remained in positon. Another notable changes is the difference in peak height between the C=C and C-C modes, whereas in chapter 3 (figure 3.7) the two modes are predominant and only differ slightly in height. This decrease can be an indication of the involvement of the C=C in complexation.

Vibrational spectroscopy proved difficult at the lower concentrations of the complexes, the characteristic functional groups peak had decreased dramatically hindering the detection of changes. The notable changes discovered included a C-Cl stretch in infrared, C-C stretch shift to a higher frequency of 1280 cm^{-1} and a CH_3 asymmetric stretch in raman.

4.2.3 Electrochemical analysis

4.2.3.1 Cyclic voltammetry

Cyclic voltammetry is implemented to measure the effect of the metal chelate complex on radical scavenging abilities of the xanthophyll astaxanthin. In figure 4.15 of the complex refluxed at 37 °C, the initial anodic scan revealed two features at a potential of 0.64 V and 1.25 V these correspond to the oxidation of the neutral carotenoid and radical cations and dications formed (Britton et al. 2008, Focsan et al. 2014). In the

reverse cathodic reduction scan two peaks were observed at 0.76 and 0.25 V corresponding to the radical dications and cations reduction. Reversible cyclic voltammograms are difficult to obtain in carotenoid studies due to the naturally low stability of the formed radicals (Focsan et al. 2014). The decreased stability accounts for the small features. Higher concentrations of copper chloride resulted in an increased peak height, i.e. increased stability. This is reflective of the stabilisation effect of copper chloride on the astaxanthin molecule.

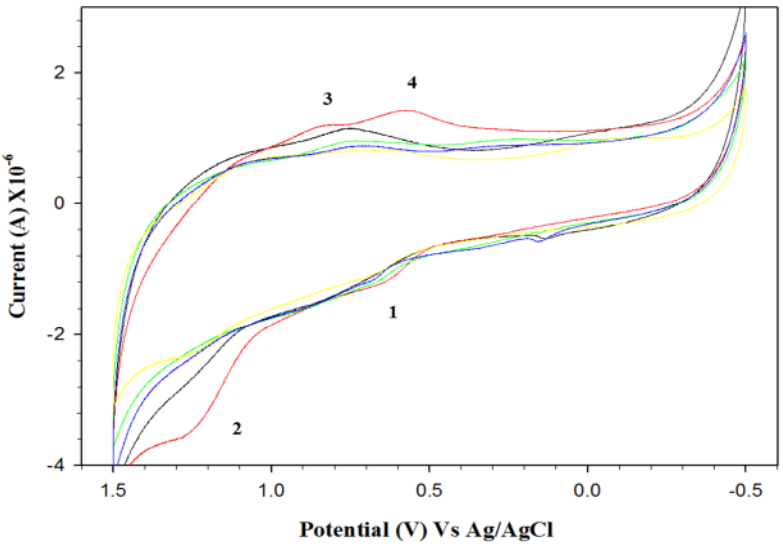

Figure 4.15: Cyclic voltammograms of refluxed astaxanthin and copper chloride complex refluxed at 37 °C in 0.1 M TBA TFO acetonitrile. Ratio of astaxanthin and $CuCl_2$ in complexes 1:3 (black), 1:2 (red), 1:1 (green), 2:1 (yellow) and 3:1 (blue).

Complexes refluxed at 78 °C produced two peaks in both the anodic and cathodic scan, proving again a more stable complex. In the anodic scan oxidation of the neutral carotenoid and production of radicals occurred at 0.69 V and 1.1 V respectively. Reduction peaks detected at 1.24 V and 0.82 V, resultants of radical dications and cations. The reversed ratio of 2 ligand: 1 metal chloride produced a single peak in both anodic and cathodic scans setting it apart from the other complexes. The oxidation peak at 0.93 V and reduction peak at 0.85 V, both are an indication of the alteration of astaxanthin two electron oxidation transfer into a single oxidation transfer hence altering the antioxidant activity. All apart from one of the complexes refluxed at 78 °C

exhibited a stabilisation effect. This is compared to the single electron oxidation transfer recorded in the previous characterisation of astaxanthin in chapter 3 as only a single notable peak is detected in each scan. Shifting of the peaks is reflective of the electrode condition as the scan rate remained constant.

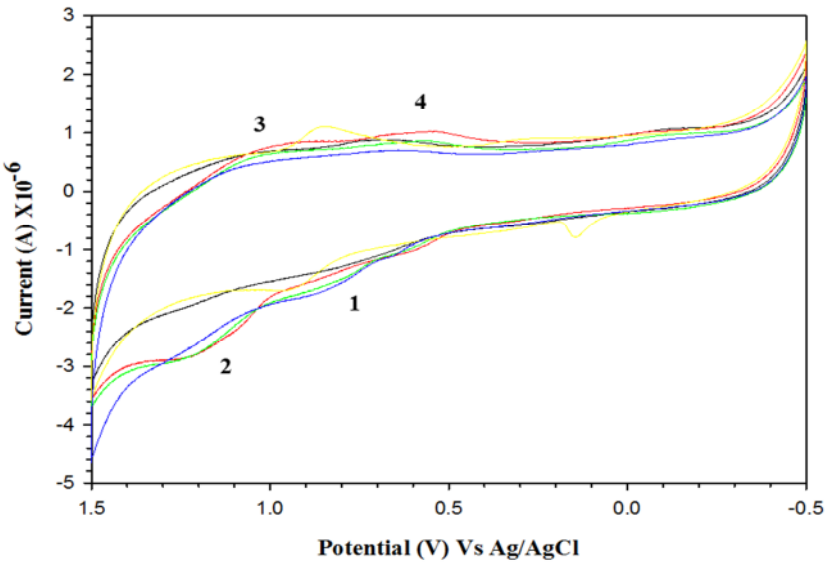

Figure 4.16: Cyclic voltammograms of refluxed astaxanthin and copper chloride complex refluxed at 78 °C in 0.1 M TBA TFO acetonitrile. Ratio of astaxanthin and $CuCl_2$ in complexes 1:3 (black), 1:2 (red), 1:1 (green), 2:1 (yellow) and 3:1 (blue).

Overall the complex formation with copper chloride altered the characteristics of astaxanthin, each technique revealing an alteration assisting in gaining a better understanding of the metal chelate complex formed. Temperature plays an important role in the arrangement of the monomers in the aggregates, lower temperatures producing J- type and higher temperatures producing a more tight packed H- type aggregate. The results obtained through electronic, vibrational and electrochemical studies demonstrated changes in the characteristics of the monomer astaxanthin involved in a complex with copper chloride. The electronic spectroscopy revealed a 1:1 ratio in the complexes, both J-type and H-type aggregates and detectable fluorescence bands. Vibrational spectroscopy presented a large decrease in the OH stretch, a C-Cl stretch and C=C decrease Electrochemical studies present a more stable complex. Accumulation of the data collected over this chapter predicted two possible structures of the astaxanthin and copper chloride complexes, these differ in the synthesis

temperature. The complexes are presented in figure 4.17. The J-type aggregate formation at a room temperature of 20 °C and a body temperature of 37 °C.

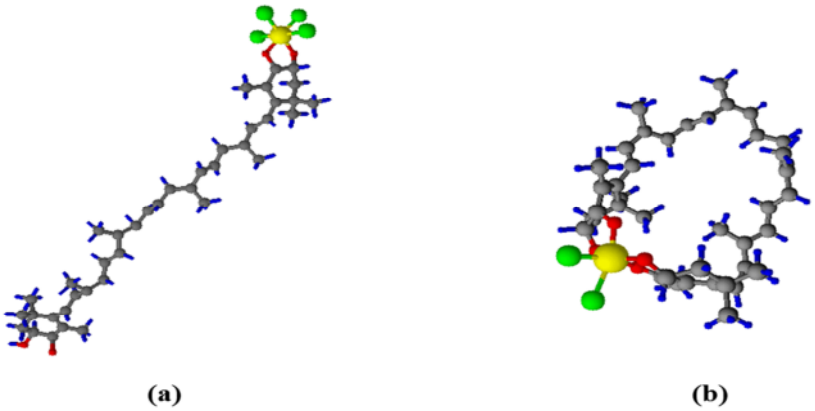

Figure 4.17: Predicted astaxanthin and copper chloride complexes formed in solution at varying temperatures, (a) J- type aggregate (head to tail) and (b) H-Type aggregate (face to face), generated through chemsketch software.

The complex synthesised at 78 °C is of a H-type aggregate exhibiting a more tight packing, the assembly of this complex is assumed as the binding of the two ends of the astaxanthin monomer to cobalt chloride complex through the carbonyl and OH groups. This assembly is implied by the electronic spectra of the complex as the astaxanthin appeared to mask the absorbance of the copper chloride peak.

Chapter 5
Cobalt chloride and astaxanthin complex

5.0 Introduction

Cobalt is one of the most common transition metals, it is found in many food supplement and naturally in vitamin B_{12} which functions as a catalyst in biochemical reactions (Mahaffy et al. 2014). Cobalt conforms to the norm of the transition metals by possessing two electrons in the 4*S* orbital. This metal is chosen due to its suitability in biochemical application and dietary intake therefore its formation of complexes with astaxanthin during the digestion is feasible. The current movement of greater antioxidants intake has increased the popularity of astaxanthin but it is questionable whether this powerful radical scavenging ability withstands the biochemical reaction incurred following ingestion or not. A biochemical reaction will be assimilated between

the carotenoid and cobalt chloride in the following chapter and the resultant complexes characterised.

5.1 Synthesis of astaxanthin and cobalt chloride complexes

The absorption difference between astaxanthin and cobalt chloride proved problematic using jobs plot method as it is essential to hold the overall concentration of the mixture. At the lower concentrations (<0.04 mM) the cobalt chloride maximum absorption peak at 657 nm is not detected. A different method by Benesi-Hildebrandt is implemented this involved the preparation of solutions with one component increasing and the next held constant. The astaxanthin and cobalt complexes were synthesised at room temperature (20 °C), this is followed by a reflux at a body temperature of 37 °C and 78 °C. A reflux at higher temperatures is to examine the effect of higher activation energy on the binding of the ligand and metal. As a general observance the astaxanthin and cobalt chloride complexes exhibited a colour change following refluxing at higher temperatures, this is more so at 78 °C as seen in figure 5.1. Another change is observed during the storage of the complexes at a lower astaxanthin preserving temperature of -20 °C, the colour of the complex in solution transforms into a more pigmented pink/ red colour, shown in figure 5.1. This colour change is attributed to thermochromism.

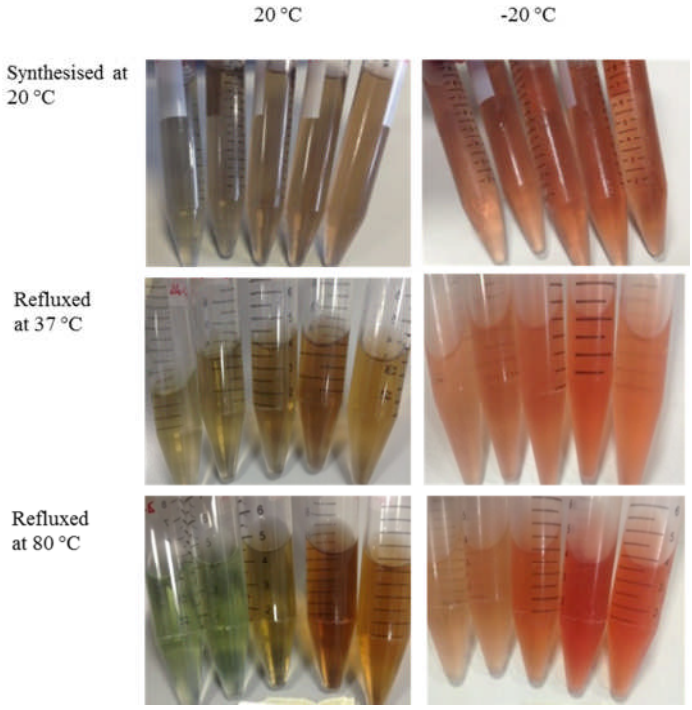

Figure 5.1: Cobalt chloride and astaxanthin complex in ethanol before and following refluxing at 37 °C and 78 °C, (a) $CoCl_2$ increase from left to right and astaxanthin constant 0.02 mM, (b) Astaxanthin increase from left to right and $CoCl_2$ constant 3 mM

Thermochromism of the complex in solution originates from the changes of the ligand coordination number, this phenomenon occurs largely with transition metal complexes involving cobalt and nickel (Seeboth and Lötzsch 2013). This change is also exhibited during the reflux of the complex at an elevated temperature of 78 °C, the complex had changed into a green colour, figure 5.2 outlines the stages of the complex colour reverting from green (78 °C) to a dark orange (20 °C). Unfortunately a closer examination of the effect on the absorbance of the complex is unfeasible in this project due to absence of a temperature controlled UV-Vis spectrophotometer.

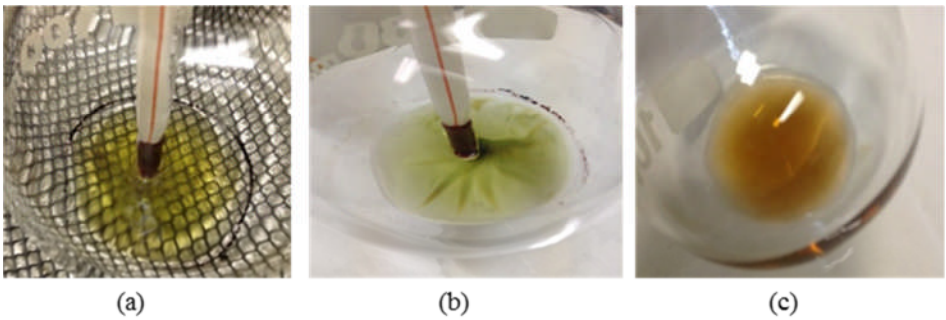

Figure 5.2: Thermochormism with heat of astaxanthin (0.024 mM) and $CoCl_2$ (3 mM) complex in ethanol, (a) precipitate during reflux at 78°C, (b) astaxanthin and metal complex at 78 °C (green) & (c) astaxanthin and metal complex at room temperature (dark orange).

5.2 Characterisation of astaxanthin and cobalt chloride complexes

5.2.1 Electronic spectroscopy

5.2.1.1 Absorption spectroscopy

The absorbance of astaxanthin increased linearly with the increase in concentration unaffected by the presence of cobalt chloride, conforming to beer's law. Whereas the constant cobalt chloride peak height changed alongside the increase in astaxanthin. The R-band absorption of astaxanthin at 294 nm is a carbonyl characteristic peak generated by the transition of the carbonyl group from n→ π* (Yuan et al. 2012), this appeared less distinctive following complex synthesis. The R- band represents the carbonyl group thus an assumption of its involvement in the binding of the complex is founded confirming its complexation role.

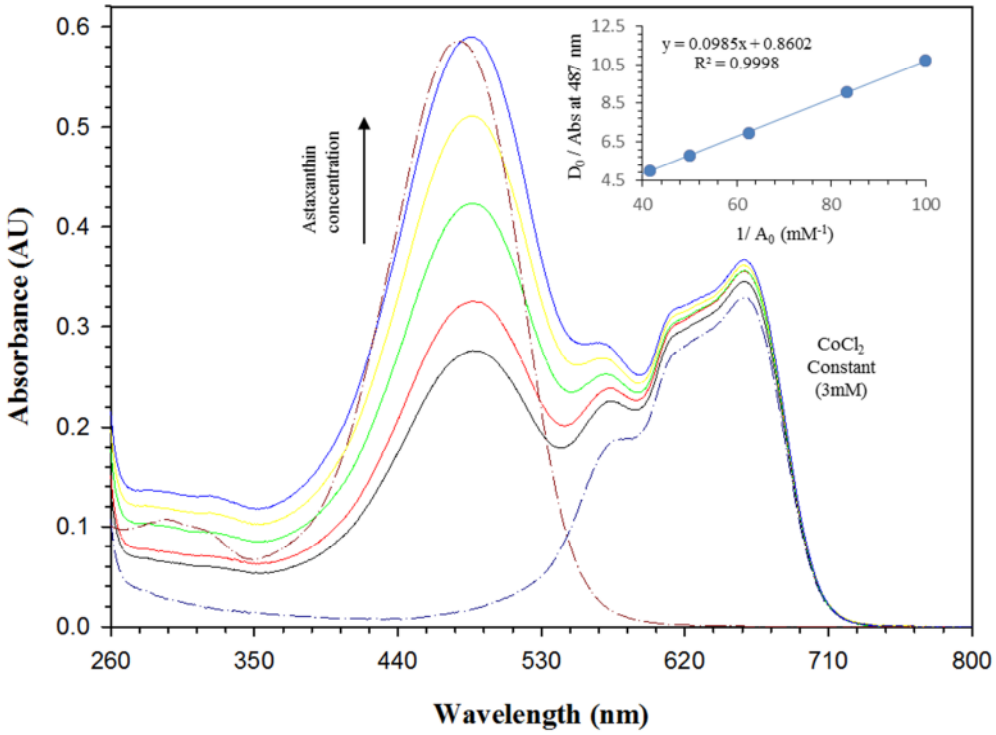

Figure 5.3: Electronic spectra of astaxanthin and $CoCl_2$ complexes synthesised at room temperature (20 °C) in ethanol (normalized), astaxanthin increasing concentrations and $CoCl_2$ held constant at 3 mM, astaxanthin (0.02 mM) (dashed dark red) and $CoCl_2$ (3 mM) (dashed dark blue) normalized. Inset of Benesi Hildebrand plot of 1/ [A_0] versus D_0 / Abs at 487 nm.

The electronic spectra of the ligand and metal complex revealed a shift of only one of the two components, the maximum K- band absorption peak ($\pi \rightarrow \pi^*$) of astaxanthin shifted 9 nm in the bathormic direction. The bathormic shift is in accordance with the molecular excitation model an indication of a loose type association (J- or head to tail) (Yadav 2005). This J- type one dimensional molecular assembly joining monomer centre end to end increases the length resulting in a higher wavelength (Johal et al. 2011). The inset of Benesi hildebrands plot in figure 5.3 is linear demonstrating a 1: 1 binding ratio of the ligand to metal (Polyakov et al. 2010).

Next the complexes synthesised at higher temperatures were examined, the first being at 37 °C matching that of body temperature. The bathormic shift presented itself again but this time a smaller shift of 5 nm is recorded.

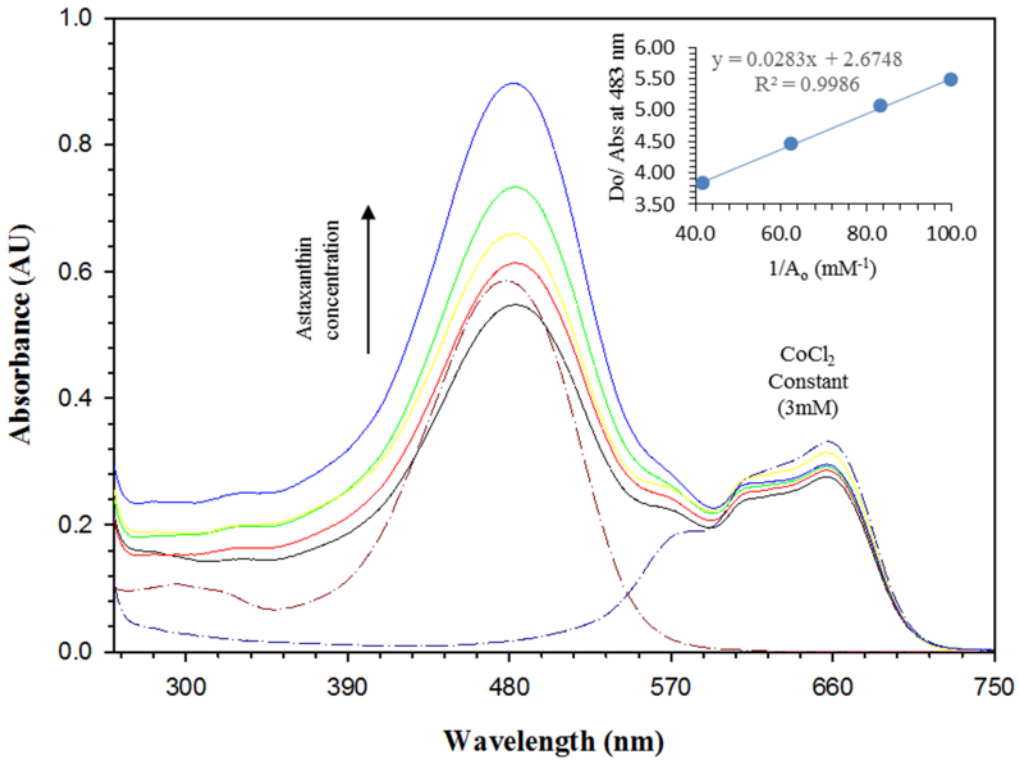

Figure 5.4: Electronic spectra of astaxanthin and $CoCl_2$ complexes refluxed at 37 °C in ethanol (normalized), astaxanthin increasing concentrations and $CoCl_2$ held constant at 3 mM, astaxanthin (0.02 mM) (dashed dark red) and $CoCl_2$ (3 mM) (dashed dark blue) normalized. Inset of Benesi Hildebrand plot of 1/ [A_0] versus D_0 / Abs at 483 nm.

This shift suggested a J-type aggregate forming between the astaxanthin and cobalt chloride. From the inset of benesi hildebrands plot in figure 5.4 it can be determined that the ratio of ligand to metal is that of 1:1. Shifts in the complexes formed have only been observed on the astaxanthin maximum K-band absorption while the cobalt chloride band remains at the original wavelength of 662 nm. Astaxanthin appears to favour a J- type aggregation at lower temperatures as also observed with the copper chloride in chapter 4.

The complexes formed at the highest temperature of 78 °C demonstrated a varied result as the peak appeared un-changed at the original wavelength of 478 nm, but through a closer examination a slight shift of 2 nm is detected, shown in figure 5.5. The interesting difference in these complexes refluxed at 78 °C is the presences of two shifts of 2 nm, one in the bathormic direction (1:3, 1:2 and 1:1) and the other in the hypsochromic direction (2:1 and 3:1). The shift in itself is but a small 2 nm but the

different direction can prove that the concentrations of the ligand and metal can impact the complex formation as opposed to the higher activation energy alone.

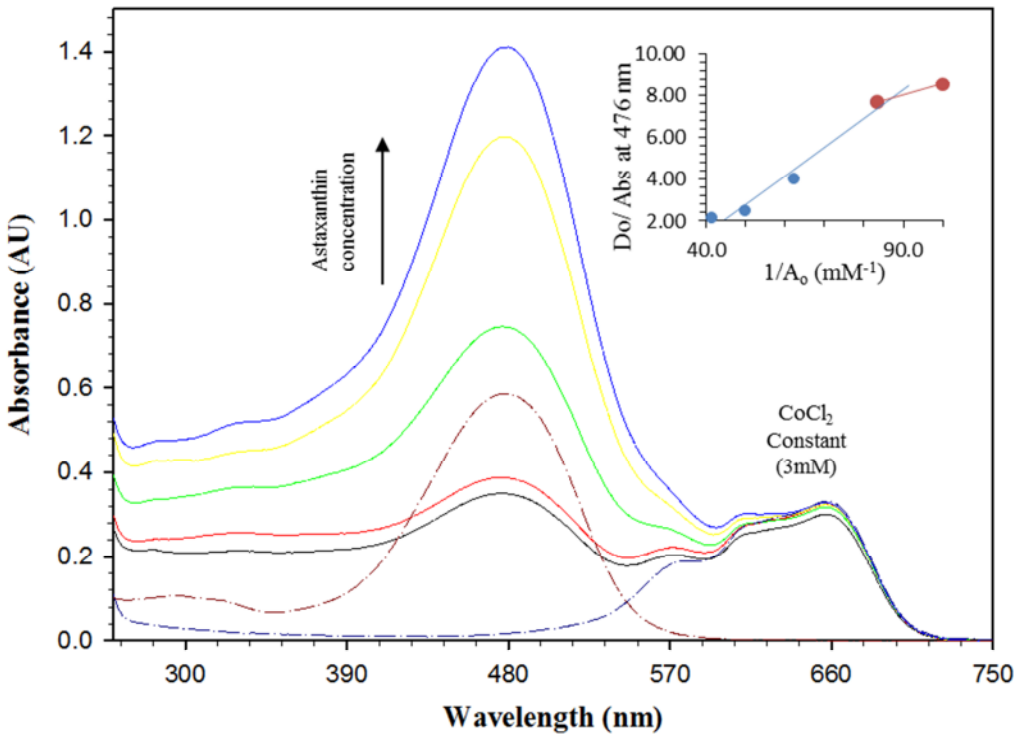

Figure 5.5: Electronic spectra of astaxanthin and $CoCl_2$ complexes refluxed at 78 °C in ethanol (normalized), astaxanthin increasing concentrations and $CoCl_2$ held constant at 3 mM, astaxanthin (0.02 mM) (dashed dark red) and $CoCl_2$ (3 mM) (dashed dark blue) normalized. Inset of Benesi Hildebrand plot of 1/ $[A_0]$ versus D_0 / Abs at 476 nm.

In the inset of figure 5.5 it can be seen that the plot the two lines intersecting shows a 2:1 binding ratio of the ligand to metal (Polyakov et al. 2010). In the plot the absorbance of astaxanthin begins to level off following a concentration of 0.02 mM this is assumed a result of aggregation of astaxanthin and cobalt chloride. The complexes formed at different temperatures with cobalt chloride demonstrated very little changes in the electronic spectra of the complex at room temperature. An interesting feature to examine would be the thermochromism distinctly shown in figure 5.1, unfortunately due to instrumentation limitations this is unattainable in this research.

In figure 5.6 the spectra of the complexes formed at different temperatures are accumulated to allow a more general comparison. Once again the cobalt chloride peaks remained strong at 662 nm as opposed to the copper chloride peak shifting in complex formation. One can argue that no changes in the wavelength of the metal chloride could

be an indication of the absence of complex formation and the astaxanthin k-band shifts were a result of the changes impacted by the metal chloride on the surrounding environment. As demonstrated in chapter 3 during the characterisation of the carotenoid that the placement of the absorbance bands are sensitive to the solvent used and previous research has shown the sensitivity of astaxanthin to the addition of salts (Britton et al. 2008).

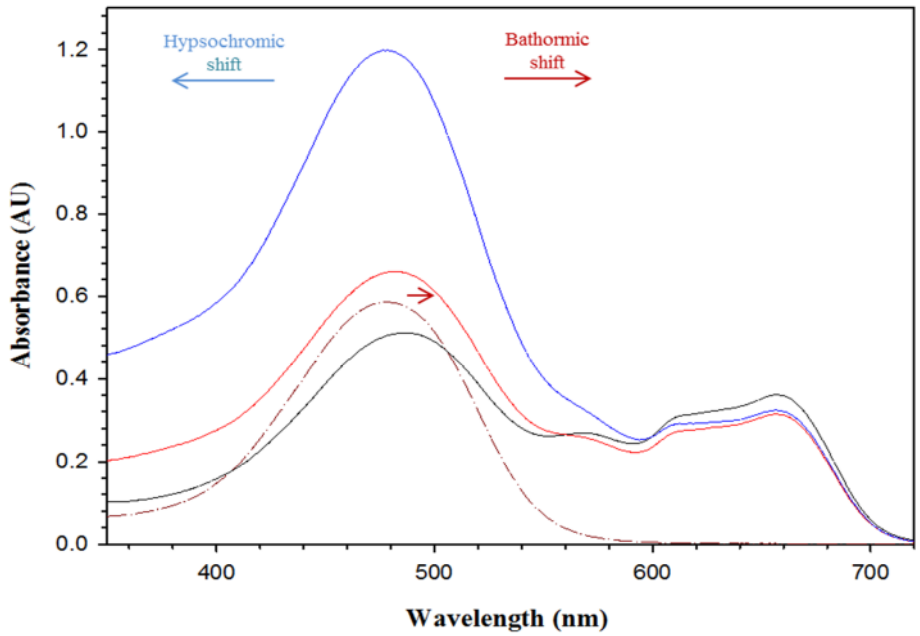

Figure 5.6: Electronic spectra comparing shift between complexes of astaxanthin and cobalt chloride (normalized) astaxanthin (0.04 mM) (dashed dark red), astaxanthin and $CoCl_2$ complexes synthesised at room temperature (black), refluxed at 37 °C (red) and refluxed at 78 °C (blue).

Table 5.1: Absorbencies of astaxanthin in all three synthesised complexes at 20, 37 and 78 °C

Synthesis temperature (°C)	20	37	78
Astaxanthin Concentration (mM)	Absorbance at 487 nm (AU) ± 0.001	Absorbance at 483 nm (AU) ± 0.001	Absorbance at 476 nm (AU) ± 0.001
0.010	0.280	9.547	0.350
0.012	0.330	0.590	0.390
0.016	0.430	0.590	0.750
0.020	0.520	0.674	1.200
0.024	0.600	0.781	1.400

The J- type (head to tail) aggregates were formed across the three complexes, the only difference is observed in the final refluxed complex at 78 °C which demonstrated a

different shifts between different concentrations of astaxanthin. The large difference in the absorption of astaxanthin and cobalt chloride caused difficulties in the preparation of the complexes, as the large absorbencies can in some cases veil the smaller changes. Next the dry state complexes were examined on quartz cells to detect any crystalline formation under a microscope at a power of 10x.

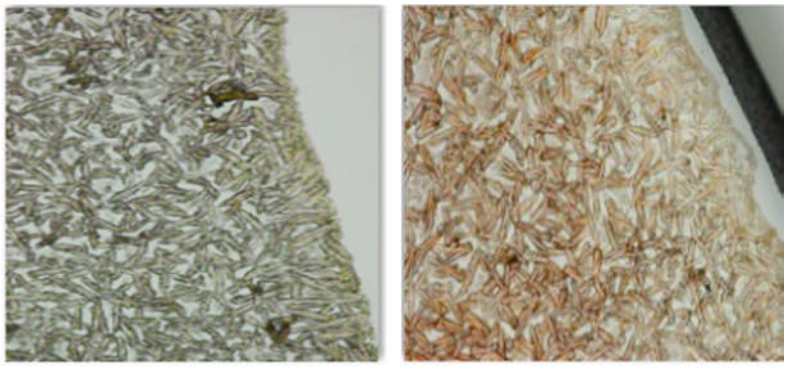

Figure 5.7: Dry state astaxanthin and $CoCl_2$ complex refluxed at 37 °C on quartz window at 10x (edge) of the highest and lowest concentrations of astaxanthin (a) 0.01 mM and (b) 0.024 mM while $CoCl_2$ constant at 3 mM.

The crystal structure appearing on the surface of the glass window is that of astaxanthin and increases in colour alongside the concentration. Between the two complexes in figure 5.7 and 5.8 barely any difference can be seen apart from the increased characteristic pigmentation of the higher astaxanthin concentration of 0.024 mM.

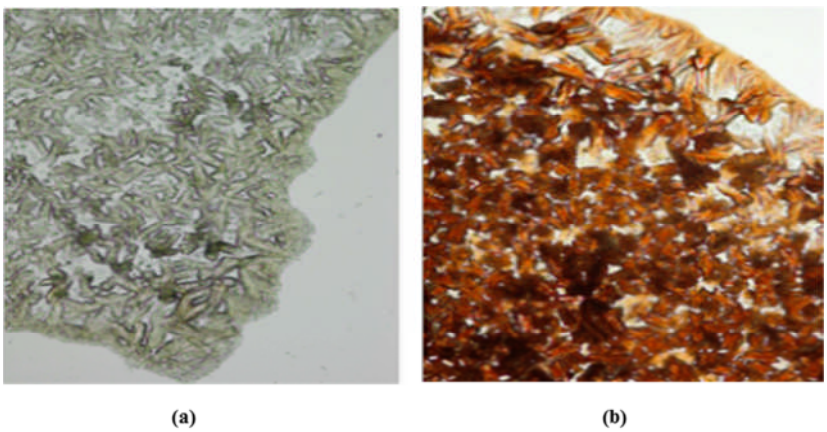

Figure 5.8: Dry state astaxanthin and $CoCl_2$ complex refluxed at 78 °C on quartz window at 10x (edge) of the highest and lowest concentrations of astaxanthin (a) 0.01 mM and (b) 0.024 mM while $CoCl_2$ constant at 3 mM.

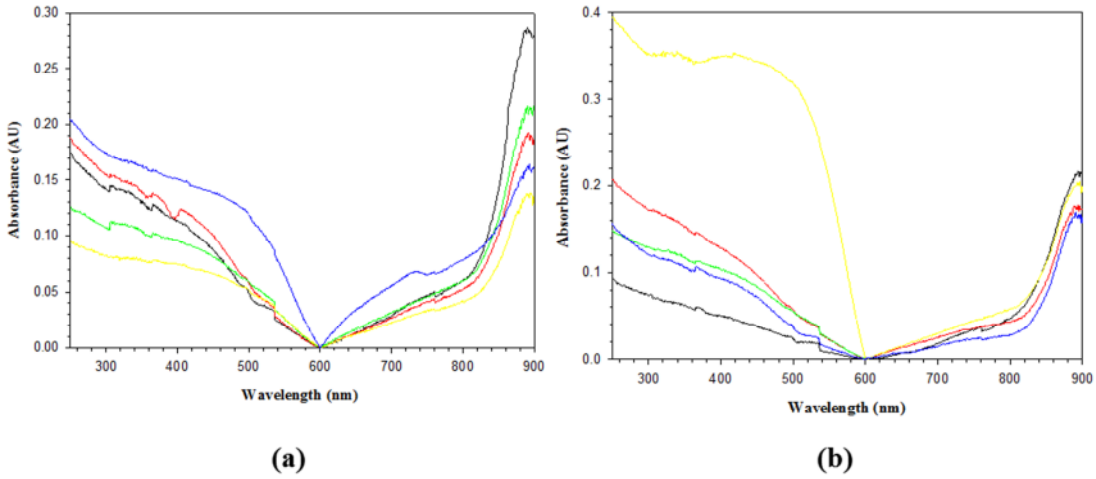

Figure 5.9: Electronic spectra of dry state astaxanthin and $CoCl_2$ complexes on quartz window (normalized), (a) refluxed at 37 °C and (b) refluxed at 78 °C (normalized). Astaxanthin concentrations 0.01 mM (black), 0.012 mM (red), 0.016 mM (green), 0.020 mM (yellow) and 0.024 mM (blue).

The Electronic spectra collected from the dry state complexes proved very weak in signal and an absorption band in the green region of 900 nm is observed. This is similarly found in the copper complexes. The absorption band weakness is caused by the non-uniform coating of the sample on the surface as seen in figures 5.7 and 5.8 the complexes were concentrated in certain area causing inaccuracies in the spectra. The comparison of the complexes absorption in solution and dry states is not feasible, an instrument capable of covering a smaller surface area is required for dry state complex examination.

5.2.1.2 Fluorescence spectroscopy

The fluorescence spectra revealed no bands as discussed previously the fluorescence lifetime measurement of carotenoid like molecules occur in picoseconds range (Bautista et al. 1999) whereas the instrument limitations of the Perkin elemer LS45 measures in milliseconds restricting the fluorescence spectroscopic analysis of the formed complexes. The formation of the astaxanthin and cobalt chloride complexes did not have a reducing effect on the speed of the electrons as with the astaxanthin and copper chloride complexes hence detection of the changes were unattainable in this instance. The absence of spectra can be an indication of the absence of complexes synthesised at the three temperatures of 20 °C, 37 °C and 78 °C

5.2.2 Vibrational spectroscopy

5.2.2.1 Infrared spectroscopy

In an attempt to determine the function al groups involved in the complex formation between the ligand and the metal salt infrared spectroscopy is employed. Dry state examination on sodium chloride windows confirms the characteristic functional groups associated with astaxanthin. These include a carbonyl stretching mode at 1660 cm^{-1} and a hydroxyl stretch at 3400 cm^{-1} (Mahaffy et al. 2014, Yuan et al. 2005).

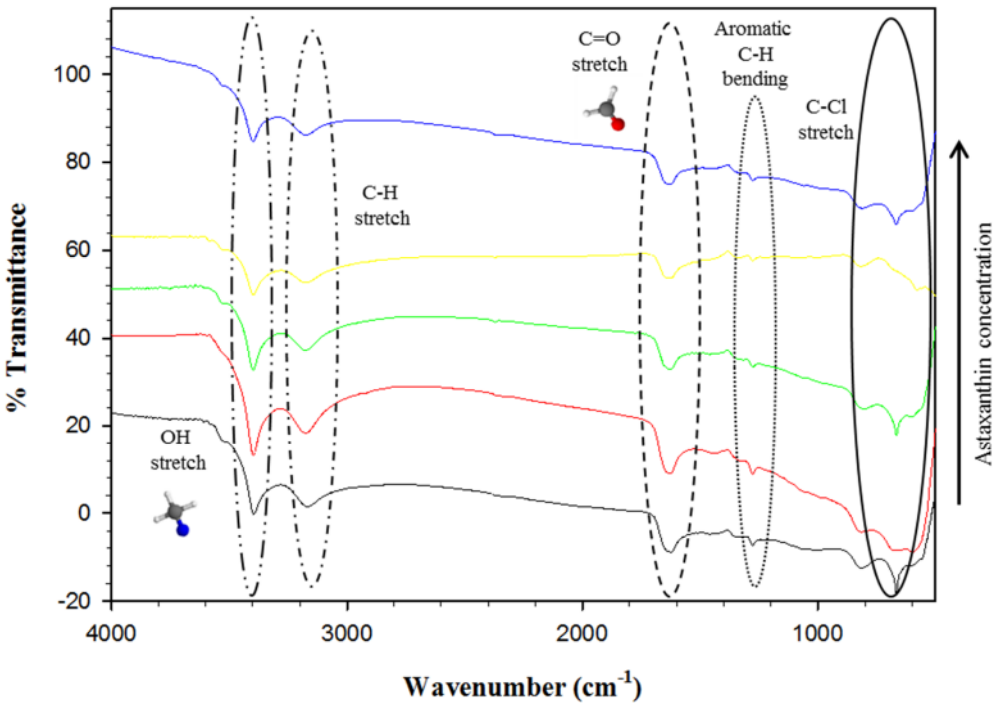

Figure 5.10: Infrared spectra of astaxanthin and complexes formed with cobalt chloride (normalized), concentration of astaxanthin 0.01 mM (black), 0.012 mM (red), 0.016 mM (green), 0.020 mM (yellow) and 0.024 mM (blue). Corresponding functional groups labelled.

Frequencies of 3170 cm^{-1} and 1270 cm^{-1} correspond to a C-H stretch and aromatic C-H bending. The C-Cl stretch is present at a frequency of 670 cm^{-1}, its presence varies with the concentration of astaxanthin and no exact pattern is deducted. The frequency with the largest shift is determined the OH group, this can assist in predicting the structure of the complex. The slight if any changes imply the absence of ligand and metal complexes.

5.2.2.2 Raman spectroscopy

Raman is employed to detect the vibration changes of the functional groups involved in the complexation of the astaxanthin and metal complexes. The raman shift is measured at an integration time of 90 sec and frame size of 30 sec. Noteworthy characteristic peaks of carotenoids occur at frequencies of 1550 cm^{-1} associated with the C-C stretching and the C=C stretch between 1400 – 1600 cm^{-1} (Deoliveira et al. 2010, Parab and Tomar 2012). These are detected in the raman spectra, matching that of the previous complex.

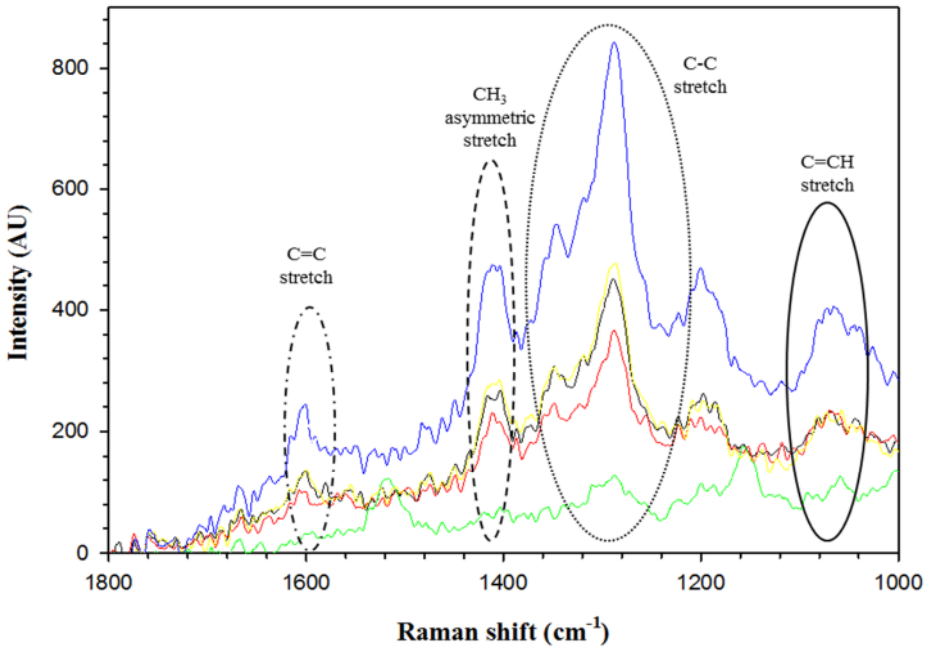

Figure 5.11: Raman spectra of astaxanthin and complexes formed with cobalt chloride (normalized), astaxanthin concentrations 0.01 mM (black), 0.012 mM (red), 0.016 mM (green), 0.020 mM (yellow) and 0.024 mM (blue). Corresponding functional groups labelled.

The characteristic frequencies of C-C and C=C are present at 1285 and 1600 cm^{-1} with little or no shifting. Similarly as with in the copper complex the cobalt complex C-C and C=C modes varied largely in peak height as opposed to the spectra of astaxanthin alone in figure 4.14. CH_3 asymmetric stretching is present at 1400 cm^{-1} and C=CH stretching at 1000 cm^{-1}. The weakness in the signal detected can prove problematic in assessing the structure in greater detail. Vibrational spectroscopy overall revealed slight changes in the detectable functional groups of the ligand.

5.2.3 Electrochemical analysis

5.2.3.1 Cyclic voltammetry

In assessment of the antioxidant activity of astaxanthin in the complex cyclic voltammetery is carried out. Originally in chapter 3 on the characterisation of astaxanthin a one electron oxidation transfer is observed in electrolyte 0.1 M TBA TFO (in acetonitrile), whereas in figure 5.12 a two electron oxidation transfer system is observed.

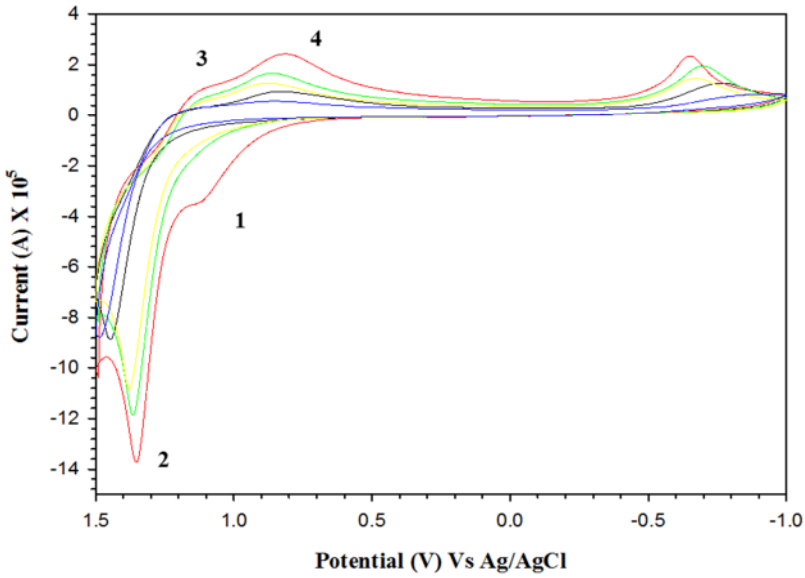

Figure 5.12: Cyclic voltammograms of refluxed astaxanthin and cobalt chloride complex refluxed at 37 °C in 0.1 M TBA TFO acetonitrile. Astaxanthin concentrations 0.01 mM (black), 0.012 mM (red), 0.016 mM (green), 0.020 mM (yellow) and 0.024 mM (blue).

In the initial anodic scan the complex refluxed at 37 °C oxidation revealed two peaks at a potential of 1.1 V and 1.35 V, these in accordance with the literature correspond to the neutral carotenoid and radical cations and dications formed (Britton et al. 2008, Focsan et al. 2014). In the cathodic scan the two characteristic peak resulting in the reduction of the astaxanthin radical dications and cations (Focsan et al. 2014) are present at 1.12 V and 1.35 V respectively.

Next the complexes refluxed at 78 °C presented similar results as a two electron oxidation transfer is revealed. A difference is observed in the anodic scan as the first

peak of the oxidation of the neutral astaxanthin is found weak in signal and undetected at certain concentrations.

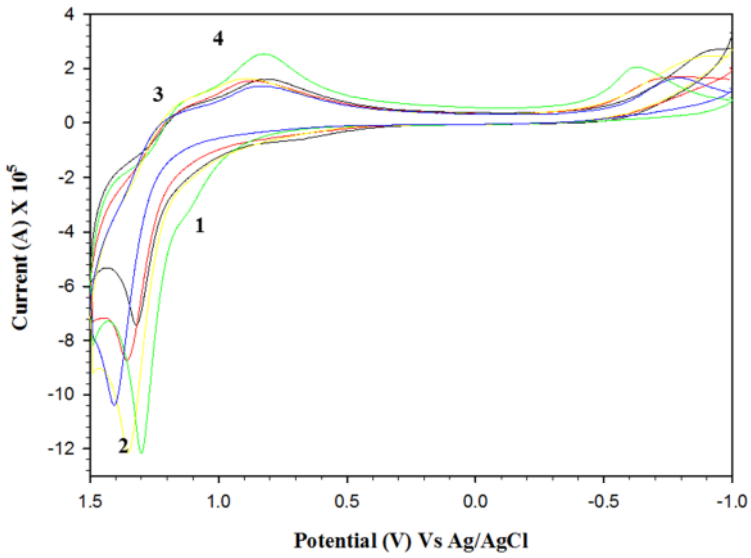

Figure 5.13: Cyclic voltammograms of refluxed astaxanthin and cobalt chloride complex refluxed at 78 °C in 0.1 M TBA TFO acetonitrile. Astaxanthin concentrations 0.01 mM (black), 0.012 mM (red), 0.016 mM (green), 0.020 mM (yellow) and 0.024 mM (blue).

On the other hand the two peaks on the return cathodic scan reveal a strong signal of the reduction of the astaxanthin radical dications and cations (Focsan et al. 2014) at potentials of 1.2 V and 0.85 V respectively. The stabilisation of the astaxanthin cobalt is demonstrated in the cyclic voltammogram as reversibility is achieved, this effect can be a result of the complexation of astaxanthin and cobalt chloride or the stabilisation of the surrounding environment in the presence of the metal salt. An additional peak in the cathodic scan is identified as oxygen and peak shifting is resultant of the condition of the electrode.

The data collected over the variety of electronic, vibration spectroscopy and electrochemical techniques reveal an absence in significant changes to imply the formation of a cobalt chloride and astaxanthin complex. The minor shift presented in the electronic spectra give the impression of a J-type formation as in figure 5.14.

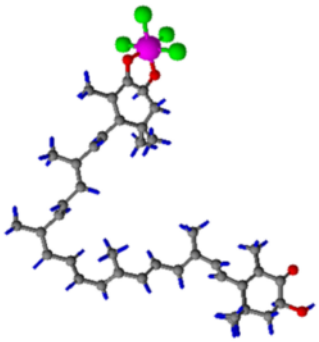

Figure 5.14: Predicted astaxanthin and cobalt chloride complexes formed in solution in a J-type arrangement (head to tail), generated through chemsketch software.

One of the significant changes presented is the stabilisation of the astaxanthin molecule. This can prove beneficial during digestion as the astaxanthin molecule can carry out its radical scavenging abilities during digestion while the cobalt helps in providing a more stable surrounding environment. The cobalt transition metal proved unreactive with the ligand astaxanthin and complexation is little if any.

Chapter 6
Summary discussion and conclusion

6.1 Summary discussion

The xanthophyll astaxanthin is proven extractable from the native Irish brown crab (*Cancer pagurus*). This is achieved using the polar solvent glacial acetic acid and a yield of 18.5 mg of extractable astaxanthin of 100g of crab shell. The choice of the solvent proved favourable in comparison with results of Vilasoa-Martínez et al. (2008) where acetone is chosen as the extracting solvent for snow crab and only a yield of 1.79± 1.03 mg/100 g of snow crab is obtained.

The characterisation of astaxanthin followed, this enlisted the use of a range of electronic, vibrational and electrochemical techniques. Each technique examined a different characteristic of the carotenoid. In electronic spectra three bands are observed,

these include a K-band generated by the transition of the large conjugated molecule from $\pi \rightarrow \pi^*$, R-band a characteristic carbonyl peak generated by the transition of the carbonyl group from $n \rightarrow \pi^*$ and the third K- band absorption as a results of the hexatomic ring absorption. The peak of interest during the synthesis of complexes is the maximum K-band absorption as any shifting assists in determining the formation of the complexes. Vibrational spectroscopy using Infrared and raman confirmed characteristic carotenoid modes. In infrared spectra the functional groups OH and C=O were detected at 3470 cm^{-1} and 1660 cm^{-1}. In raman spectra the characteristic three modes C=C,C-C and C=CH were detected at 1510 cm^{-1},1155 $cm^{-1}$and 1004 cm^{-1} respectively. The establishment of these characteristics allowed a close examination of the changes in the structure of the carotenoid and the functional groups responsible for the complexation with the transition metals. As a final technique cyclic voltammetry is applied to assess the electron transfer kinetics in the carotenoid before and following complexation. The electrochemical investigation of astaxanthin revealed a one electron transfer oxidation as opposed to the literature of a two electron transfer oxidation (Focsan, et al 2014), this variation is attributed to the sensitivity of the molecule.

The synthesis of the complexes follows and is carried out using two metal chloride these include copper chloride dehydrate ($CuCl_2.2H_2O$) and cobalt chloride hexahydrate ($CoCl_2.6H_2O$). The complexes were formed at three temperatures 20 °C, 37 °C and 78 °C. Body temperature is examined to attempt and replicate the temperature at which reactions would occur within the body following ingestion. The elevated temperatures at 78 °C is applied in an attempt to apply sufficient activation energy. Previously employed characterising techniques are applied to formed complexes. Successful complexation occurred with copper chloride as opposed to cobalt chloride proving futile. The electronics spectra proved insightful into the formation of the aggregates. Cobalt yielded very little change whereas copper exhibited a large hypsochromic shift in complexed refluxed at 78 °C proving an H-type aggregation. The large shift is also accompanied by a masking effect of the copper chloride absorbance band by that of the astaxanthin proving problematic in jobs plot and in turn the estimation of the binding ratio.

One of the main differences between the copper and cobalt complexes is the fluorescence life time measurements. As previously mentioned the fluorescence spectra

of astaxanthin are undetectable due the instrumental limitations as fluorescence lifetime measurement of carotenoid molecules are in picoseconds (Bautista et al. 1999). The complexes refluxed at 78 °C alone presented fluorescence bands, this is an indication of complexation. A plot of the absorbance and fluorescence bands revealed an exception to the mirror rule with a change in the peak shape. This change is attributed to geometric changes in the nuclei in the excited state in comparison to the ground state (Lakowicz 1999).

Vibrational spectroscopy yielded weak signals and very little changes were detected. Characteristic modes of astaxanthin are detected. The copper complex in comparison with that of the cobalt produced smaller peaks indicating complexation. Infrared spectra detected a C-Cl stretch peak corresponding to the metal chlorides. Raman spectra also revealed no significant changes as the sample concentrations proved too low.

Electrochemical investigation of the complexes revealed an overall stabilisation effect brought about by the metal salts. A two electron transfer oxidation is obtained in accordance with the literature (Focsan et al. 2014). Initial testing of the astaxanthin revealed a single electron transfer due to the production of the less stable radical cations and dications. This stabilisation effect can prove beneficial during the assimilation of astaxanthin improving its potential.

The synthesis of an astaxanthin and copper chloride complexes proved effective as changes are observed. An astaxanthin and cobalt chloride complex proved unfeasible as no significant changes are observed. Hence the assumption that astaxanthin is absorbed through metabolic reactions within the human body is founded. Further investigation of the exploiting these changes can be applied in industry. The wide variety of benefits associated with astaxanthin gives it the potential to be a powerful nutraceutical, these benefits include antioxidant and anti-inflammatory activity (Bagchi et al. 2010). The interferences within the digestion of the xanthophyll can improve or hinder these abilities.

6.2 Conclusion

Astaxanthin is a proven powerful antioxidant and anti-inflammatory. However the reactions the molecule undertakes following consumption can impair or hinder these abilities. Its extractability using glacial acetic acid, a high eutrophic strength solvent is proven effective. Characterisation of the molecule using a range of electronic, vibrational and electrochemical techniques provided a comparison platform for the changes incurred by the molecule following complexation. The formation of astaxanthin and metal complexes proved successful with the reactive copper as opposed to the unsuccessful cobalt chloride. Significant changes were recorded in the electronic spectra with a large maximum absorption band shift and life time fluorescence measurements. These occurred with the copper complexes refluxed at 78 °C demonstrating a need for a higher activation energy. The cobalt proved unreactive in this instance with astaxanthin and no detectable changes were recorded. The possibility of the use of astaxanthin as powerful nutraceutical must incorporate the changes during their assimilation across the intestinal wall before proving effective, as these biochemical reaction can hinder its activity or promote it through a stabilisation effect.

Chapter 7
Bibliography

7.1 Bibliography

Albertsson, J., et al. (1979) ‘Compounds with intermediate spin.3. Structure of tris [N, N-bis (2-hydroxyethyl) dithiocarbamato] iron (III) at 150 and 295 K’, ActaCrystallographica Section B: Structural Crystallography and Crystal Chemistry, 35(6), 1473-1476.

Alexandropoulou, I., Komaitis, M., and Kapsokefalou, M. (2006) ‘Effects of iron, ascorbate, meat and casein on the antioxidant capacity of green tea under conditions of in vitro digestion’, Food chemistry, 94(3), 359-365.

Ahmed, F., Li, Y., Fanning, K., Netzel, M. and Schenk, P. M. (2015) 'Effect of Drying, Storage Temperature and Air Exposure on Astaxanthin Stability from Haematococcus pluvialis', Food Research International, 74, 231-236.

Bagchi, D. (2001) 'Oxygen free radical scavenging abilities of vitamins C. E, β-carotene, pycnogenol, grape seed proanthocyanidin extract, astaxanthin and BioAstin® in vitro', Omaha: Creighton University School of Health Sciences.

Bagchi, D., Lau, F. and Ghosh, D. K. (2010) Biotechnology In Functional Foods and Nutraceuticals, Boca Raton, Fla.: CRC.

Bautista, J. A., Connors, R. E., Raju, B. B., Hiller, R. G., Sharples, F. P., Gosztola, D., Wasielewski M. R. and Frank, H. A. (1999) 'Excited state properties of peridinin: observation of a solvent dependence of the lowest excited singlet state lifetime and spectral behaviour unique among carotenoids', The Journal of Physical Chemistry B, 103(41), 8751-8758.

Benesi, H. A. (1949) 'The Benesi-Hildebrand Method for Determination of Kf for DA association and ε Values for DA CT absorption', Journal American Chemical Society, 71, 2703.

Bernstein, P. S., Yoshida, M. D., Katz, N. B., McClane, R. W. and Gellermann, W. (1998) 'Raman Detection of Macular Carotenoid Pigments in Intact Human Retina', Investigative Ophthalmology and Visual Science, 39, 2003-2011.

Britton, G., Pfander, H., & Liaaen-Jensen, S. (1996) Carotenoids, Volume 2: Synthesis, Germany: BirkhäuserVerlag,

Britton, G., Liaaen-Jensen, S., and Pfander, H. (2008) Carotenoids, Vol. 4: Natural Functions., Germany: BirkhäuserVerlag, 167-188.

Burnie, D. and D. E. Wilson (2001), Animal: The Definitive Visual Guide to the World's Wildlife, DK publishing.

Ramaa, C. S., Shirode, A. R., Mundada, A. S. and Kadam, V. J. (2006) 'Nutraceuticals-an emerging era in the treatment and prevention of cardiovascular diseases', Current pharmaceutical biotechnology, 7(1), 15-23.

Rivera, S. M. and R. Canela-Garayoa (2012) 'Analytical tools for the analysis of carotenoids in diverse materials', Journal of Chromatography A, 1224(0), 1-10.

Cotton, F. A. and G. Wilkinson (1988) Advanced Inorganic Chemistry, New York: Wiley.

Compton, R. G. and C. E. Banks (2011) Understanding Voltammetry, London: Imperial College Press.

Cornelis, R., Caruso, J. A., Crews, H. and Heumann, K. G. (Eds.) (2005) Handbook of Elemental Speciation, Handbook of Elemental Speciation II: Species in the Environment, Food, Medicine and Occupational Health, England: John Wiley & Sons.

Chan, T. R., et al. (2004) 'Polytriazoles as copper (I)-stabilizing ligands in catalysis', Organic letters, 6(17), 2853-2855.

Chunhua, Y. I. N., Shuzhen, Y. A. N. G., Xiaolu, L. I. U., and Hai, Y. A. N (2013) 'Efficient Extraction of Astaxanthin from Phaffiarhodozyma with Polar and Non-polar Solvents after Acid Washing'. Chinese Journal of Chemical Engineering, 21(7), 776-780.

Chen, C. S., Wu, S. H., Wu, Y. Y., Fang, J. M. and Wu, T. H. (2007) 'Properties of astaxanthin/Ca2+ complex formation in the deceleration of cis/trans isomerization', Organic letters, 9(16), 2985-2988.

Capelli, B. and G. Cysewski (2007) 'Natural Astaxanthin: King of the Carotenoids', USA, Cyanothech Corporation.

Dash, D. C. (2011) Analytical Chemistry, New Delhi: PHI Learning Private Ltd.

De Azevedo-Meleiro, C. H. and Rodriguez-Amaya, D. B. (2009) 'Qualitative and Quantitative Differences in the Carotenoid Composition of Yellow and Red Peppers Determined by HPLC-DAD-MS', Journal of Separation Science, 32(21), 3652-3658.

De Oliveira, V. E., Castro, H. V., Edwards, H. G., and De Oliveira, L. F. C. (2010) 'Carotenes and carotenoids in natural biological samples: a Raman spectroscopic analysis', Journal of Raman Spectroscopy, 41(6), 642-650.

Deman, J. M. (1999), Principles of Food Chemistry, Gatherburg: Aspen Publishers.

Elumalai, S., Santhose, B. I., and Kanna, G. R (2014) 'Extraction of carotenoid and thin layer chromatography (TLC), GC-MS, FT-IR and HPLC analysis of pharmaceutically important pigment astaxanthin from a new strain of Haematococcus pluvialis', Weekly Science Research Journal, 2(8), 2321- 7871.

Ewald, A. H., Martin, R. L., Sinn, E. and White, A. H. (1969) 'Electronic equilibrium between the 6A1 and 2T2 states in iron (III) dithio chelates', Inorganic Chemistry, 8(9), 1837-1846.

Focsan, A. L., Pan, S., & Kispert, L. D. (2014) 'Electrochemical Study of Astaxanthin and Astaxanthin n-Octanoic Monoester and Diester: Tendency to Form Radicals', The Journal of Physical Chemistry B, 118(9), 2331-2339.

Frank, H. A., et al. (1999) The Photochemistry of Carotenoids. Dordrecht: Kluwer Academic.

Frost and Sullivan (2011), Global Nutraceutical Industry: Investing in healthy living, Frost-FICCI report.

Gillbro, T. and Cogdell, R. J. (1989) 'Carotenoid fluorescence', Chemical Physics Letters 158(3), 312-316.

Goyal, M. R. (2013) Biofluid Dynamics of Human Body Systems, Canada: Apple Academic Press Inc.

Griffiths, P. R. and De Haseth, J. A. (2007) Fourier Transform Infrared Spectrometry. Chichester : John Wiley & Sons.

Gütlich, P. and Goodwin, H. A. (2004) Spin Crossover in Transition Metal Compounds, Berlin: Springer.

Hegedus, L. S. (1999) Transition metals in the synthesis of complex organic molecules, U.S.: University Science Books.

Hernández-Marin, E., Barbosa, A., and Martínez, A. (2012) 'The metal cation chelating capacity of astaxanthin. Does this have any influence on antiradical activity?', Molecules, 17(1), 1039-1054.

Hu, X., Jandacek, R. J. and White, W. S. (2000) 'Intestinal absorption of β-carotene ingested with a meal rich in sunflower oil or beef tallow: postprandial appearance in triacylglycerol-rich lipoproteins in women', The American journal of clinical nutrition, 71(5), 1170-1180.

Janes, R. and E. Moore (2004) Metal-Ligand Bonding, Cambridge: Royal Society of Chemistry.

Jelley, E. E. (1936) 'Spectral absorption and fluorescence of dyes in the molecular state', Nature, 138(3502), 1009-1010.

Johal, M. S. and Johnson L. E. V. (2011) Understanding nanomaterials, USA: CRC Press.

Kaczor, A., Turnau, K. and Baranska, M. (2011) 'In situ Raman imaging of astaxanthin in a single microalgal cell', Analyst, 136(6), 1109-1112.

Kamberg, M. L. (2010) The Transition Elements: The 37 Transitions Metals, USA: The Rosen Publishing Group Inc.

Ke, B. (2001) Photosynthesis: Photobiochemistry and Photobiophysics. Dordrecht: Kluwer Academic.

Khanafari, A., Saberi, A., Azar, M., Vosooghi, G., Jamili, S. and Sabbaghzadeh, B. (2007) 'Extraction of astaxanthin esters from shrimp waste by chemical and microbial methods', Iranian Journal of Environmental Health Science & Engineering, 4(2), 93-98.

Lakowicz, J. R. (1999) Principles of Fluorescence Spectroscopy, New York: Kluwer Academic.

Landrum, J. T. (2009) Carotenoids: Physical, Chemical and Biological Functions and Properties, CRC Press.

Larkin, P. (2011) Infrared and Raman Spectroscopy; Principles and Spectral Interpretation. USA: Elsevier Inc.

Leipoldt, J. G. and Coppens P. (1973) 'Correlation between structure-and temperature-dependent magnetic behavior of iron dithiocarbamate complexes.Crystal structure of tris

(N, N diethyldithiocarbamato) iron (III) at 297.deg. and 79. deg. K', Inorganic Chemistry, 12(10), 2269-2274.

Li, H. P., Gong, G. C., & Hsiung, T. M. (2002) 'Phytoplankton pigment analysis by HPLC and its application in algal community investigations', Botanical Bulletin of Academia Sinica, 43, 283-290.

Mahaffy, P., et al. Bucat, B., Tasker, R., Kotz, J. C., Weaver, G. C., Treichel, P. M. and McMurry, J. E. (2014) Chemistry: Human Activity, Chemical Reactivity, USA: Nelson Education Ltd.

Manjabhat, S. N., Narayan, B. and Subbanna, M. N. (2006) 'Carotenoids in Solonoceraindica and Aristeusalcocki, deep-sea shrimp from Indian waters', Journal of aquatic food product technology, 15(2), 5-16.

Martell, A. E. and Smith, R. M. (1974) Critical Stability Constants, New York: Plenum Press.

Meyer, V. (2010) Practical High-Performance Liquid Chromatography, 5th ed., Chichester: Wiley & Sons.

Miao, F., Geng, Y., Lu, D., Zuo, J., & Li, Y. (2013) Stability and Changes in Astaxanthin ester Composition from Haematococcus pluvialis during storage', Chinese Journal of Oceanology and Limnology, 31(6), 1181-1189.

Mohan, J. (2004) Organic Spectroscopy: Principles and Applications, India: CRC Press.

Pacheco, N., Garnica-González, M., Ramírez-Hernández, J. Y., Flores-Albino, B., Gimeno, M., Bárzana, E. and Shirai, K. (2009) 'Effect of Temperature on Chitin and Astaxanthin Recoveries from Shrimp Waste using Lactic Acid Bacteria', Bioresource technology, 100(11), 2849-2854.

Palanna, O. G. (2009) Engineering Chemistry, New Delhi: Tata McGraw Hill Education Private Limited.

Parab, N. D. T., & Tomar, V. (2012) 'Raman spectroscopy of algae: A review', J Nanomedic Nanotechnol, 3(131), 2.

Polyakov, N. E., Focsan, A. L., Bowman, M. K. and Kispert, L. D. (2010), 'Free radical formation in novel carotenoid metal ion complexes of astaxanthin', The Journal of Physical Chemistry B, 114(50), 16968-16977.

Pham-Huy, L. A., He, H. and Pham-Huy, C. (2008) 'Free radicals, antioxidants in disease and health', International Journal of Biomedical Science: IJBS, 4(2), 89.

Sachindra, N. M., Bhaskar, N. and Mahendrakar, N. S. (2005) 'Carotenoids in crabs from marine and fresh waters of India', LWT - Food Science and Technology, 38(3), 221-225.

Sachindra, N. M. and. Mahendrakar N. S (2005) 'Process Optimization for Extraction of Carotenoids from Shrimp Waste with Vegetable Oils', Bioresource Technology, 96(10), 1195-1200.

Sachindra, N. M., Bhaskar, N., AND Mahendrakar, N. S. (2006) 'Recovery of carotenoids from shrimp waste in organic solvents', Waste Management, 26(10), 1092-1098.

Sasic, S. (2008) Pharmaceutical applications of Raman spectroscopy, Oxford: Wiley-Interscience.

Sathyanarayana, D. N. (2001). Electronic absorption spectroscopy and related techniques, India: Universities Press.

Seeboth, A., and Lötzsch, D. (Eds.) (2013) Thermochromic and thermotropic materials, U.S.: CRC Press.

Schmid, H. and Stich, H. B. (1995) 'HPLC-analysis of algal pigments: comparison of columns, column properties and eluents', Journal of applied phycology, 7(5), 487-494.

Scholz, F. and A. M. Bond (2005) Electroanalytical Methods: Guide to Experiments and Applications, Berlin: Springer.

Shahidi, F. (2000) 'Antioxidants in food and food antioxidants', Food / Nahrung, 44(3), 158-163.

Shimidzu, N., Goto, M., and Miki, W. (1996) 'Carotenoids as singlet oxygen quenchers in marine organisms', Fisheries science, 62(1), 134-137.

Siems, W. G., Sommerburg, O. and Van Kuijk, F. J. (1999) 'Lycopene and β-carotene decompose more rapidly than lutein and zeaxanthin upon exposure to various pro-oxidants in vitro', BioFactors, 10(2-3), 105-113.

Simonyi, M., Bikadi, Z., Zsila, F. and Deli, J. (2003) 'Supramolecular Excitation Chirality of Carotenoid Aggregates', Chirality, 15(8), 680-698.

Smith, B. C. (2011) Fundamentals of Fourier Transform Infrared Spectroscopy, London: CRC Press.

Smith, J. L. and Gropper, S. S. (2012) Advanced Nutrition and Human Metabolism, USA: Cengage Learning.

Trimm, H. H. and Hunter, W. J. (2011) Dyes and Drugs: New Uses and Implications, Canada: Apple Academic Press.

Ukibe, K., Katsuragi, T., Tani, Y. and Takagi, H. (2008) 'Efficient screening for astaxanthin-overproducing mutants of the yeast Xanthophyllomycesdendrorhous by flow cytometry', FEMS Microbiology Letters, 286(2), 241-248.

Yadav, L. D. S. (2005) Organic Spectroscopy, Boston: Kluwer Academic Publishers.

Yuan, C., Jin, Z., & Xu, X. (2012) 'Inclusion complex of Astaxanthin with Hydroxypropyl-β-cyclodextrin: UV, FTIR, 1H NMR and Molecular Modeling studies', Carbohydrate Polymers, 89(2), 492-496.

Yuan, Y. V., Bone, D. E. and Carrington, M. F. (2005) 'Antioxidant activity of Dulse (*Palmaria palmata*) extract evaluated in vitro', Food Chemistry, 91(3), 485-494.

Vilasoa-Martínez, M., Calaza-Ramos, C., López-Hernández, J., Lage-Yusty, M. A., Losada, P. P. and De Quirós, A. R. B. (2008) 'Determination of vitamin E and carotenoid pigments by High Performance Liquid Chromatography in Shell of Chionoecetes Opilio', Analytica chimica acta, 617(1), 225-229.

Valeur, B. and Berberan-Santos M. N. (2012) Molecular Fluorescence: Principles and Applications, Weinheim: Wiley-VCH.

Varsányi, G. (2012). Vibrational Spectra of Benzene derivatives, Hungary: Elsevier.

Vidussi, F., Claustre, H., Bustillos-Guzmàn, J., Cailliau, C. and Marty, J.-C. (1996) 'Determination of chlorophylls and carotenoids of marine phytoplankton: separation of chlorophyll a from divinylchlorophyll a and zeaxanthin from lutein', Journal of plankton research, 18(12), 2377-2382.

Vilasoa-Martínez, M., Calaza-Ramos, C., López-Hernández, J., Lage-Yusty, M. A., Losada, P. P. and Rodríguez-Bernaldo de Quirós, A. (2008) 'Determination of vitamin E and carotenoid pigments by high performance liquid chromatography in shell of Chionoecetesopilio', AnalyticaChimicaActa, 617(1–2), 225-229.

Weinhold, F. and Landis C. R. (2005) Valency and Bonding: A Natural Bond and Orbital donor-acceptor perspective, CambridgE: Cambridge University Press.

Withnall, R., Chowdhry, B. Z., Silver, J., Edwards, H. G. and De Oliveira, L. F. (2003) ‘Raman spectra of carotenoids in natural products’, Spectrochimica Acta Part A: Molecular and Biomolecular Spectroscopy, 59(10), 2207-2212.

Wu, T. H., Liao, J. H., Hou, W. C., Huang, F. Y., Maher, T. J. and Hu, C. C. (2006) ‘Astaxanthin protects against oxidative stress and calcium-induced porcine lens protein degradation’, Journal of Agricultural and Food Chemistry, 54(6), 2418-2423.